

BEHAVIOUR OF COMPOSITE BEAMS
WITH RIBBED METAL DECK



By

MOHAMED SHERIF ELKELISH

A Thesis
Submitted to the School of Graduate Studies
in Partial Fulfilment of the Requirements
for the Degree
Doctor of Philosophy

McMaster University
March, 1979

BEHAVIOUR OF COMPOSITE BEAMS

WITH RIBBED METAL DECK

To My Dear Wife Maha
and
to the Light of my Life,
my Daughter, Rhonda
Whose
Patience, Understanding and Assistance
Are Deeply Appreciated.

DOCTOR OF PHILOSOPHY (1979)
(Civil Engineering)

MCMMASTER UNIVERSITY
Hamilton, Ontario.

TITLE: Behaviour of Composite Beams with Ribbed Metal Deck

AUTHOR: Mohamed Sherif Elkelish, B.Sc. (Cairo University)
M.Eng. (McMaster University)

SUPERVISOR: Dr. H. Robinson

NUMBER OF PAGES: xviii , 190

ACKNOWLEDGEMENTS

The author wishes to express his sincere gratitude to Dr. H. Robinson for his guidance, encouragement, and supervision during the course of this study. The valuable comments offered by Dr. Robinson and the effort he expended in reviewing the manuscript are greatly appreciated.

Appreciation is extended to the other committee members, Dr. M. Levinson, Dr. G. Oravas and Dr. R. Sowerby for their valuable suggestions.

Acknowledgement is due to McMaster University, the National Research Council of Canada and the Ministry of Colleges and Universities for financial support.

Finally, a special note of deep appreciation is due to my wife, my daughter and my parents for their help and encouragement without which this thesis would have been difficult to complete.

ABSTRACT

This dissertation presents an inelastic analysis of the behaviour of composite beams with ribbed metal deck.

A layered finite element model is used to allow for any variation in material properties through the thickness. An incremental and iterative technique is adopted using the tangent modulus stiffness approach.

The dependability of the model is checked by means of comparison with some experimental results, obtained from testing composite beams with solid and ribbed slabs.

A study of the effect of the type of loading and the transverse moment in the slab on the deformation and the ultimate capacity of composite beams with ribbed metal deck, is presented.

The effective width of composite beams with ribbed metal deck, subjected to uniformly distributed load, is investigated. The effective width in the inelastic stage and at the ultimate load are also studied.

Finally, a study of the longitudinal cracking of composite beams with ribbed metal deck, is presented. Some design recommendations are presented to account for

the longitudinal cracking of composite beams with ribbed metal deck, subjected to a uniformly distributed load over the entire slab.

TABLE OF CONTENTS

	PAGE
CHAPTER 1: INTRODUCTION	
1.1 General	1
1.2 Objectives and Scope	4
Chapter 2: MATERIAL BEHAVIOUR CHARACTERISTICS	
2.1 General	8
2.2 Stress-Strain Curves for Steel and Concrete	9
2.3 Failure Criteria for Concrete	11
2.4 Constitutive Relations of Concrete	15
2.4.1 Elastic Concrete	15
2.4.2 Inelastic Concrete	16
2.4.3 Singly-cracked Concrete	16
2.4.4 Doubly-Cracked Concrete	19
2.4.5 Crushed Concrete	20
2.5 Constitutive Relations of the Steel Reinforcement	20
2.6 Constitutive Relations of the Metal Deck	21
2.7 Constitutive Relations of the Steel Beam	22
CHAPTER 3: NUMERICAL MODEL AND INCREMENTAL ANALYSIS	
3.1 General	24
3.2 Numerical Model	25
3.3 Layering Concept	26
3.4 Solution Steps	28
3.5 Boundary Conditions	30
3.6 Computer Program	31
CHAPTER 4: NUMERICAL EXAMPLES	
4.1 General	33
4.2 Centrally Loaded Rectangular Plate	34
4.3 McNiece's Reinforced Concrete Slab	34
4.4 Barnard's Test on a Composite Beam with a Solid Slab	37
4.5 Robinson's and Wallace's Tests on Composite Beams with Ribbed Metal Decks	40
4.6 Fisher's Test on a Composite Beam with a Ribbed Metal Deck	47

	PAGE
4.7 Henderson's Tests on Composite Beams with Ribbed Metal Decks	49
4.8 Effect of the Type of Loading and boundary Conditions on the Behaviour of Composite Beams with Ribbed Metal Deck	49
 CHAPTER 5: EFFECTIVE WIDTH OF COMPOSITE BEAMS WITH RIBBED METAL DECK	
5.1 General	59
5.2 Definition of the Effective Width	63
5.3 Comparison with Available Solutions	64
5.4 Effective Width of Composite Beams with Ribbed Slabs	64
5.5 Effective Width Variation with the Span to Width Ratio	72
5.6 Effect of the Concrete Compressive Strength on the Effective Width Ratio Distribution	77
5.7 Effect of Beam Size on the Effective Width Ratio Distribution	77
5.8 Effect of Type of Loading on the Effective Width Ratio Distribution	77
5.9 Effective Width of Composite Beams with Ribbed Metal Deck in the Inelastic Stage	80
5.10 Comparison with the CISC and AIJ Specifications	83
5.11 Conclusions	87
 CHAPTER 6: LONGITUDINAL CRACKING OF COMPOSITE BEAMS WITH RIBBED METAL DECKS	
6.1 General	90
6.2 Effect of the Type of Loading	95
6.3 Effect of the Compressive Strength of Concrete	99
6.4 Effect of the Beam Span to Slab Width Ratio	102
6.5 Effect of the Metal Deck	106
6.6 Effect of Beam Size	106
6.7 Effect of the Thickness of the Solid Part of the Slab	109
6.8 Effect of the Transverse Reinforcement	109
6.9 Design Recommendations and Conclusions	113
 CHAPTER 7 SUMMARY AND CONCLUSIONS	
7.1 Summary	123
7.2 Conclusions	124

APPENDIX A: FINITE ELEMENT APPROACH

A.1	Introduction	131
A.2	Derivation of Bending and In-Plane Plate Stiffness Matrix	136
A.3	Determination of the Reference Surface Strains	148
A.4	Determination of the Layer Stresses	148
A.5	Determination of the Excess Nodal Forces	149
A.6	Derivation of Bending and In-Plane Beam Stiffness Matrix	150
A.7	Stiffness Matrices of the Beam Elements Representing the Vertical Parts of the Metal Deck	155
A.8	Assembly of the Element Stiffness Matrices	156
A.9	Displacement Compatibility	157

APPENDIX B: COMPUTER PROGRAM

B.1	General Description	159
B.2	Program Subroutines	159
B.3	Notations	162
B.4	Program Listing	165

REFERENCES :	185
--------------	-----

LIST OF FIGURES

FIGURE		PAGE
2.1	Assumed Stress-Strain Curves for Steel and Concrete	10
2.2	Biaxial Strength of Concrete Proposed by Kupfer et al.	13
2.3	Adopted Failure Criteria	13
3.1	Intermediate Composite Beam with the Assumed Boundary Conditions	32
4.1	Element Grid for a Rectangular Plate Fixed at all Edges	35
4.2	Element Grid for Jofreit and McNiece's Slab	36
4.3	Load-Deflection Curve of McNiece's Slab	38
4.4	Details of Barnard's Composite Beam	38
4.5	Layered Finite Element Grid for a Composite Beam with a Solid Slab	39
4.6	Moment-Curvature Curve for Barnard's Beam	39
4.7	Details of Robinson and Wallace's Composite Beam with Ribbed Metal Deck	42
4.8	Layered Finite Element Grid for a Composite Beam with Ribbed Metal Deck	43
4.9	Moment-Deflection Curve of Robinson and Wallace's Beam B_4	44
4.10	Load Versus Steel Bottom Fibre Strain of Robinson and Wallace's Beam B_4	45
4.12	Details of Fisher's Composite Beam	48

	PAGE
4.13 Load-Deflection Curve of Fisher's Beam B_4	48
4.14 Details of Henderson's Composite Beams with Ribbed Metal Deck	50
4.15 Load-Deflection Curve of Henderson's Beam B_2	51
4.16 Load-Deflection Curve of Henderson's Beam B_3	52
4.17 Load-Deflection Curve of Henderson's Beam B_8	53
4.18 Typical Composite Beam with Different Boundary Conditions	55
4.19 Effect of Type of Loading on the Behaviour of Composite Beams with Ribbed Metal Deck	56
5.1 Effective Width of Composite Beams	60
5.2 Comparison with Adekola's Effective Width Distribution ($L/b=3$)	60
5.3 Comparison with Adedola's Effective Width Distribution ($L/b=4$)	65
5.4 Effective Width of an Intermediate Beam in a System of Composite Beams	67
5.5 Effective Width Ratio Distribution for a Composite Beam with a Solid Slab under a UDL over the Slab Area	70
5.6 Effective Width Ratio Distribution for a Composite Beam with a Ribbed Metal Deck under a UDL over the Slab Area	71
5.7 Effective Width Ratio Distribution for a Solid and Ribbed Slab under UDL over Slab	73
5.8 Effective Width Ratio Distribution for a Solid and Ribbed Slab under UDL over Slab	73
5.9 Variation of Mid-Span Effective Width with Span-to-Width Ratio for a UDL over the Slab Area	76
5.10 Effect of Type of Loading on the Effective Width Ratio Distribution for a Composite Beam with Ribbed Metal Deck	79

	PAGE
5.11 Variation of the Effective Width of a Composite Beam with a Ribbed Metal Deck with the Stage of Loading ($L/b=4$)	81
5.12 Variation of the Effective Width of a Composite Beam with a Ribbed Metal Deck with the Stage of Loading ($L/b=3$)	82
5.13 Comparison between the Analytical Model and the CISC and the AIJ Specifications	86
6.1 Relationship between Longitudinal Cracking Moment and the Properties of the Composite Beam	115
6.2 Relationship between Longitudinal Cracking Moment and the Properties of the Composite Beam (using the Ultimate Stress Block Method)	117
6.3 Effect of the Thickness of the Solid Part of the Slab on the Longitudinal Cracking of Composite Beams with Ribbed Metal Deck	118
6.4 Composite Beam Properties to Achieve the Ultimate Capacity Simultaneously with the Longitudinal Cracking	120
A.1 Plate and Beam Nodal Numbering System and Local Element Coordinate System	133
A.2 Layered Beam and Plate Finite Elements	133
A.3 Composite Beam Modelling	135
A.4 Positive Orientation of the Nodal Degrees of Freedom	137
A.5 Position of the J^{th} Layer	137

LIST OF TABLES

TABLE

4.1	Comparison of the Maximum Deflection of a Plate Fixed at All its Edges	35
4.2	Comparison of the Maximum Deflection of a Rectangular Plate Simply Supported at All its Edges	36
4.3	Effect of Type of Loading on the Behaviour of Composite Beams with Ribbed Metal Deck	58
5.1	Comparison with Adekola's Effective Width Ratios	65
5.2	Effective Width of an Intermediate Composite Beam	67
5.3	Effect of Boundary Conditions on the Effective Width of Composite Beams with Ribbed Metal Deck Subjected to One Point Load at the Mid-Span of the Beam ($L/b=4$)	68
5.4	Effect of Boundary Conditions on the Effective Width of Composite Beams with Ribbed Metal Deck Subjected to UDL over the Slab Area ($L/b=4$)	68
5.5	Effective Width-to-Width Ratio Distribution for a Solid and Ribbed Slab under UDL over the Slab Area ($L/b=4$)	74
5.6	Effective Width-to-Width Ratio Distribution for a Solid and Ribbed Slab under UDL over the Slab Area ($L/b=5$)	74
5.7	Moment to Effective Width Ratio along a Composite Beam with a Ribbed Metal Deck under a UDL over the Slab Area ($L/b=4$)	75

5.8	Effective Width-to-Width Ratio for Two Composite Beams with Ribbed Metal Deck Having the Same L/b Ratio ($L/b=4$)	76
5.9	Effect of Concrete Strength on the Effective Width-to-Width Ratio Distribution in a Ribbed Slab under UDL over Slab Area ($L/b=4$)	78
5.10	Effect of Beam Size on the Effective Width-to-Width Ratio of a Composite Beam with a Ribbed Metal Deck ($L/b=4$)	78
5.11	Effect of Type of Loading on the Effective Width Ratio of a Composite Beam with a Ribbed Metal Deck ($L/b=4$)	79
5.12	Comparison with the Effective Width of a Composite Beam with a Ribbed Metal Deck according to the Canadian and Japanese Specifications	85
5.13	Effective Width Ratios of a Composite Beam with 1-1/2 in Ribbed Metal Deck under a UDL over the Slab Area	86
6.1	Effect of Type of Loading on the Longitudinal Cracking ($f'_c = 5800$ psi)	96
6.2	Effect of Type of Loading on the Longitudinal Cracking ($f'_c = 3000$ psi)	97
6.3	Effect of Concrete Strength on the Longitudinal Cracking of Composite Beams Loaded with 2-Point Load at 1/3 Points of Beam Span ($L/b=4$)	100
6.4	Effect of Concrete Strength on the Longitudinal Cracking of Composite Beams Loaded with a UDL over the Slab Area ($L/b=4$)	100
6.5	Longitudinal Cracking for Composite Beams having the Same Steel Beam Yield Stress to Concrete Compressive Strength Ratios	101
6.6	Effect of L/b Ratios on the Longitudinal Cracking of Composite Beams Loaded with One Point Load at Mid-Span of the Beam ($f'_c = 5822$ psi)	103
6.7	Effect of L/b Ratio on the Longitudinal Cracking of Composite Beams Loaded with a UDL over the Slab Area ($f'_c = 4000$ psi)	103

6.8	Longitudinal Cracking of Composite Beams having the Same Span to Width Ratio ($L/b=3$)	105
6.9	Longitudinal Cracking of Composite Beams having the Same Span to Width Ratio ($L/b=4$)	105
6.10	Effect of the Metal Deck on the Longitudinal Cracking of Composite Beams under one Point Load at Mid-Span of the Beam	107
6.11	Effect of the Metal Deck on the Longitudinal Cracking of Composite Beams under UDL over the Slab Area	107
6.12	Effect of the Steel Beam Size on the Longitudinal Cracking	108
6.13	Effect of the Thickness of the Solid Part of the Slab on the Longitudinal Cracking	108
6.14	Effect of the Transverse Reinforcement on the Longitudinal Cracking of Composite Beams under UDL over the Slab Area ($L/b=3$)	110
6.15	Effect of the Transverse Reinforcement on The Longitudinal Cracking of Composite Beams under UDL over the Slab Area ($L/b=4$)	110
6.16	Effect of the Transverse Reinforcement on The Longitudinal Cracking of Composite Beams under UDL over the Slab Area ($L/b=5$)	111
6.17	Effect of the 6 x 6/10 x 10 Welded Wire Mesh on the Longitudinal Cracking of Composite Beams under UDL over the Slab Area ($L/b=3$)	111

LIST OF SYMBOLS

a_1	Half-element dimension in x-direction
A	Matrix relating nodal displacements and generalized unknowns
b	Total width of the concrete slab (Centreline to centreline distance between the adjacent beams)
b_1	Half-element dimension in y-direction
b_e	Effective width of the concrete slab
B	Matrix relating generalized unknowns and middle surface strains and curvatures
B_ϵ, B_χ	Submatrices of B representing membrane and bending parts, respectively
c	Material properties matrix
c_j	j^{th} layer material properties matrix
D, H, F	Submatrices of \bar{D}
D_j, H_j, F_j	Submatrices of \bar{D}_j
\bar{D}	Matrix representing $[G]^T [C] [G]$
\bar{D}_j	D evaluated for the j^{th} layer
E_c, E_{c1}, E_{c2}	Tangent moduli of concrete
E_s, E_{s1}, E_{s2}	Tangent moduli of the steel beam
E_s, E_{s1}	Tangent moduli of the steel reinforcement and the metal deck
f	Stress vector : $\{f_x, f_y, f_{xy}\}$

f_1, f_2	Principal stresses in a concrete layer
f'_c	Compressive Strength of Concrete
f_{c1}	Transition stress between first and second linear regions for concrete
f_{c2}	Transition stress between second and third linear regions for concrete
f_{cu}	Maximum compressive stress in the transition criteria for concrete
f_{ex}	Excess layer stress vector
f_{tu}	Tensile strength of concrete
F_{ex}	Excess element nodal force vector
F_{jex}	j^{th} layer excess element nodal force vector
F_y	Yield stress of steel
G	Matrix relating strain vector to middle surface strains and curvatures
K	Element stiffness matrix
L	Span of the simply supported composite beam
M'_u	Ultimate Moment of the Composite Beam (Ultimate Stress Block Method)
M_{Lc}	Longitudinal cracking moment of the composite beam
M_u	Ultimate moment of the composite beam
M_y	Yield moment of the composite beam
N	Number of layers
p_T	Percentage of the transverse reinforcement in the slab
t_j, t_{j+1}	Distance from reference surface to the top, bottom of the j^{th} layer

t_s	Overall thickness of the ribbed concrete slab
T	Transformation matrix
u, v, w	Displacements in the x, y and z directions, respectively
U	Element displacements vector
\bar{U}	Vector of nodal displacements
W_{int}	Internal work
θ_x, θ_y	Slope of $w(x,y)$ in the y and x-directions, respectively
x, y, z	Rectangular cartesian coordinates
α	Vector of generalized coordinates
β	Shear retention factor for concrete
δW_{int}	Internal virtual work
ϵ	Strain vector : $\{\epsilon_x, \epsilon_y, \epsilon_{xy}\}$
ϵ_0	Reference surface strain vector : $\{\epsilon_{x_0}, \epsilon_{y_0}, \epsilon_{xy_0}\}$
$\bar{\epsilon}$	Reference surface strains and curvatures vector
ν	Poisson's ratio for concrete
χ	Reference surface curvatures vector : $\{\chi_x, \chi_y, 2\chi_{xy}\}$

CHAPTER 1

INTRODUCTION

1.1 General

In recent years there has been an increased use of ribbed metal decking in the floor slabs of buildings⁽¹⁶⁾. This metal decking has a single or multi-purpose role dependent to a large extent upon the cross-sectional configuration, Fig. (4.7).

The prime role of the ribbed deck may be deemed to be the action as the structural floor slab spanning between the steel beams. The ribbed slab supports the superimposed load and transfers it to the steel beams while acting as the compression flanges for the simply supported composite beams. The shallow decking acts as in-situ form work for the concrete floor slab and may be designed to act compositely with the concrete slab. An additional attribute of the steel deck is that it can provide duct space in the floor slab for electrical and communications wiring.

The stress conditions within the concrete slab of a composite beam are quite complex⁽¹⁷⁾. First, the concrete floor slab itself is normally continuous over

the steel beams resulting in the transverse slab moment along the length of the beams. Secondly, due to the composite action between the slab and the beam, a longitudinal shear stress is produced in the concrete slab. These effects are additional to the basic longitudinal flexural stresses set up by the principal bending moment applied to the composite beam.

Moreover, in the inelastic stage of deformation, the flexural and longitudinal cracking of the concrete slab and the yielding of the steel beam affect the behaviour of the composite beam. The transverse and longitudinal slab reinforcements, and the ribbed metal deck may also have a significant effect on the composite beam behaviour.

In recent years, a variety of methods have been developed for the determination of the structural response of composite floor systems. However, most of these methods did not account for the behaviour of such structures in the inelastic stage of deformation.

Most of the work done on composite beams has dealt with composite beams with solid concrete slabs. Allen and Severn⁽⁵⁾, discussed the basis for the determination of stresses and deflections in composite beams with solid slabs in the elastic stage. They divided the structure into two parts, the slab and beam, with the former being analysed by thin-plate theory and the latter by simple bending theory. The effect of the slab reinforcement

and the cracking of concrete was not included in this study.

Adekola^(3,4) has presented an elastic solution of an equally spaced system of composite beams with solid concrete slabs under symmetrical point loads over the beams, by using the basic plane-stress equations. The cracking of the concrete slab and the effect of the steel reinforcement are not included in this analysis.

Barnard et al^(9,10) made a thorough study of simple flexure of composite beams with solid concrete slabs. This included some tests on simply supported composite beams with solid slabs. They presented a method for the calculation of the ultimate strength of composite beams. The effect of the transverse bending of the slab and the effect of cracking were not included in this study.

Heins et al^(21,27) utilized a finite difference approach to find the load-deformation response of composite beams with solid slabs in the inelastic stage of deformation. The cracking of the concrete slab and the effect of the reinforcement were not included in this study. A finite element analysis was presented⁽²³⁾ to study the elastic behaviour of composite girder bridges with solid concrete slabs. The reinforcement and the cracking of the concrete slab were not considered.

Recent progress in the application of the finite element technique has led to a reliable approach for

finding the inelastic response of eccentrically stiffened plates^(60,61). The cracking of the solid concrete slab and the yielding of the steel beam were accounted for in this approach.

Robinson^(50,51) investigated experimentally the behaviour of composite beams with ribbed metal deck. He observed that in many cases, the concrete slab began to show failure by longitudinal cracks extending from the load points to the ends of the beams prior to the attainment of the theoretical ultimate moment.

Ma⁽⁴²⁾ presented an inelastic analysis of composite beams with ribbed metal deck using the finite difference method. However, he did not include the longitudinal cracking and the effective width of the slab in his study. Also, the metal deck and the concrete ribs were not taken into consideration. The model did not include the effect of transverse bending of the slab.

1.2 Object and Scope

The goal of the present investigation is the development of an analytic procedure capable of predicting the complete inelastic response of composite beams with ribbed metal deck. The investigation involves the inclusion of the effects of the longitudinal and flexural cracking of the concrete, and the yielding of the steel beam and the steel reinforcement. The contribution of the metal deck and the

concrete ribs are also included in this study.

The current investigation is restricted to short-term monotonically increasing loads. Therefore, the nonlinear behaviour of the composite beam can mainly be attributed to four sources: the tensile cracking and compressive crushing of concrete, and the yielding of reinforcing steel and the girder steel.

The characteristic behaviour of the different materials used in composite beams with ribbed metal deck are presented in Chapter 2. A biaxial failure criterion is adopted to deal with the biaxial state of stress in the concrete slab.

A layered finite element^(25,26,39) technique is used in this study to permit any variation in material properties through the thicknesses of the concrete slab and the steel beam flange and web. It allows the inclusion of the cracking of the concrete slab and the yielding of the steel beam. It also allows the inclusion of the steel reinforcement and the metal deck in the study.

The nonlinear solution scheme is presented in Chapter 3. An incremental and iterative process^(25,26,39,61) is adopted to reduce the nonlinear problem to a piece-wise linear one. The loads are applied to the structure by increments. At each stage of loading, the material properties are checked and the structural stiffness is updated to accommodate any changes in these properties.

The finite element model is compared in Chapter 4 to some experimental results obtained from testing composite beams with solid and ribbed slabs. The comparison is aimed at demonstrating the capability of the model in predicting the inelastic behaviour of composite beams.

One of the objects of this investigation is to study the load-deformation behaviour of composite beams with ribbed metal deck in the inelastic stage. The effect of the type of loading and the transverse negative moment in the slab on the ultimate capacity of composite beams with ribbed metal deck is also presented.

A study of the effective width of composite beams with ribbed metal deck subjected to uniformly distributed load is presented in Chapter 5. The effective width variation in the inelastic stage as well as the effective width at the ultimate load are studied. The different parameters affecting the effective width of composite beams with ribbed metal deck are also considered. A comparison with the Canadian and Japanese specifications, together with some conclusions and recommendations are presented.

Chapter 6 contains a parametric study of the slab longitudinal cracking developed along the length of the steel beams in a composite floor system. The different factors affecting the longitudinal cracking, such as the strength of concrete, the transverse reinforcement, the ribbed metal decking, the beam-span-to-slab-width ratio, the thickness of

the solid part of the slab and the size of the steel beam, are presented in this study. The effect of the type of loading and the transverse negative moment in the slab are also considered in this investigation. Some design recommendations are proposed concerning the longitudinal cracking of composite beams with ribbed metal deck under a uniformly distributed load over the entire slab.

Chapter 7 includes some general conclusions with respect to the inelastic behaviour of a composite beam with ribbed metal deck: its strength, stiffness, effective width and longitudinal cracking.

CHAPTER 2

MATERIAL BEHAVIOUR CHARACTERISTICS.

2.1 General

In a composite beam with a reinforced concrete slab, the slab acts compositely with the steel beam in resisting the applied loads. The accuracy of any analysis attempting to predict the nonlinear behaviour of composite beams will invariably depend on the ability of the material models used to represent the complex behaviour of the reinforced concrete slab.

In modelling the reinforced concrete slab, several difficulties arise. Reinforced concrete is not homogeneous, being composed of two different materials, concrete and steel. Moreover, concrete, itself, is non-homogeneous, having aggregates and cement paste as the main components. The structural properties of concrete, such as strength and deformation, can only be determined at the macroscopic level using averaged values. The variations due to the microscopic structure are generally ignored because of the complexities involved and because satisfactory prediction of structural response can be made using

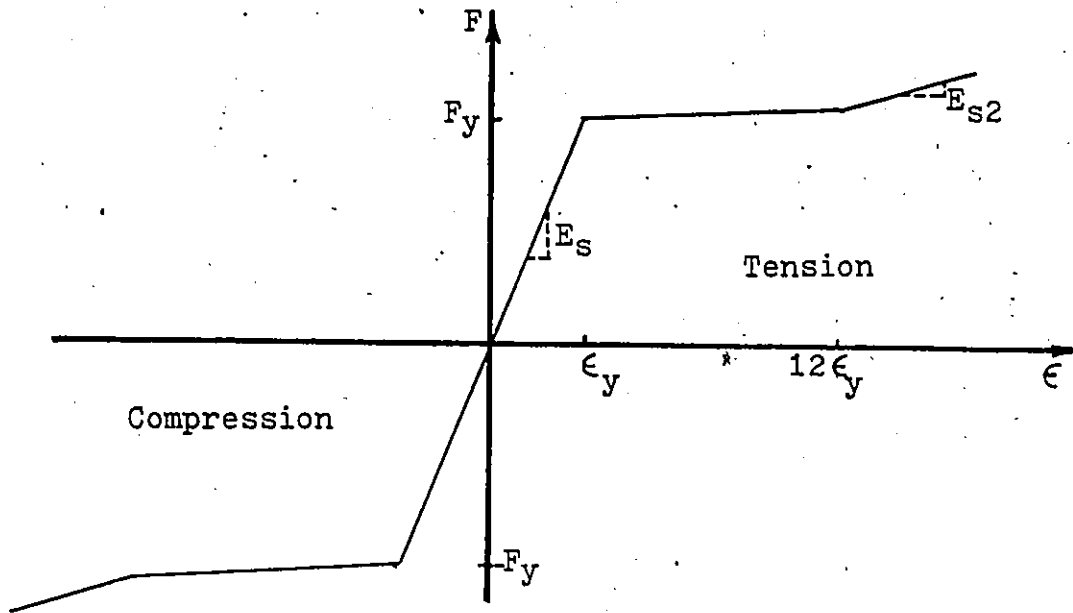
properties at the macroscopic level. Cracking in concrete shows randomness in the sense that although it is possible to predict the region where cracking will occur, the actual location and direction of cracks will depend on the local variations in the microstructure.

On the other hand, the properties of the steel reinforcement and the steel beam can be specified more consistently because of the superior homogeneity of this material in the macroscopic sense.

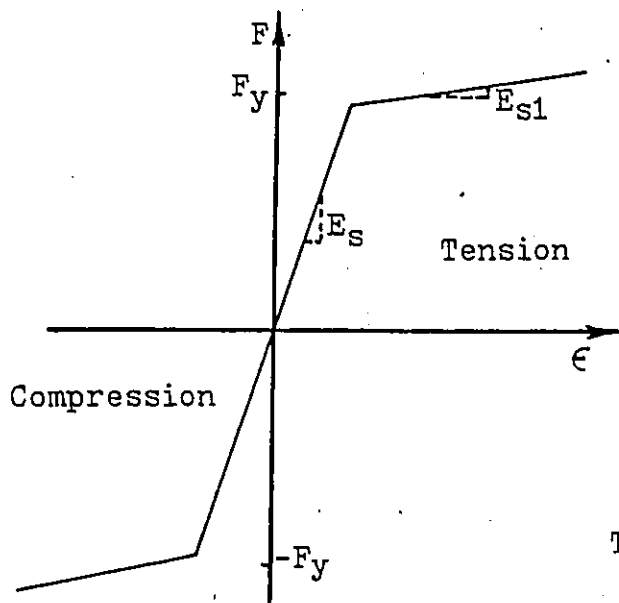
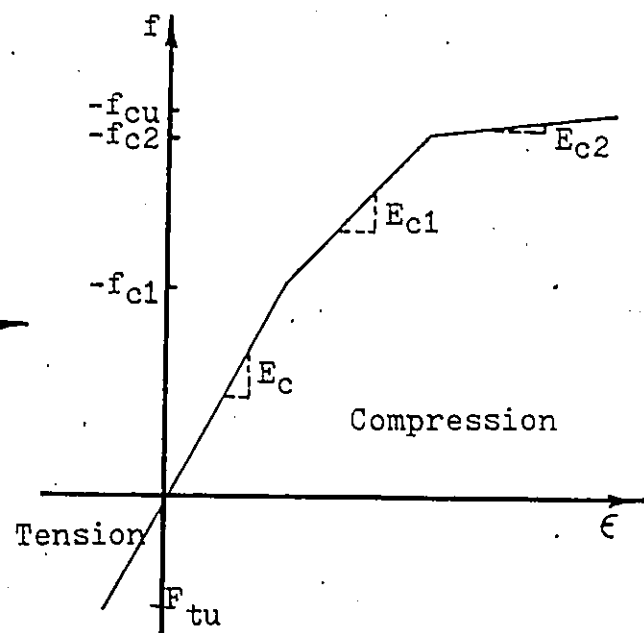
In order to analyse a composite beam in the inelastic stage, several simplifying assumptions regarding the behaviour of the materials have to be made. The purpose of this Chapter is to state explicitly what material properties are assumed for the plain concrete, the steel reinforcement, the metal deck and the steel beam.

2.2 Stress-Strain Curves for Steel and Concrete

The assumed uniaxial stress-strain curves for the steel beam, the reinforcing steel, the metal deck and the concrete slab are shown in fig.(2.1). The stress-strain curve for the steel beam is assumed to be elastoplastic-strain-hardening curve, fig.(2.1-a). The reinforcing steel and the metal deck are considered to be of an elastic material with strain-hardening response, fig.(2.1-b). The bilinear elastic-perfectly plastic stress-strain curve^(25,47) is modified to a trilinear curve with a very small tangent



(a) Steel Beam

(b) Steel Reinforcement
and Metal Deck

(c) Concrete

Fig.(2.1) Assumed Stress-Strain Curves
for Steel and Concrete

modulus in the third segment for iteration purpose, fig.(2.1-c).

2.3 Failure Criteria for Concrete

Concrete under a biaxial state of stress, as is assumed to occur in such structural elements as concrete slabs, shows a different behaviour than that under a uniaxial state of stress. Several investigators^(7,12,13,36,40,41,49,52) presented experimental data on concrete specimens under biaxial states of stress.

The experimental works of Kupfer et al⁽³⁶⁾, indicate that the major difference in the stress-strain relations between uniaxial and biaxial states is that the biaxial states have a higher capacity. The works indicate also that the biaxial states of stress have a minor effect on the modulus of elasticity of concrete. The biaxial strength of concrete is as much as 27 percent higher than the uniaxial strength. In the compression-tension region, the results obtained⁽³⁶⁾ show that the compressive stress at failure decreases as the simultaneously acting tensile stress is increased. The experimental results also show that the strength of concrete under biaxial tension is almost independent of the stress ratio f_1/f_2 and equal to the uniaxial tensile strength. Kupfer's⁽³⁶⁾ biaxial strength envelope with the different failure modes for various stress ratios is shown in fig.(2.1).

Kupfer and Gerstle⁽³⁵⁾ have used a curve fitting technique to represent the experimental results for various combinations of biaxial stresses. They proposed expressions in terms of the principal stresses to cover the tension-tension, tension-compression and compression-compression regions, fig.(2.2).

For the compression-compression zone;

$$(f_1/f_{cu} + f_2/f_{cu})^2 + (f_1/f_{cu}) + 3.65(f_2/f_{cu}) = 0$$

For the compression-tension zone;

$$f_2/f_{tu} = 1.0 + 0.80(f_1/f_{cu})$$

For the tension-tension zone;

$$f_2 = f_{tu} = 1.55(\sqrt[3]{f_{cu}^2})$$

Several investigators^(25,34,39,45,48,54,55,59) studying the inelastic behaviour of concrete element, have used the biaxial failure criterion envelope, determined by Kupfer⁽³⁶⁾, as a basis for their investigations.

A failure criterion to be used should be simple if possible. It should provide a reliable prediction of the

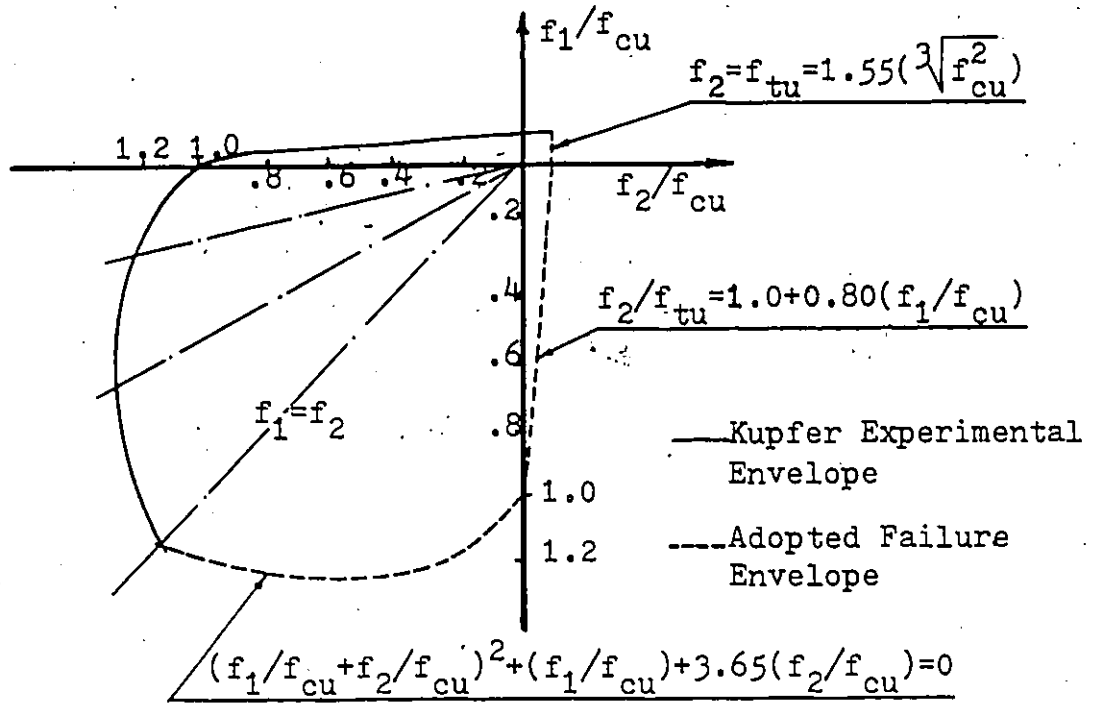


Fig.(2.2) Biaxial Strength of Concrete Proposed by Kupfer et al (35&36)

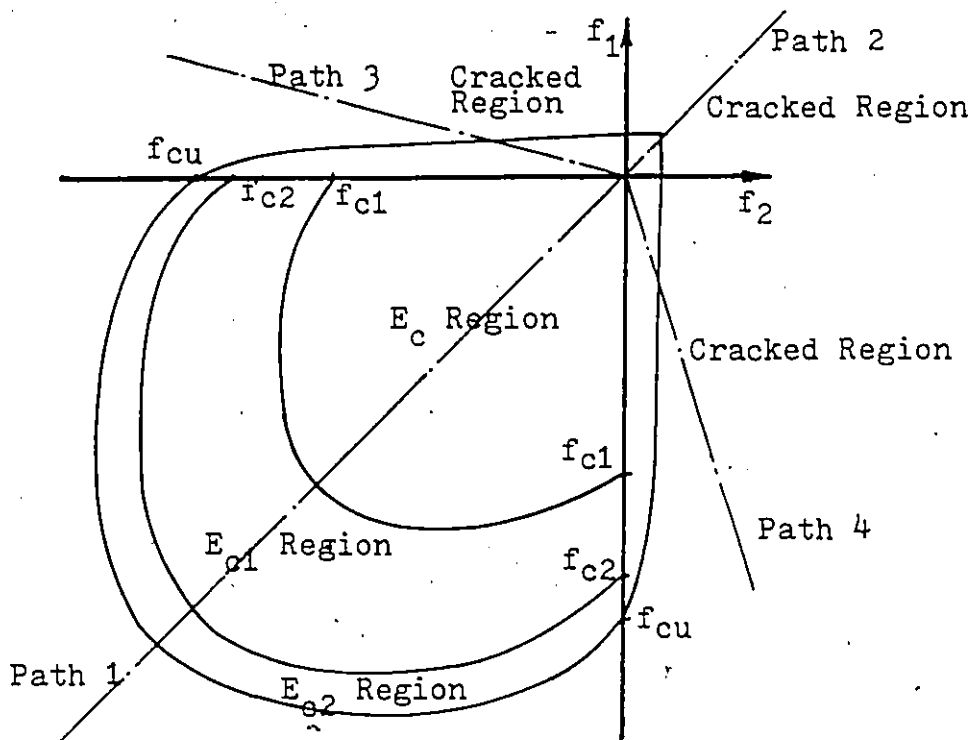


Fig.(2.3) Adopted Failure Criterion

failure for those combinations of stresses which can occur in the structure. The reliability of the criteria should be confirmed by test results. Recognizing all these facts, the criterion suggested by Kupfer⁽³⁵⁾ and confirmed by his experimental studies⁽³⁶⁾, is used in this research as a failure criterion for the concrete in the ribbed slab.

In the adopted failure criteria, fig.(2.3), there are three basic failure modes for plain concrete layers as illustrated by the loading paths:

1. Elastic behaviour, inelastic behaviour and crushing of concrete (path 1).
2. Elastic behaviour, cracking in one direction and crushing of concrete compressive struts (path 3 and 4).
3. Elastic behaviour, cracking in one direction and cracking in two perpendicular directions (path 2).

The adopted failure criterion is modified to serve as the transition criterion for defining the boundaries of the different material properties, fig.(2.3). This is accomplished by simply scaling the failure surface of Kupfer. In order to determine the boundaries of the elastic and inelastic regions, f_{c1} and f_{c2} replace f_{cu} respectively in the biaxial compression region. Through the use of these transition criteria it is possible to extend the assumed uniaxial stress-strain curve for concrete to cover biaxial stress states.

2.4 Constitutive Relations of Concrete

The main purpose of this section is to present the properties of concrete in its different states. Concrete can be elastic, inelastic, singly-cracked, doubly-cracked, or crushed. In the following discussion, the matrix of material properties, $[c]$, relates the stress vector, $\{f\}$, to the strain vector, $\{\epsilon\}$, by

$$\begin{Bmatrix} f_x \\ f_y \\ f_{xy} \end{Bmatrix} = [c] \begin{Bmatrix} \epsilon_x \\ \epsilon_y \\ \epsilon_{xy} \end{Bmatrix}$$

2.4.1 Elastic Concrete

Concrete is assumed here to act as an isotropic and homogeneous material. The incremental stress-strain relation is of the form:

$$\{f\} = \left[\frac{E_c}{(1-\nu^2)} \right] \begin{bmatrix} 1 & \nu & 0 \\ \nu & 1 & 0 \\ 0 & 0 & (1-\nu)/2 \end{bmatrix} \{\epsilon\}$$

Where

ν = Poisson's ratio for concrete

E_c = Modulus of elasticity of concrete

2.4.2 Inelastic Concrete

The constitutive relationship will be quite similar to that in section 2.4.1, except that the tangent modulus E_{c1} or E_{c2} should be used instead of the modulus of elasticity, E_c . The selection of the tangent modulus to be used in the constitutive relationship should be done according to the transition criteria, fig.(2.3). Thus, the incremental stress-strain relation can be written as

$$\{f\} = [(E_{c1} \text{ or } E_{c2})/(1-\nu^2)] \begin{bmatrix} 1 & \nu & 0 \\ \nu & 1 & 0 \\ 0 & 0 & (1-\nu)/2 \end{bmatrix} \{\epsilon\}$$

It is to be mentioned that, according to experimental evidence, poisson's ratio can be reasonably assumed constant up to 80 percent of the ultimate load, but after this point it starts to deviate. However, there is no dependable body of experimental data for such a deviation, especially for the biaxial state of stresses. Therefore, it is assumed in this study that poisson's ratio is constant in the elastic and the inelastic stage^(25,26,34,39,48,60,61)

2.4.3 Singly-cracked concrete

When a principal tensile stress exceeds its limiting value, according to the adopted cracking criterion, a crack

is assumed to occur in a plane normal to the direction of the tensile principal stress. This is in accordance with the experimental work of Kupfer⁽³⁶⁾. The crack direction is then fixed for all subsequent loading. In this context, a crack is not discrete but implies an infinite number of parallel fissures across the element

Once a crack has formed, it is assumed that tensile stresses cannot be supported perpendicular to the crack and the stiffness of the material is reduced to a negligible value in this direction. However, material parallel to the crack is still capable of carrying stress according to the uniaxial conditions prevailing parallel to the crack.

The assumed material properties matrix for concrete with a crack oriented at an angle θ counter-clockwise from the x-axis is,

$$[c] = [T^{-1}] \begin{bmatrix} E & 0 & 0 \\ 0 & 0 & 0 \\ 0 & 0 & \beta E/2(1+\nu) \end{bmatrix} [T^{-1}]^T \quad (2.1)$$

Where

E = Tangent modulus of concrete according to the level of loading.

β = A factor to account for aggregate interlock and any doweling action that may be present. It provides the shear-strength capacity of the cracked concrete

and it is called the shear-retention factor.

$[T]$ = The transformation matrix to go from the θ -direction coordinate system to the x and y coordinate system.

Its inverse is,

$$[T^{-1}] = \begin{bmatrix} \cos^2 \theta & \sin^2 \theta & -2 \cos \theta \sin \theta \\ \sin^2 \theta & \cos^2 \theta & 2 \cos \theta \sin \theta \\ \cos \theta \sin \theta & -\cos \theta \sin \theta & \cos^2 \theta - \sin^2 \theta \end{bmatrix}$$

A few remarks are in order regarding the shear retention factor, β , used here. To omit this effect altogether implies that cracked concrete would behave as a bundle of uniaxial fibres capable of sustaining only a tensile or compressive load parallel to the direction of the crack. However, this is not a very realistic representation of the load carrying capacity of cracked concrete. In reality the cracks in the concrete are not smooth, but rather consist of irregular rough planes arbitrary finite distances apart. The shear retention factor, β , accounts for the aggregate interlock and any dowling action that may be present in the crack. By using this factor, a shear force is induced along the cracked planes. It is recognized that the shear strength along the crack is a function of the crack-width, among other factors, and would have an upper and a lower bound of one and zero, respectively, relative to the uncracked

shear strength capacity. In the present study, the value of β was arbitrary selected as 0.5 because it was found^(25,61) that the shear retention factor only slightly affects the behaviour of reinforced concrete slabs.

The incremental stress-strain relationship for a singly-cracked concrete can be written as

$$\{f\} = [c] \{\epsilon\}$$

Where the constitutive matrix, $[c]$, can be determined from eqn.(2.1).

2.4.4 Doubly Cracked Concrete

Concrete is assumed to crack a second time when singly cracked concrete develops a tensile stress in excess of the tensile strength capacity. This set of cracks is assumed to develop perpendicular to the first crack and, although theoretically a doubly cracked layer could still transmit some shear stresses, it is assumed here that doubly cracked concrete has no shear stiffness left. The incremental, as well as the total stresses vanish for any additional applied load increment. The material properties matrix is

$$[c] = \begin{bmatrix} 0 & 0 & 0 \\ 0 & 0 & 0 \\ 0 & 0 & 0 \end{bmatrix}$$

2.4.5 Crushed Concrete

Crushed concrete is assumed unable to support any load, which will imply a zero stiffness. Thus, the material properties matrix can be written as

$$[c] = \begin{bmatrix} 0 & 0 & 0 \\ 0 & 0 & 0 \\ 0 & 0 & 0 \end{bmatrix}$$

For any crushed layer, it is again assumed that there is no stiffness left after crushing, and hence, incremental stresses as well as total stresses vanish for any applied load increment.

2.5 Constitutive Relations of the Steel Reinforcement

In the present approach, the reinforcing steel is replaced by an equivalent smeared steel layer with stiffness only in the direction of the reinforcement. The equivalent thickness of the steel layer is determined such that the corresponding cross-sectional area of the reinforcement in the layer remains unchanged. Generally, the slab in a composite beam is reinforced by at least two sets of steel bars: transverse reinforcement and longitudinal reinforcement running parallel to the steel beam. Perfect bond is assumed to exist between the reinforcing steel and the surrounding concrete.

The material properties matrix for the transverse steel reinforcement running in the x-direction, in the elastic region, can be written as

$$[c] = \begin{bmatrix} E_s & 0 & 0 \\ 0 & 0 & 0 \\ 0 & 0 & 0 \end{bmatrix} \quad (2.2)$$

where E_s is the modulus of elasticity of the steel

Similarly, the material properties matrix for the longitudinal reinforcement running in the y-direction, can be written as

$$[c] = \begin{bmatrix} 0 & 0 & 0 \\ 0 & E_s & 0 \\ 0 & 0 & 0 \end{bmatrix} \quad (2.3)$$

For the strain hardening region, the material properties matrix can simply be determined, for the reinforcement in the transverse and the longitudinal direction, by substituting the tangent modulus E_{s1} instead of the modulus of elasticity E_s in eqns.(2.2) and (2.3), respectively.

2.6 Constitutive Relations of the Metal Deck

It is assumed that the layers of the deck have stiffness only in the transverse direction which is perpendicular

to the steel beam; in other words, it has stiffness only in the ribbed direction, where embossments exist to provide mechanical interlock between concrete and the deck. Perfect bond is assumed between the deck and the surrounding concrete.

The material properties matrix for the metal deck, in the elastic region, can be written as

$$[c] = \begin{bmatrix} E_s & 0 & 0 \\ 0 & 0 & 0 \\ 0 & 0 & 0 \end{bmatrix}$$

In the inelastic region the material properties matrix for the metal deck can be written as

$$[c] = \begin{bmatrix} E_{s1} & 0 & 0 \\ 0 & 0 & 0 \\ 0 & 0 & 0 \end{bmatrix}$$

2.7 Constitutive Relations of the Steel Beam

The stress in the steel beam is computed on the basis of a linear distribution of strain extending to the bottom fibre of the beam, and the state of stress at the centroid of the layer is taken as the representative stress for this layer. A layer of the beam is assumed to be in a state of uniaxial stress for the consideration of yielding.

In the elastic stage, the stress-strain relation may

be written as

$$f_y = E_s \epsilon_y$$

In the inelastic stage, before the strain hardening point is reached, the incremental stress-strain relation may be written as

$$f_y = E'_{s1} \epsilon_y,$$

where E'_{s1} is taken as a very small value just for iteration purpose,

In the strain hardening stage, the incremental stress-strain relation may be written as

$$f_y = E_{s2} \epsilon_y$$

CHAPTER 3

NUMERICAL MODEL AND INCREMENTAL ANALYSIS

3.1 General

An incremental iterative solution^(25,34,39,60) technique is employed in the present approach to obtain the nonlinear response of composite beams with ribbed metal deck using the finite element formulation based on the displacement method. The solution progresses through the use of an iterative or step-by-step procedure with the nonlinearity of the problem entering through the material properties.

The following incremental analysis incorporates the layered concept^(25,34,39,56,60). This also includes the use of the transitions between the zones of the material properties discussed in Chapter 2. The layered concept requires that at any given level of load, a layer of an element is composed of material of only a single property state.

The incremental procedure will analyse the structure, generate the layer stress states, check these against the adopted transition criterion, make any necessary material property modifications, obtain any necessary correction

forces, and then reanalyse the structure.

The total load is applied incrementally, and for each load increment the overall tangent modulus stiffness matrix is modified to account for any changes in material properties. This procedure has the advantage of giving, at every stage of loading, the complete state of stress and deformation of the structure. Therefore, it is possible to predict the cracking loads in concrete, and the yielding in the steel beam and the reinforcing steel.

The incremental iterative technique is used to find the equilibrium configuration for each applied load increment. Iteration is required until the structure reaches a state of equilibrium compatible with the property state of each slab and beam layer. Once equilibrium is reached, the next load increment is applied and the process is repeated. The structural stiffness matrix must be updated at the beginning of each load increment and after each cycle within the iteration.

3.2 Numerical Model

The method of analysis used in the present study is the displacement formulation of the finite element method. An incremental, iterative solution procedure using the tangent stiffness approach is adopted. A layered finite element approach is used to represent the variation in material properties through the depth and to account for the material

nonlinearity. The formulation of the finite element approach used in this investigation is presented in Appendix A.

3.3 Layered Concept

By introducing the layered system^(25,34,39,56,60), it is possible to have an out-of-plane variation in material properties while not suffering the consequences of going to a complete three dimensional finite element analysis. Furthermore, it is possible to retain the limited number of degrees of freedom from the two-dimensional approach while at the same time conserving the material variation with depth. The total number of degrees of freedom depends solely on the number of nodal points and not on the number of layers introduced.

The beam and slab elements are subdivided into a suitably chosen number of layers in order to describe the process of cracking and crushing in the slab and the yielding of the steel beam (Appendix A). The layered system will also allow for the consideration of the longitudinal and transverse reinforcement in the slab and the ribbed metal deck.

The stress resultants are defined separately for each layer. Thus, it is conceivable that a particular finite element employing the layered approach could contain as many different material properties as it has layers. This allows for any material property variation through the thickness of the beam or the slab.

To demonstrate the desirability of this out-of-plane variation, consider a real reinforced concrete member loaded to failure. Presumably, but most definitely at failure, a vertical section cut through the concrete member would reveal that the compression region would contain elastic, inelastic and possibly crushed concrete. Also, the tensile region would contain elastic, singly cracked and possibly doubly cracked concrete. There is also the possibility of the reinforcing steel being elastic or even in the strain hardening region. Moreover, a vertical cut through the steel beam would reveal that it would contain elastic, yielded and possibly strain-hardened layers. The influences of such variations can be achieved through the layered structure approach.

The use of the layered concept to study the inelastic behaviour of composite beams with ribbed slabs involves the use of four distinctly different sets of layers (Appendix A) as follows:

1. Plain concrete layers;

These layers could be elastic, inelastic, singly-cracked, doubly-cracked or crushed concrete layers.

2. Smearred reinforcing steel layers;

These layers could be elastic or in the strain-hardening state.

3. Metal deck layers;

Metal deck is divided into two types of layers:

a. Horizontal deck layers

b. Vertical parts of the deck layers ;

These layers could be elastic or in the strain-hardening state.

4. Steel beam layers;

These layers could be elastic, yielded or in the strain-hardening state.

Thus, the layered system can trace the progressive cracking in the reinforced concrete slab and the progressive yielding of the steel beam. The occurrence of other failures and their progression is also possible. It should, however, be emphasized that, for each layer, stresses are based on an averaging concept, and thus tensile cracks or steel yielding can only be indicated relative to an area. Thus, only averaged values are being considered.

3.4 Solution Steps

The essential steps in the solution process for a typical load increment are as follows:

1. Apply a load increment and analyse the structure to obtain the nodal displacements. Then perform the following for each element i :
2. Convert the nodal displacements to reference surface strains and curvatures. Then perform the following for each layer j of element i :
3. Convert the reference surface strains and curvatures

- to layer strains.
4. Determine the layer stresses using the previous material properties for each layer.
 5. Check the layer stress state against the applicable transition criterion. If none of the transition zones are exceeded, go to step 8.
 6. Calculate the excess amount of stress present in layer j and convert it to the excess amount of resultants.
 7. If more unprocessed layers of element i exist, repeat steps 3 through 6. If not, go to the next step.
 8. If no transition criteria were exceeded for the i^{th} element, go to step 10. Otherwise, convert the excess stress resultants into excess element nodal forces and put these forces in the excess force vector.
 9. If the structural stiffness matrix is to be changed, update the element stiffness matrix so that it will yield a new system stiffness matrix with the new material properties.
 10. If all elements have not been checked repeat steps 2 through 9. Otherwise, reanalyse the structure using the excess force vector.
 11. Check the displacements from step 10 for convergence. The iterations about a load increment are assumed

to have converged when all the displacements due to the correction forces are small compared to all corresponding incremental displacements caused by the last load increment. The system is assumed to have converged when no more than ± 5 percent change occurs in any quantity. If displacements from step 10 have not converged, repeat steps 2 through 11 until convergence is obtained or until the maximum number of allowed iterations about a load increment have been completed. In the examples processed in this work, four was the maximum number of allowed iterations about a load increment. If this specified number of iterations is exhausted without convergence, a smaller load increment would be necessary. Generally, relatively small increments lead to a faster convergence and less computational time.

3.5 Boundary Conditions

All nodal degrees of freedom are considered at the reference surface used in defining the element stiffness matrix. Accordingly, boundary conditions are also specified at the same reference surface.

In the study of intermediate simply supported composite beams, for the effective width and longitudinal cracking investigations, one beam is analysed using a slab width equal to the centreline to centreline spacing between the

beams, b. The edges of the slab are assumed to have zero slope, θ_y , and zero in-plane displacement in the x-direction, u , as shown in fig(3.1).

However, in the comparisons done with some of the available experimental results, free slab edges are considered to represent the actual conditions in the laboratory tests.

3.6 Computer Program

A computer program has been developed to implement the method described in this work. This program is capable of handling reinforced concrete slabs and beams, and composite beams with solid and ribbed reinforced concrete slabs under any type of loading. The program can be used to trace the entire load-deformation response of composite beams with ribbed metal decks through the elastic and inelastic stages up to the ultimate load. It can provide a complete listing of stress and strain states in the concrete, the steel reinforcement, the metal deck and the steel beam at any stage of loading of the structure's response history.

The program is coded in Fortran IV language and has been developed and tested on a CDC 6400 computer at McMaster University, Hamilton, Ontario. A full description of the computer program with the details of the notations used are presented in Appendix B.

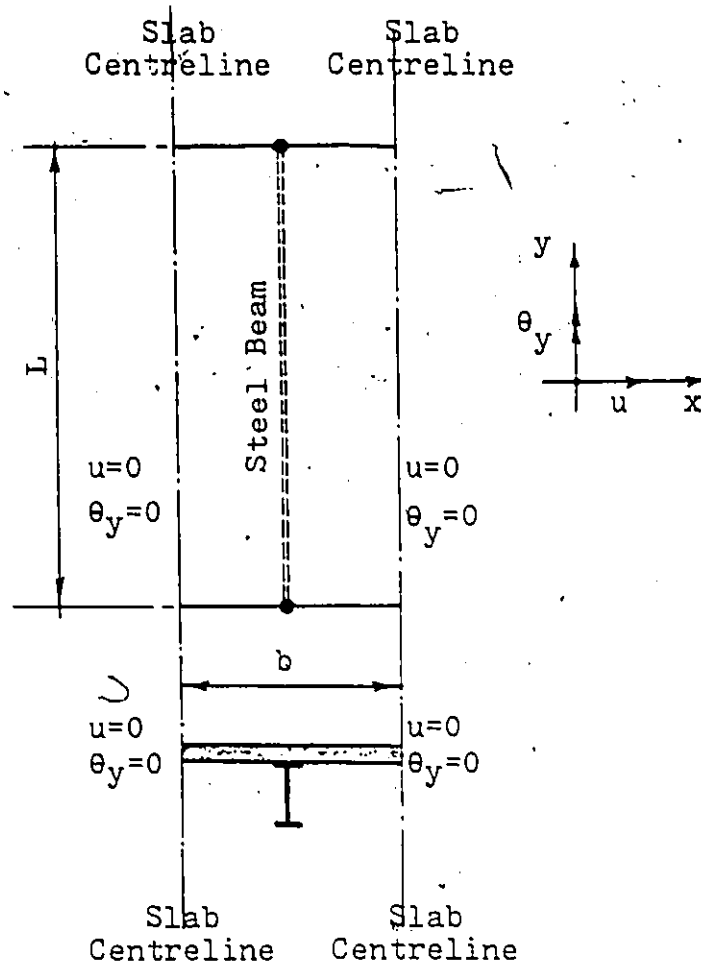


Fig.(3.1) Intermediate Composite Beam with the Assumed Boundary Conditions

CHAPTER 4

NUMERICAL EXAMPLES

4.1 General

To demonstrate the applicability and flexibility of the proposed analysis, a series of numerical examples are presented. The examples are presented in a sequence of increasing complexity; plates then composite beams with solid and ribbed slabs. The purpose of these numerical examples is to check the validity of the material idealizations and the structural model and to demonstrate the applicability of the proposed model to different types of loading.

The plate examples considered are of two types : theoretical and experimental. The theoretical plate ⁽⁵⁷⁾ example is for comparison of the theoretical and computational procedures in the elastic stage. The experimental slab of Jofreit and McNiece ⁽³⁰⁾ is analysed to demonstrate the applicability of the model in the inelastic stage.

The numerical results obtained from the analyses of composite beams with solid and ribbed slabs are compared with the available experimental data ^(10,22,28,50). Comparison

is made with one of the composite beams with solid concrete slabs tested by Barnard⁽¹⁰⁾. For composite beams with ribbed slabs, six experimental beams^(22,28,50) have been selected to test the validity of the analytical model.

Finally, a numerical example is presented to study the effect of the type of loading on the inelastic behaviour of composite beams with ribbed metal decks.

4.2 Centrally Loaded Rectangular Plate

To demonstrate the applicability of the numerical analysis in the elastic stage, a rectangular plate fixed at all of its edges is analysed under a central point load, fig.(4.1).

Table (4.1) shows a comparison between the theoretical maximum central deflection⁽⁵⁷⁾ and the maximum central deflection computed from the layered finite element model for a rectangular plate fixed at all of its edges. The percentage difference between the two solutions is less than two percent which can be considered to be satisfactory.

Table (4.2) shows a similar comparison but for a rectangular plate simply supported at its four edges. It shows very good agreement between the theoretical and the numerical results with a difference of less than 1.5 percent.

4.3 Jofreit and McNiece's⁽³⁰⁾ Reinforced Concrete Slab

In the test performed by Jofreit and McNiece⁽³⁰⁾,

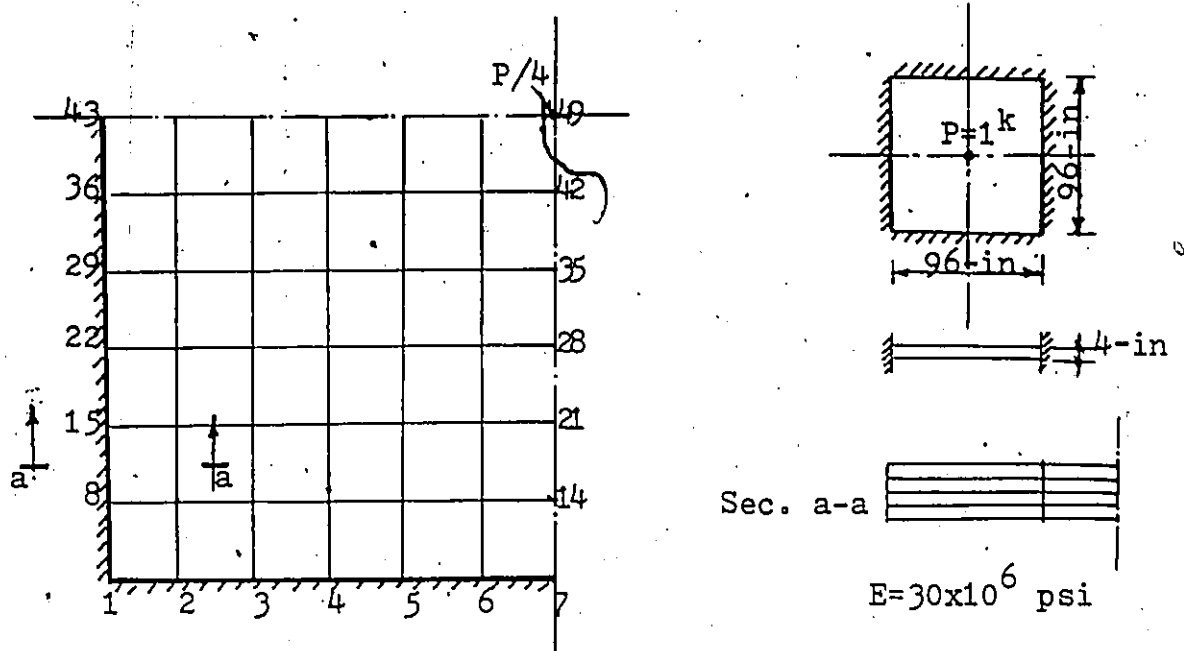


Fig.(4.1) Element Grid for a Rectangular Plate Fixed at all Edges

Maximum Deflection at Centre of Plate (in)		
Theoretical	Layered Plate Model	Percentage Difference
0.000294	0.000299	1.70

Table(4.1) Comparison of the Maximum Deflection of a Plate Fixed at all its Edges

a square corner supported two-way slab was considered, fig.(4.2). The concrete slab was reinforced with a mesh of .85 percent reinforcing steel. It was tested under a central concentrated load.

A layered finite element analysis was performed and a comparison between the experimental and the computed results are presented in fig.(4.3). The finite element grid used with the different layers of the slab is shown in fig.(4.2).

The main conclusion from this comparison is that the chosen analytical technique is capable of handling a reinforced concrete slab in different stages of the loading.

4.4 Barnard's Test⁽¹⁰⁾ on a Composite Beam with a Solid Slab

In the test performed by Barnard⁽¹⁰⁾, a composite beam with a solid concrete slab was loaded with a symmetrical two-point loading system over the beam length, fig.(4.4). The composite beam was simply supported over a ~~12-ft~~ span. It consisted of a W8 x 20 lb per ft steel section and a 5-in thick concrete slab with 24-in width.

A layered finite element analysis, fig.(4.5), was performed and a comparison between the experimental and the computed results is presented in fig.(4.6).

It was experimentally observed that the first flexural cracking in the bottom of the slab appeared after first yield of the steel beam. Near the ultimate load, a

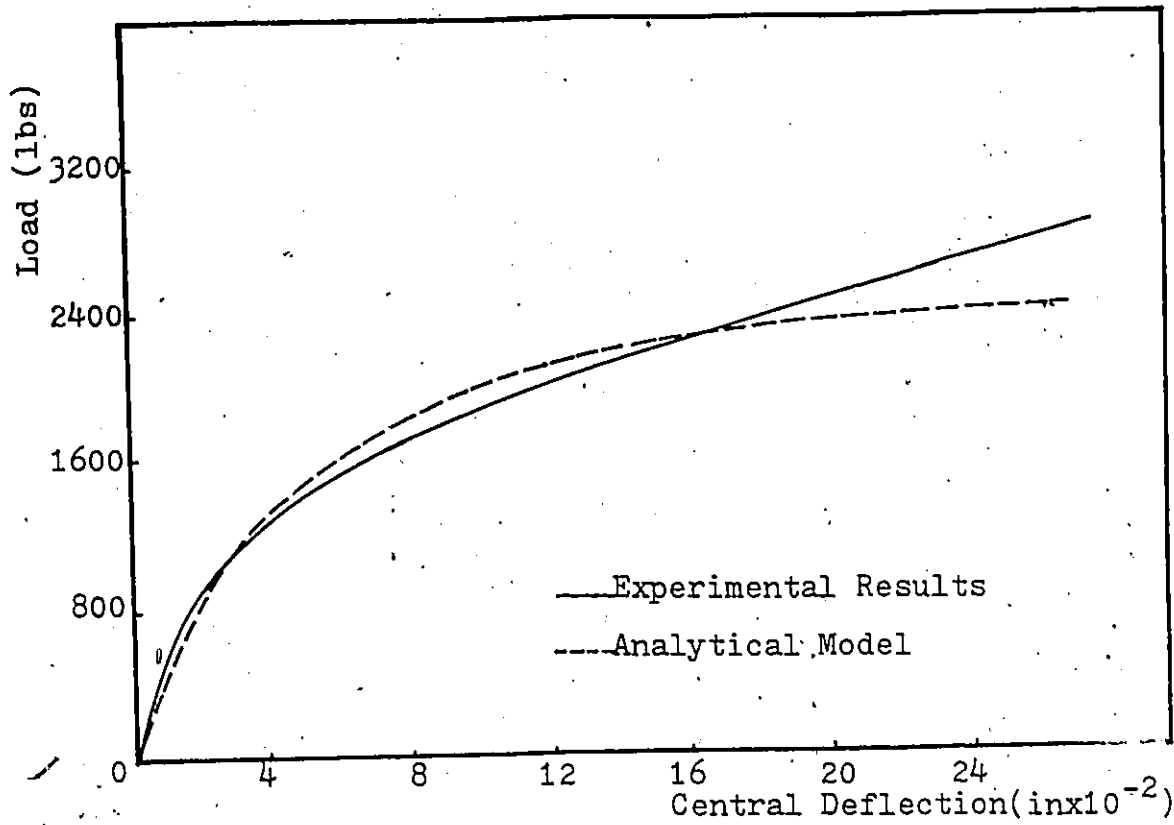


Fig.(4.3) Load-Deflection Curve of McNiece Slab⁽³⁰⁾

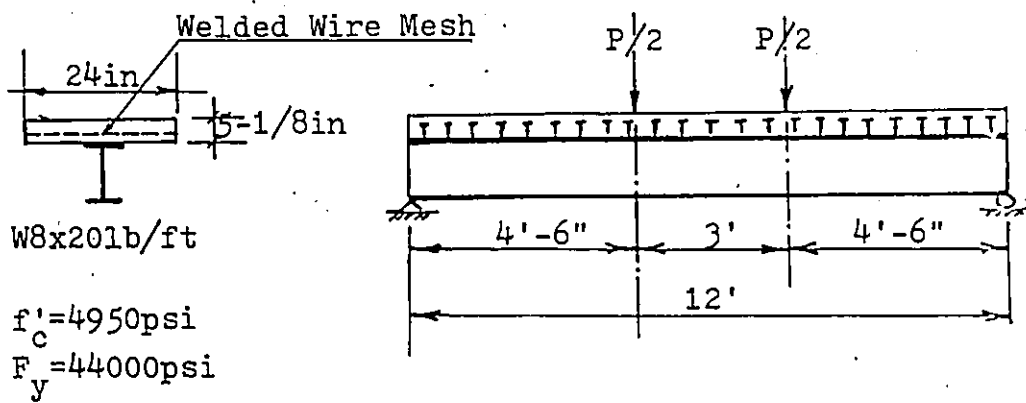


Fig.(4.4) details of Barnard's Composite Beam⁽¹⁰⁾

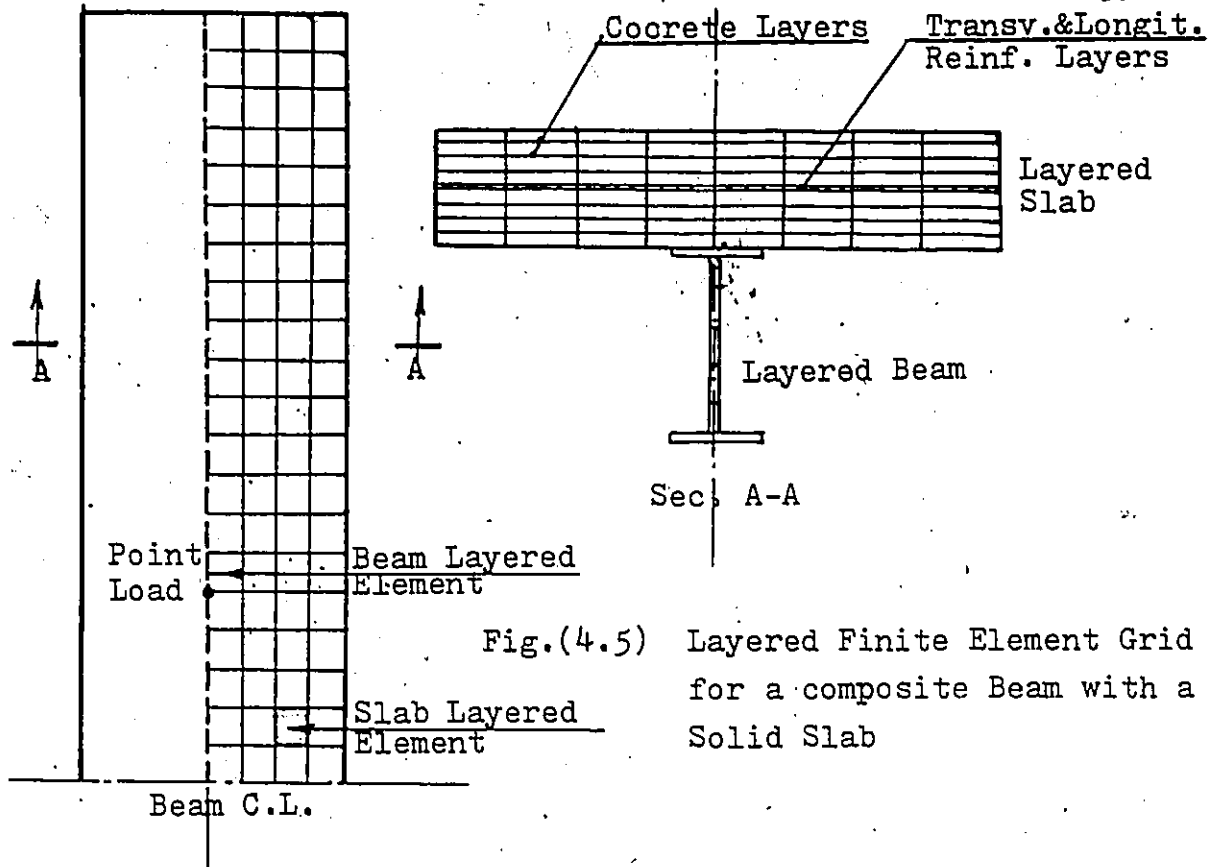


Fig.(4.5) Layered Finite Element Grid for a composite Beam with a Solid Slab

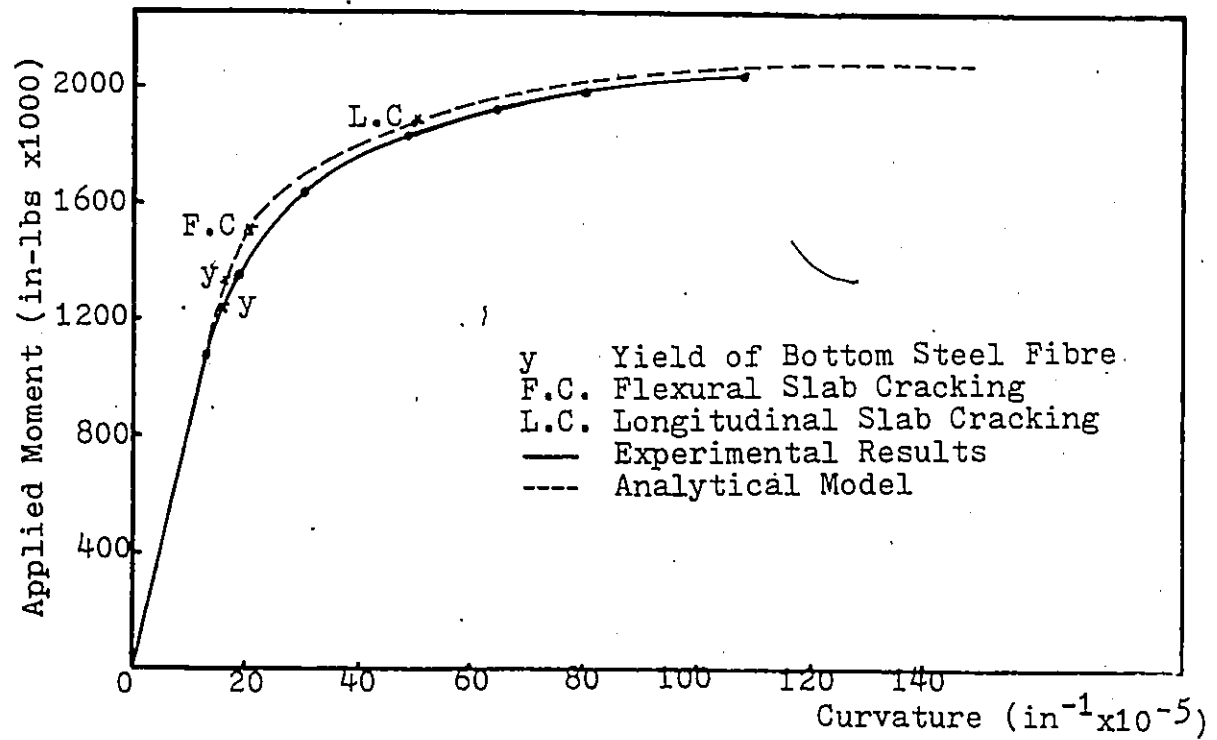


Fig.(4.6) Moment-Curvature Curve for Barnard's Beam

longitudinal crack appeared near the top of the slab. In the analytical model, the first flexural crack started at the bottom fibre of the slab near the point loads a little after the yield of the steel beam. The longitudinal crack started at the bottom fibre of the slab under the point loads at about 92 percent of the ultimate load. Then the crack extended longitudinally toward the supports and vertically through the slab depth. At the ultimate load, the crack propagation reached about 90 percent of the slab depth.

The main conclusion that can be drawn from this comparison is that the numerical technique is capable of handling a composite beam with a solid slab in the different stages of loading up to the ultimate load. The computed yield load of the steel beam and the ultimate load are in quite good agreement with the corresponding experimental results.

4.5 Robinson's and Wallace's Tests⁽⁵⁰⁾ on Composite Beams with Ribbed Metal Decks

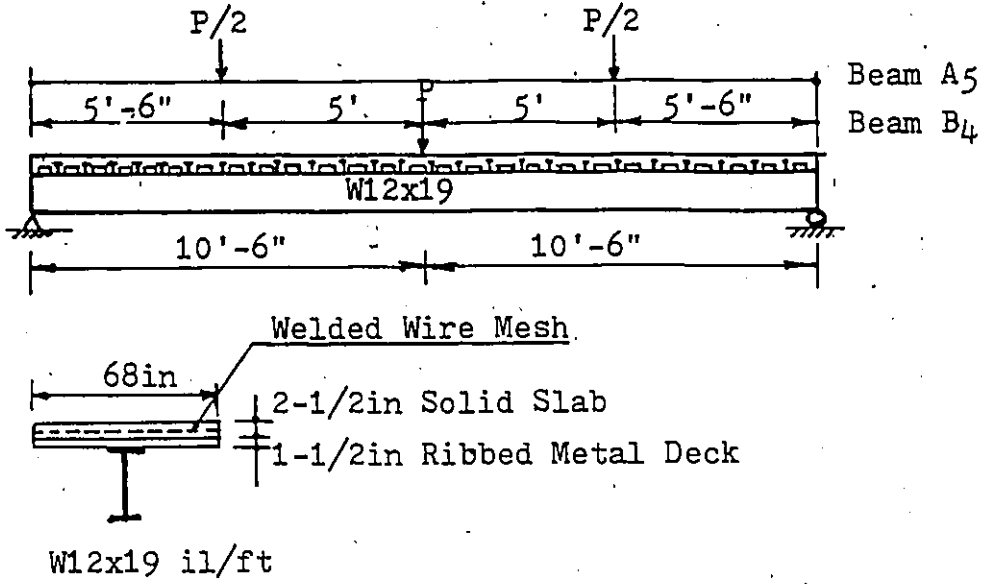
In the tests performed by Robinson and Wallace⁽⁵⁰⁾, two composite beams with ribbed slabs were loaded at two points 5-ft either side of the centreline and at one point at mid-span of the beam, respectively, fig.(4.7). The composite beams were simply supported over a 21-ft span. They consisted of W12 x 19 lb per ft steel sections and 4-in ribbed slabs with 68-in width. The concrete slabs had 1-1/2-in

ribbed metal deck and were reinforced with 6 x 6/10 x 10 welded wire mesh at the middle surface of the solid concrete parts.

The relationships of the moment to mid-span deflection and to the bottom steel fibre strain, as determined from the tests, are plotted up to the ultimate capacity of the composite beams, figs.(4.9,4.10 & 4.11). Also, the yield loads, the flexural cracking and longitudinal cracking loads as observed in the tests are shown on these diagrams.

A layered finite element analysis, fig.(4.8), was performed and comparisons between the experimental and the computed results are presented in figs.(4.9,4.10 & 4.11). It is shown that an excellent agreement was achieved in the elastic stage. The predictions of the yield loads, the longitudinal cracking load, the flexural cracking loads and the ultimate loads using the finite element model are quite satisfactory. However, it is worthwhile mentioning that the model is not capable to predict the behaviour beyond the ultimate load (the falling branch of the load-deflection curve) because the softening of concrete was not included in the idealized stress-strain curve.

It can be concluded from the comparison that the numerical method is capable of predicting the behaviour of a composite beam with a ribbed concrete slab in the different stages of loading up to the ultimate load.



Beam No.	f'_c (psi)	F_y (flange) (psi)	F_y (web) (psi)
B4	3530	42000	46000
A5	3890	40700	46300

Fig.(4.7) Details of Robinson and Wallace's(50)
Composite Beam with Ribbed Metal Deck

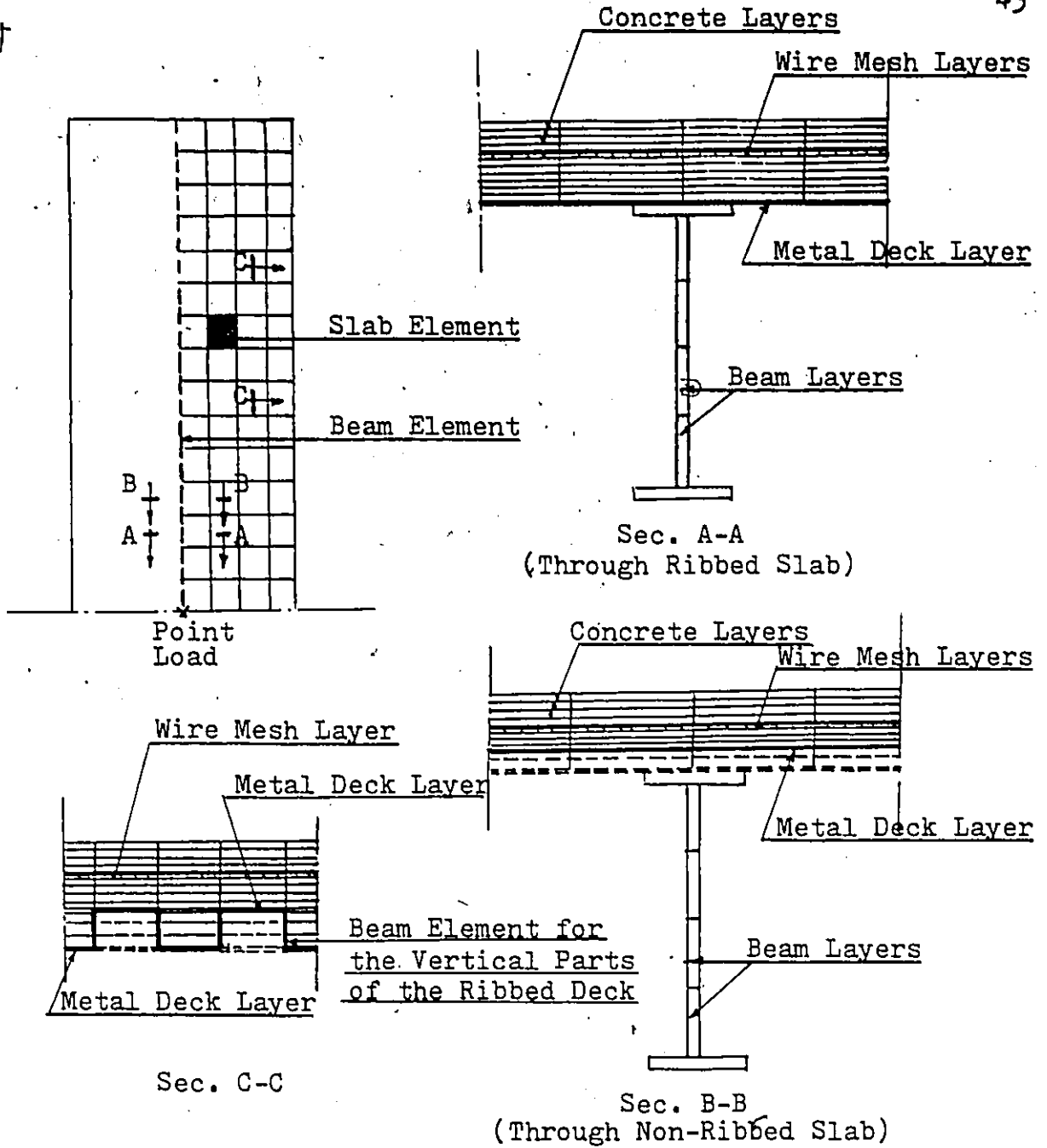


Fig.(4.8) Layered Finite Element Grid for a Composite Beam with a Ribbed Metal Deck

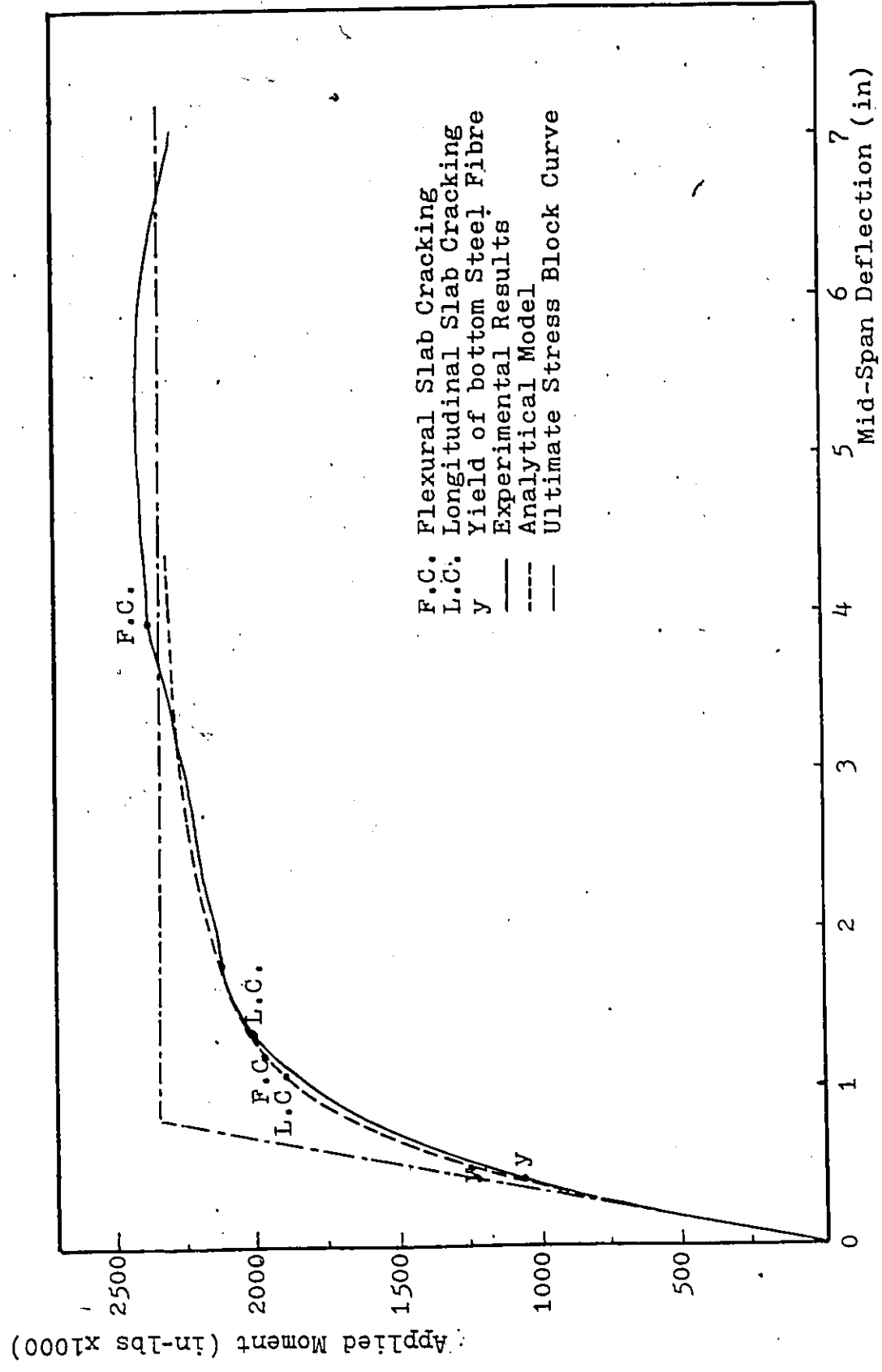


Fig.(4.9) Moment-Deflection Curve of Robinson and Wallace's (50) Beam B₄

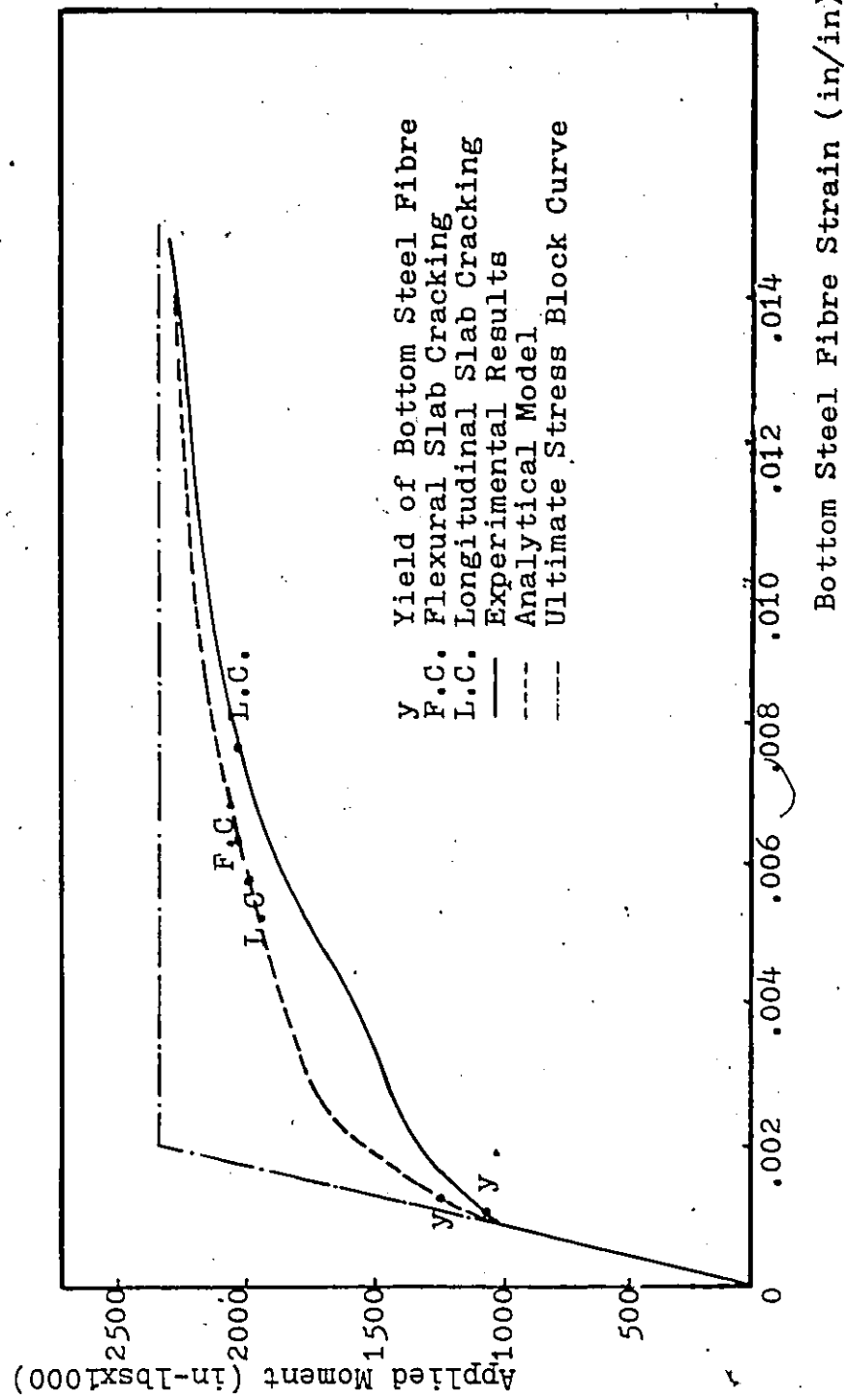


Fig.(4.10) Moment Versus Steel Bottom Fibre Strain of Robinson and Wallace's (50) Beam B₄

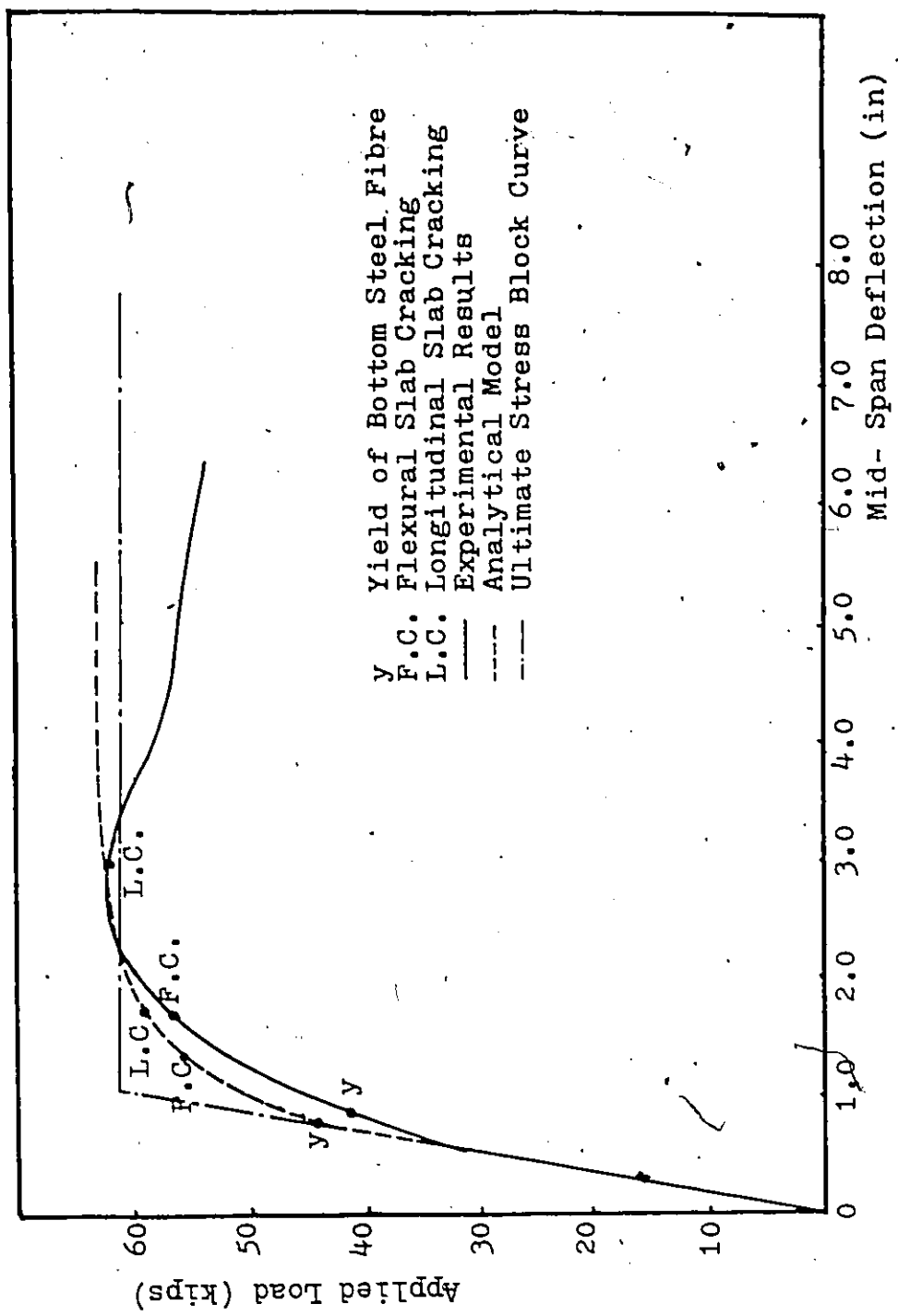


Fig.(4.11) Load-Deflection Curve of Robinson and Wallace's (50) Beam A₅

4.6 Fisher's test⁽²²⁾ on a Composite Beam with a Ribbed Metal Deck

In one of the tests performed by Fisher⁽²²⁾, a composite beam with a ribbed slab simply supported over a 15-ft span was loaded with two-transverse line loads 13-in either side of the centreline of the beam, fig.(4.12). The beam consisted of a W12 x 27 lb per ft steel section and a 5-1/2-in ribbed slab with 48-in width. The lightweight concrete slab has 3-in ribbed metal deck and is reinforced by an 8 x 8 in-grid of #4 bars placed one inch below the top of the slab.

The relationship of the load to mid-span deflection, as determined from the test, is plotted up to the ultimate capacity of the composite beam, fig.(4.13). Also, the yield load of the bottom steel flange and the ultimate load, as observed in the tests, are shown in this figure.

A layered finite element analysis was performed considering two-uniformly distributed transverse line loads 13-in either side of the centreline of the beam. A comparison between the experimental⁽²²⁾ and the computed results is presented in fig.(4.13). It is shown that a very good agreement was achieved in the elastic stage. The predictions of the yield load and the ultimate load using the finite element model are also quite acceptable.

The comparison shows quite good agreement which demonstrates the applicability of the proposed model to predict the behaviour of composite beams with ribbed slabs. It also demonstrates the validity of the material models and the structural idealizations.

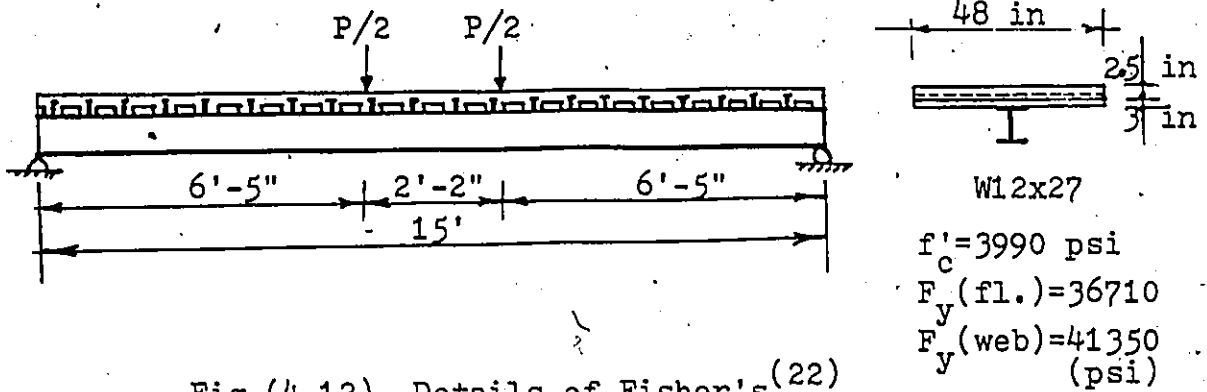


Fig.(4.12) Details of Fisher's⁽²²⁾ Composite Beam

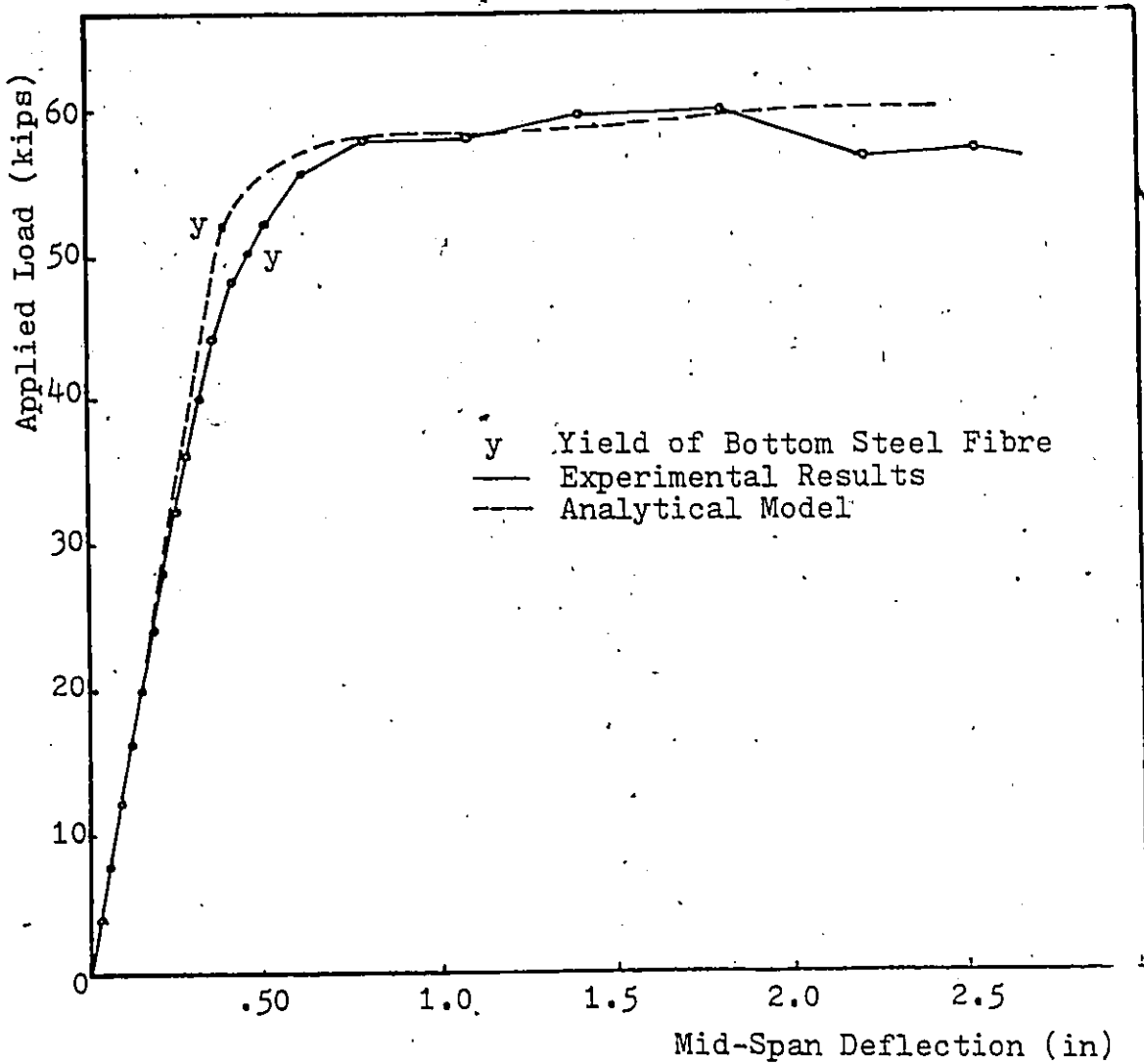


Fig.(4.13) Load-Deflection Curve of Fisher's⁽²²⁾ Beam B₄

4.7 Henderson's Tests⁽²⁸⁾ on Composite Beams with Ribbed Metal Decks

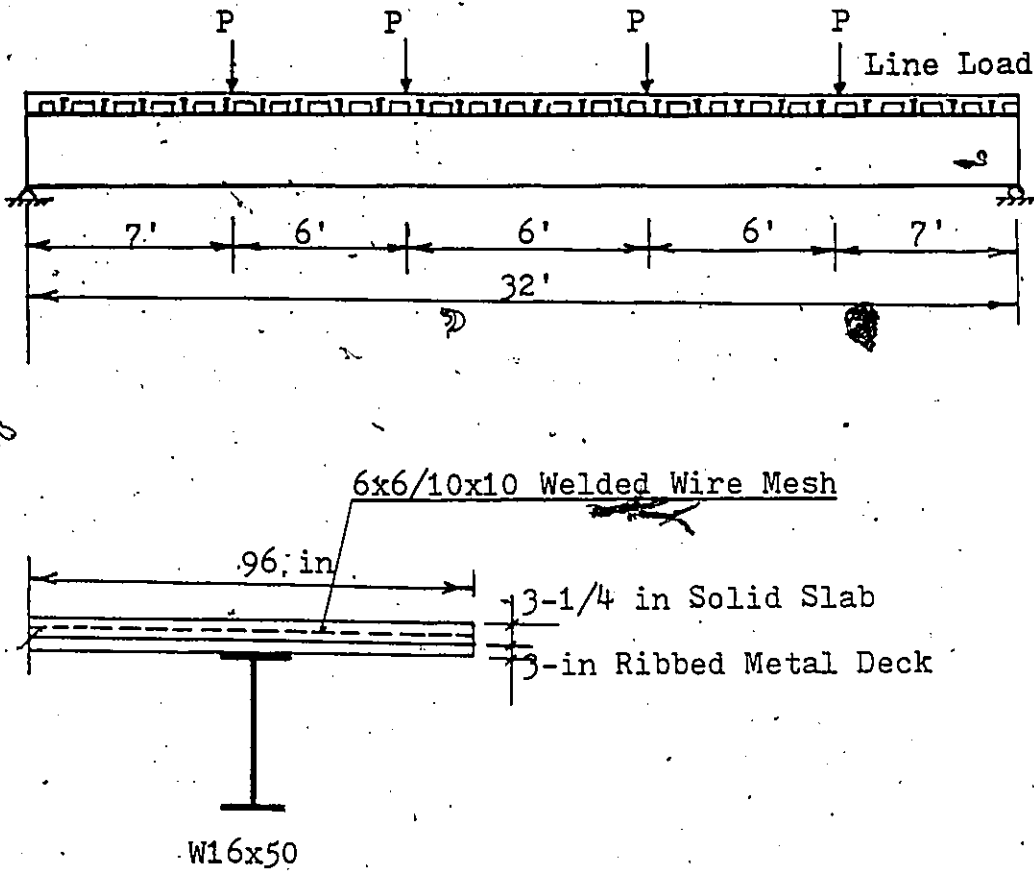
Three composite beams with ribbed slabs simply supported over a 32-ft span were tested by Henderson⁽²⁸⁾. The beams were loaded with 4-transverse line loads using 4-spreader beams, fig.(4.14). They consisted of W16 x 50 lb per ft steel sections and 6-1/4-in ribbed slab. A 3-1/4-in thick slab was cast in a 3-in ribbed metal deck. For the first two specimens, wire mesh for the slabs was placed 1-1/2-in above the deck. The wire mesh was placed 2-1/2-in above the deck for the third specimen.

A layered finite element analysis was performed considering 4-uniformly distributed transverse line loads along the beam length. Comparisons between the experimental and the computed results are presented in figs.(4.15,4.16&4.17). The comparisons show that a very good agreement was achieved in the elastic stage. The predictions of the longitudinal cracking loads and the ultimate loads using the finite element model are also quite satisfactory.

The previous comparisons, figs.(4.15,4.16&4.17), demonstrates the applicability of the proposed numerical model in following the behaviour of composite beams in the different stages of loading.

4.8 The Effect of Type of Loading and Boundary Conditions on the Behaviour of Composite Beams with Ribbed Metal Deck

A layered finite element analysis of a typical composite beam with a ribbed concrete slab is presented for three different



Beam No.	f'_c (psi)	F_y (flange) (psi)	F_y (Web) (psi)
B ₂	3855	35830	45220
B ₃	3776	35780	36740
B ₈	4046	39800	39000

Fig.(4.14) Details of Henderson's⁽²⁸⁾ Composite Beams with Ribbed Metal Deck

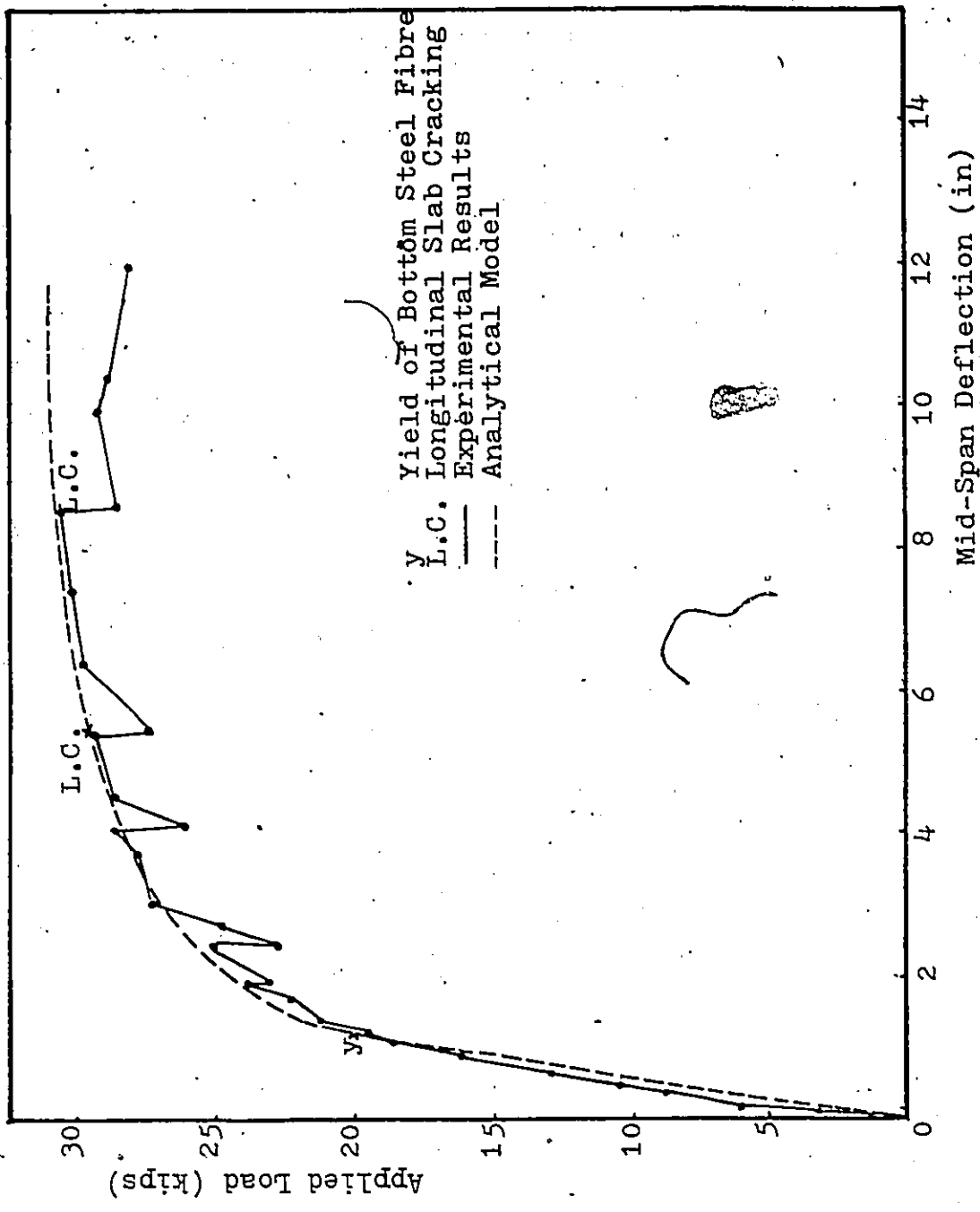


Fig.(4.15) Load-Deflection Curve of Henderson's (28) Beam B₄

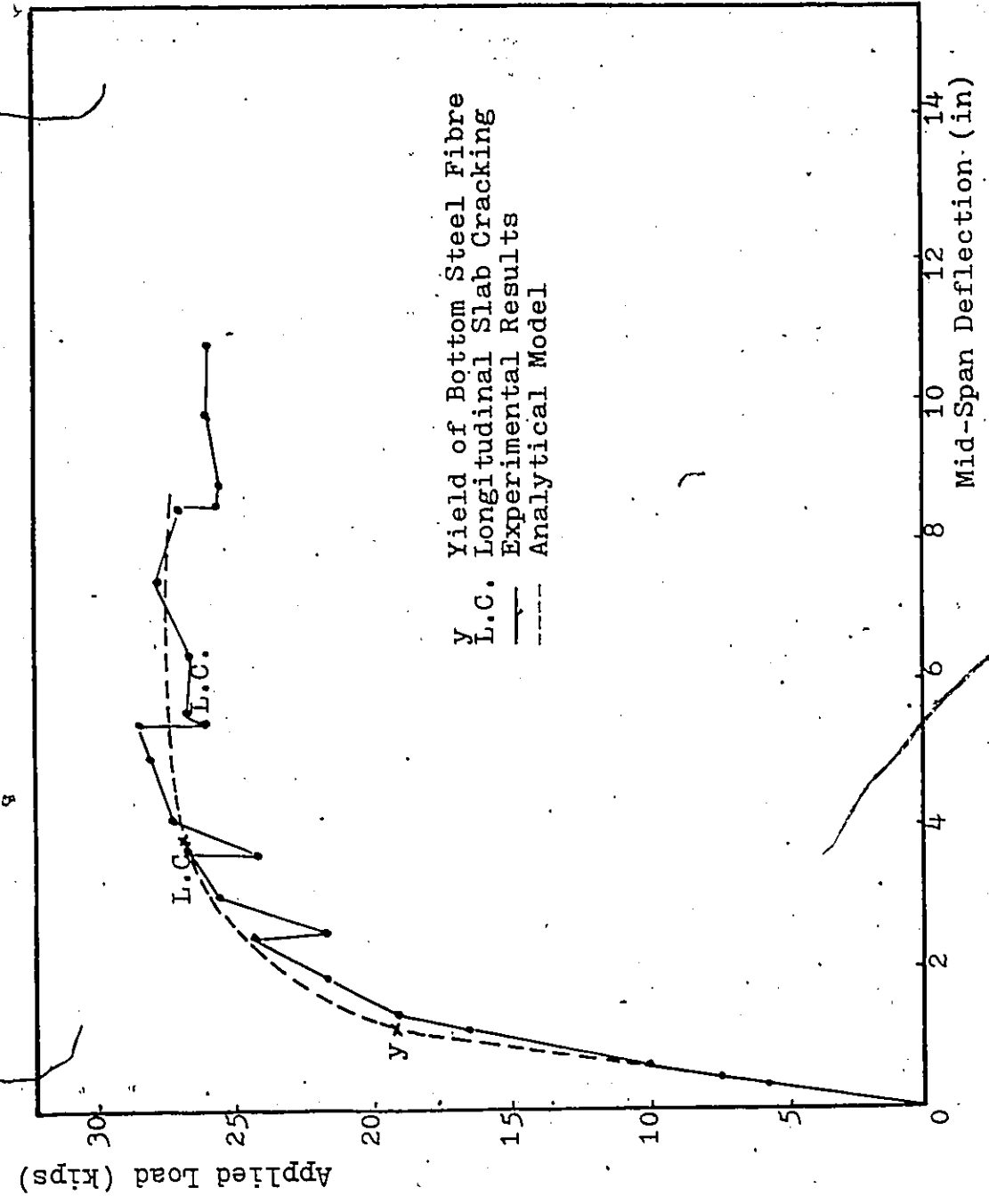


Fig.(4.16) Load-Deflection Curve of Henderson's (28) Composite Beam B₃

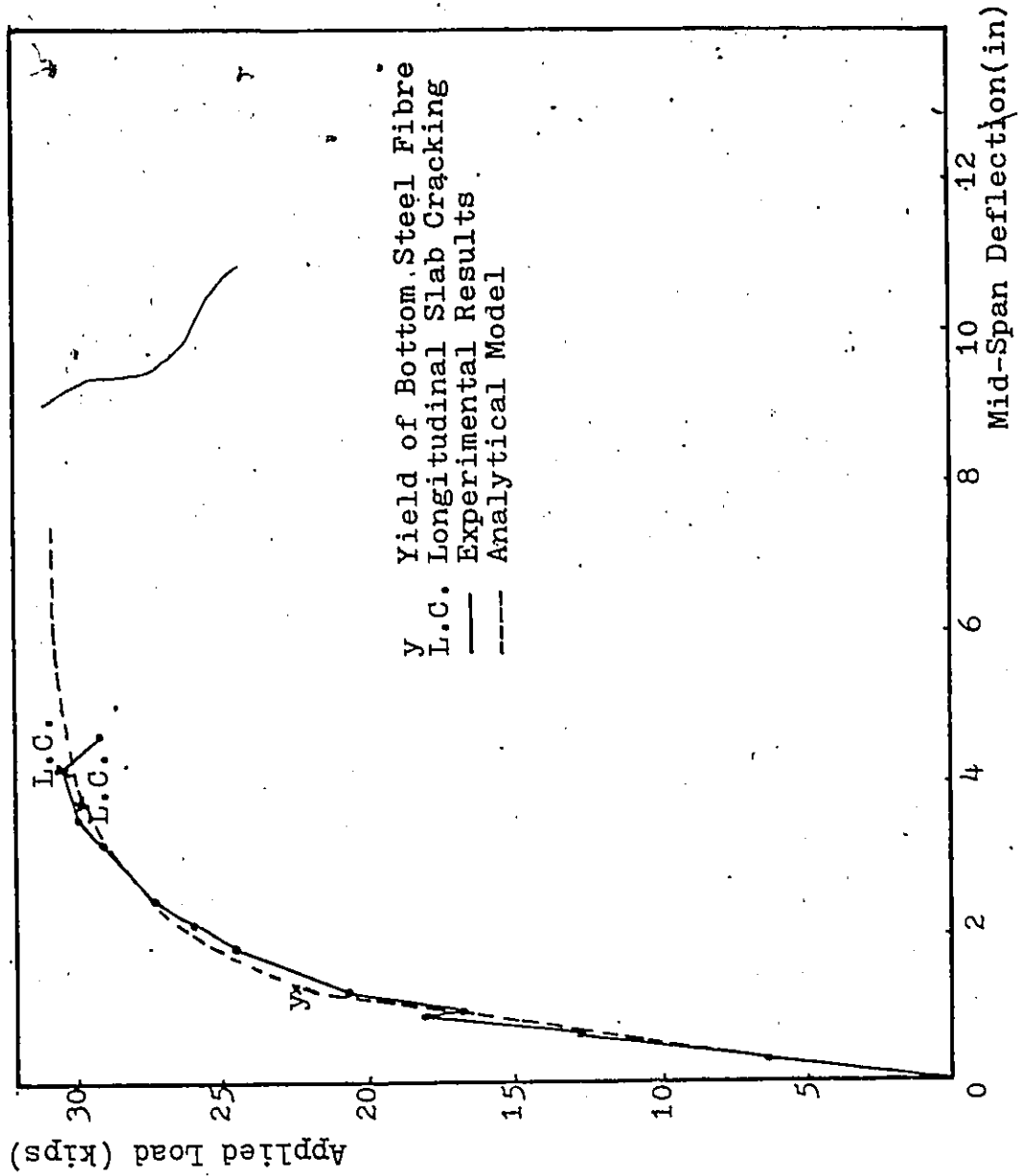


Fig.(4.17) Load-Deflection Curve of Henderson's (28) Composite Beam B8

loading conditions:

1. Uniformly distributed load over the slab area.
2. One point load at mid-span of the steel beam.
3. Two point load at $1/3$ points of the steel beam length.

Two different boundary conditions are considered for the above mentioned types of loading:

a. Zero slope, θ_y , and zero displacement, u , at the slab edges, fig.(4.18-a).

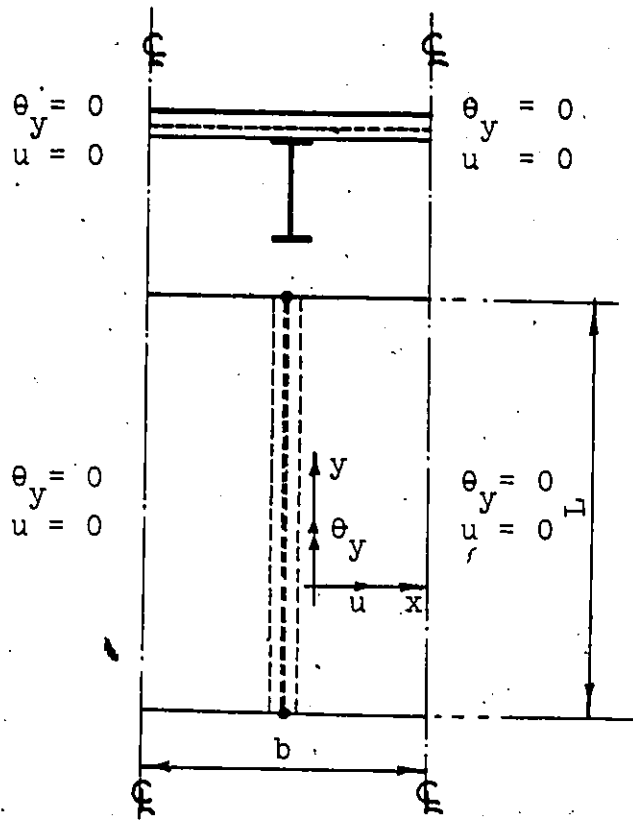
These are considered to represent the boundary conditions for an intermediate beam in a system of composite beams.

b. Free slab edges, fig.(4.18-b).

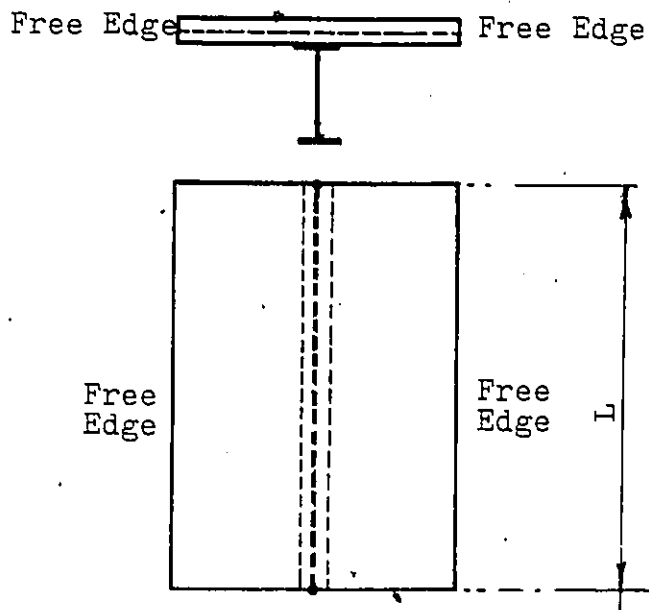
These are considered to represent the boundary conditions in a laboratory test^(10,22,28,50) on a composite beam.

Figure(4.19) shows the resulting moment-deflection curves for the different loading and boundary conditions. It shows that for the three types of loading, the composite beams have achieved almost the same ultimate moment capacity. It also shows that the moment-deflection curves for the uniformly distributed load over the slab area and for the two-point loading are almost identical. Thus, a test with two point loads performed in the laboratory can provide a legitimate appraisal of the performance of a uniformly loaded composite beam.

Figure(4.19) also shows that the effect of the boundary conditions at the edges of the slab, on the deflection and the ultimate moment capacity of a composite beam with a ribbed metal deck, is almost negligible. The percentage



a. $u = \theta_y = 0$ at the Slab Edges



b. Free Slab Edges

Fig.(4.18) Typical Composite Beam with Different Boundary Conditions

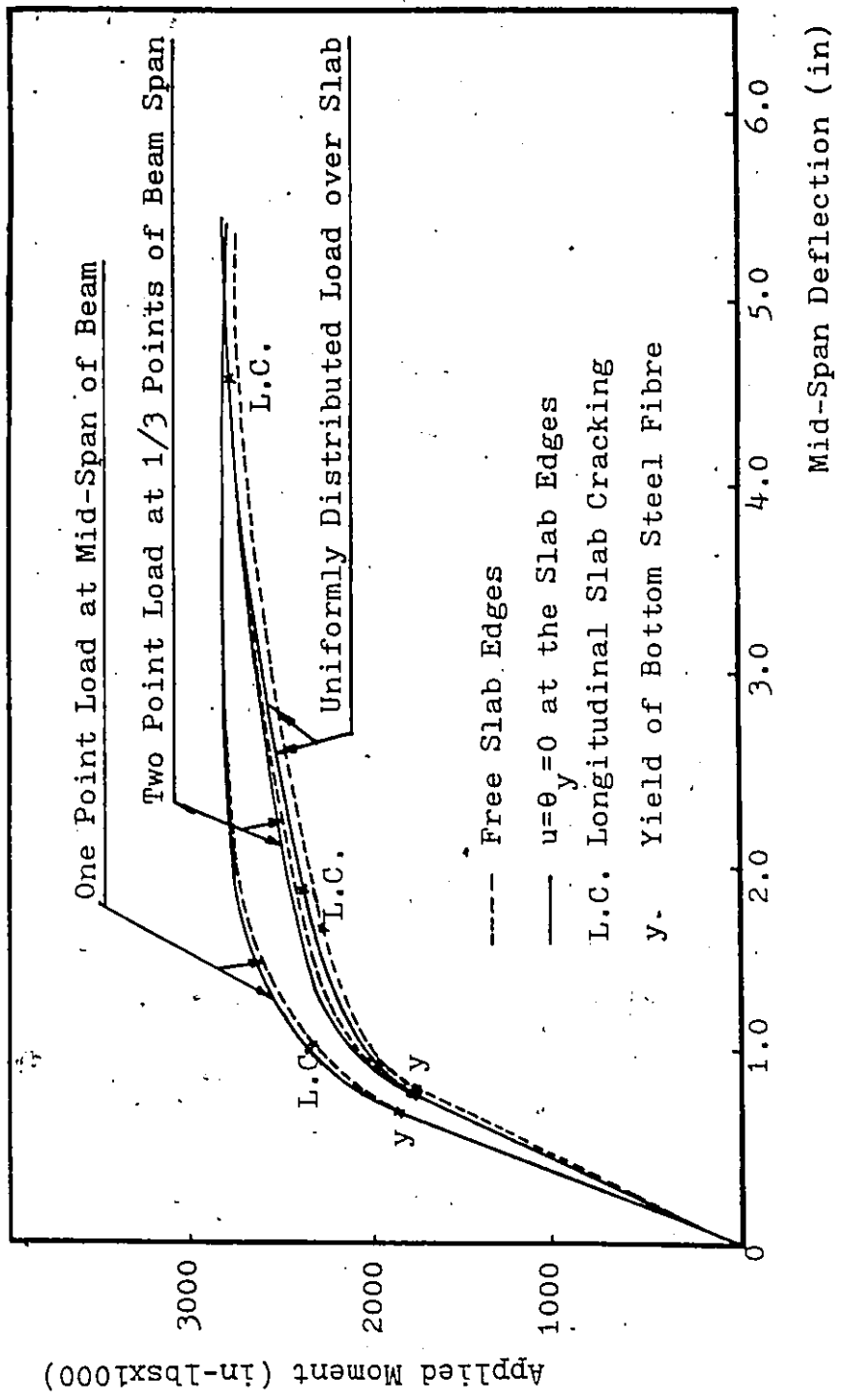


Fig.(4.19) Effect of Type of Loading and Boundary Conditions on the Behaviour of Composite Beams with Ribbed Metal Deck

difference is less than 3 percent for the point and two point cases of loading whereas it is less than 6 percent for the case of a uniformly distributed load over the entire slab. However, in all cases of loading, the beams with free slab edges show less stiffness and ultimate moment capacity than the beams with constrained boundary conditions ($\theta_y = u = 0$ at the slab edges).

Table(4.3) gives the moments at which longitudinal cracking first occurs. In the case of a uniformly distributed load over the entire slab, when considering constrained boundary conditions at the slab edges, the first longitudinal crack occurred along the top fibre of the slab over the beam and was due to transverse bending. However, in the cases of one and two point loads, longitudinal cracking started at the bottom fibre of the slab over the steel beam, near the load points, and was caused by longitudinal shear.

It may be concluded that the current method of testing composite beams with ribbed metal deck, by loading over the steel beams and considering free slab edges, gives satisfactory results with respect to the ultimate capacities of the beams and their stiffnesses. However, when it comes to the transverse stresses in the slab, as in a study of the effect of the transverse reinforcement in resisting longitudinal cracking of the slab, the type of loading has a drastic effect on the results such that it is not possible to rely on the current method of testing to predict the transverse behaviour of the slab.

Type of Loading	M_y (in-kips)	M_{Lc} (in-kips)		M_u (in-kips)
		Top Crack	Bottom Crack	
One Point Load at (free Edges or $u=0$ at Edges) (y)	1795	-----	2370	2765
Two Point Load at (Free Edges)	1750	-----	2760	2775
UDL over Slab ($u=0$ at Edges) (y)	1760	2400	-----	2780

Table(4.3) Effect of Type of Loading on the Behaviour of Composite Beams with Ribbed Metal Deck

CHAPTER 5

EFFECTIVE WIDTH OF COMPOSITE BEAMS WITH RIBBED METAL DECK

5.1 General

In a composite beam, the shear connectors restrain the concrete slab immediately above the beam so that there is a nonuniform longitudinal stress distribution across the transverse cross section of the slab. The portion of the slab directly above the steel section, which is bonded to the steel section, naturally contributes most fully to the composite action.

Thus, when the slab of a composite beam is subjected to transverse bending loads, the longitudinal stresses in the slab cannot be obtained accurately from the elementary theory of bending for the entire composite beam. Due to the shear strain in the plane of the slab, the parts of the slab remote from the steel beam lag behind the longitudinal flexural deformation of the parts near the beam. This effect, often termed shear lag^(15,46,58), causes a nonuniform stress distribution across the width of the slab, fig.(5.1).

Simple bending theory will give good approximation to the maximum stress at point D, fig.(5.1), if the true flange

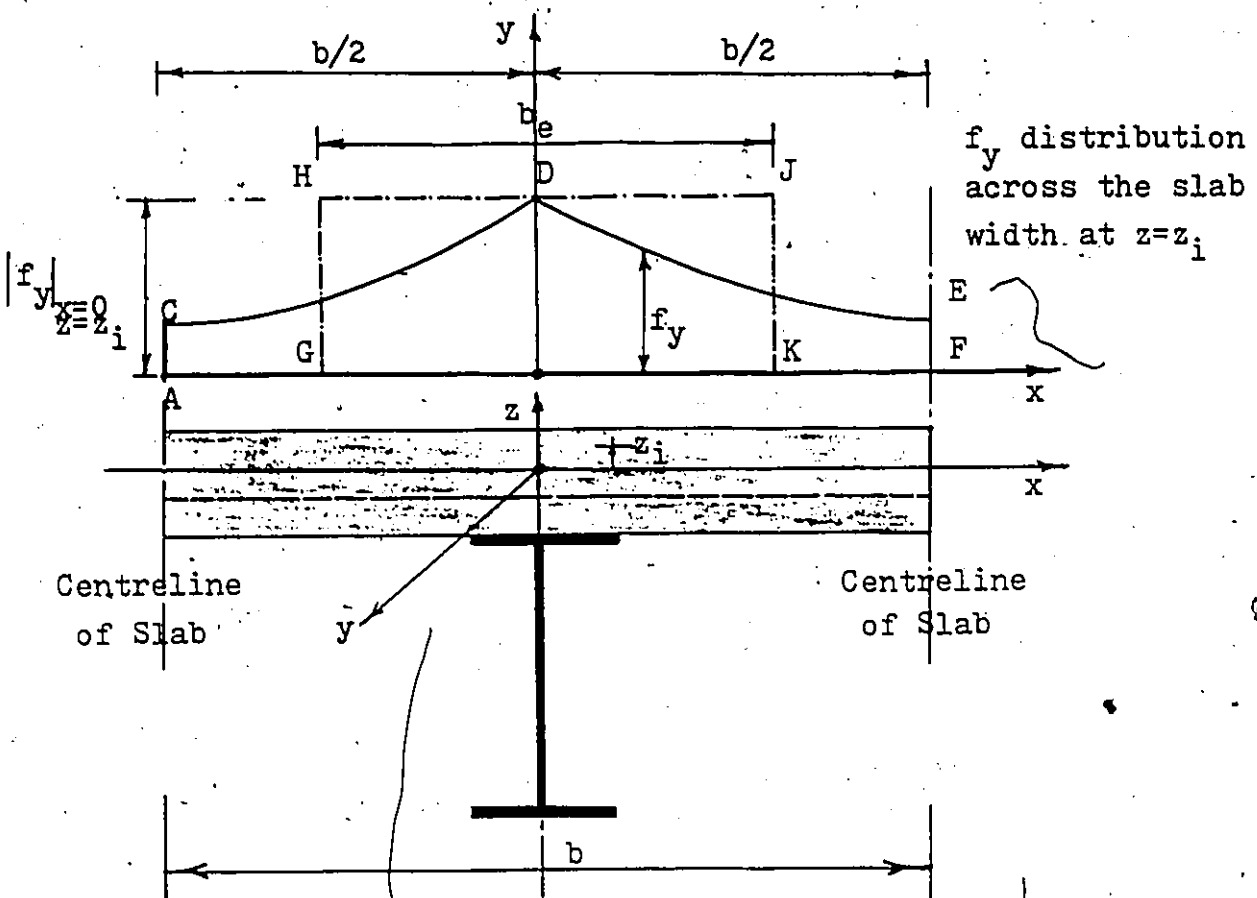


Fig.(5.1) Effective Width of Composite Beams

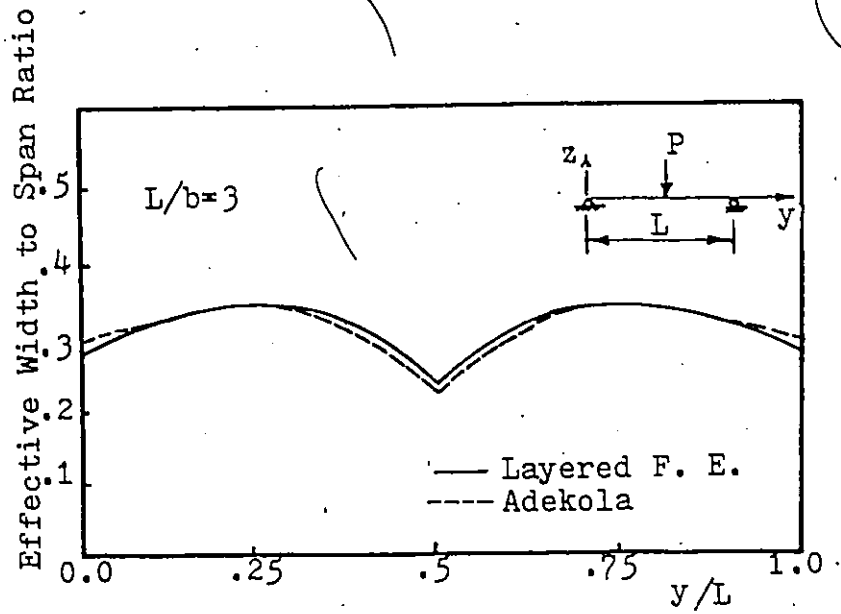


Fig.(5.2) Comparison with Adekola's⁽⁵⁾ Effective Width Distribution ($L/b=3$)

width, b , is replaced by an imaginary width, b_e , referred to as the effective width. The longitudinal stress is considered constant over the width, b_e , and equal to the maximum stress over the steel beam. Thus, the area GHJK should be equal to the area ACDEF, fig.(5.1).

Several investigators^(1,2,3,5,6,11,14,24,37,43) have studied theoretically and experimentally the effective width of composite beams in the elastic stage. Linear elastic analyses, with the properties of sections calculated for a homogeneous material, ignoring cracking, were performed to investigate the variation of the effective width with the span, the cross-sectional properties and the load distribution. Most of these investigators have presented values of effective widths for variations in some of the parameters noted above. However, not one of them have provided sufficient information with respect to composite beams loaded with a uniformly distributed load over the slab area, which is actually the practical type of loading specified in the code.

Little research^(21,27) has been done on the effective slab width at the ultimate capacity of the composite beams. Heins and Fan^(21,27) evaluated the effective composite slab width at ultimate load for bridges subjected to standard truck wheel loads. Cracking of concrete was not included in this analysis. One study of the effective width at ultimate load⁽³¹⁾ has concluded that it is on the safe side to use the effective width based on elastic theory even at the ultimate

state.

None of the investigations that have been done on the problem of the effective width of composite beams, have studied the effective width of a composite beam with a ribbed metal deck. All these studies were performed on composite beams with solid slabs. However, certain codes^(29,38) have established requirements for the evaluation of the effective width of composite beams, which can be used for solid or ribbed concrete slabs.

The purpose of the work described in this chapter is to establish design recommendations for estimating the effective width of composite beams with ribbed slabs. The effective width is studied in the elastic and inelastic stages and at the ultimate load. Some conclusions are drawn with respect to the estimation of the effective width at the ultimate load. Cracking of concrete, effect of metal deck and steel reinforcement and the yield of the steel beam is included in the analysis. The variation of the effective width with the span to width ratio, the type of loading and the cross-sectional properties, is studied. Since the majority of governing loads considered in the design approximate to uniformly distributed loads, it was decided to study mainly the effective width ratios for uniformly distributed load over the concrete slab area.

5.2 Definition of the Effective Width

In this work, the following definitions hold:

1. The strength effective width of the concrete slab in a composite beam is that width of the slab which would sustain a force equal to the force in the actual slab at the section of maximum strength assuming the longitudinal stresses across the effective slab width are constant and equal to the stress over the centreline of the steel beam, fig.(5.1). This definition is expressed mathematically as follows:

$$b_e = \frac{\int_z \int_{-b/2}^{b/2} f_y \cdot dx \cdot dz}{\int_z |f_y|_{x=0} \cdot dz} \quad (5.1)$$

(through the slab thickness)

where f_y is the longitudinal stress at any point in the cross-section of the concrete slab..

2. An effective width ratio is the ratio of an effective width of the slab to the actual width of the slab which is the average spacing between the beams, at any cross section along the beam length (i.e. sections across the ribbed parts or the solid parts of the slab).

5.3 Comparison with Available Solutions

Simply supported composite beams with solid concrete slabs, having span to width ratios of 3 and 4, were analysed using the layered finite element model. These beams were subjected to point loads at mid-span. The distribution of the effective width to span ratio along the beam length was compared to Adekola's⁽³⁾ curves determined from his elastic analytical model, figs.(5.2 & 5.3). The values of the effective width ratios obtained at mid-span are given in table (5.1). It can be seen that the agreement between the results given is satisfactory.

5.4 Effective Width of Composite Beams with Ribbed Slabs

In this study, simply supported composite beams with 1-1/2-in. ribbed metal deck, are considered under a uniformly distributed load over the slab area. The configuration of the ribbed metal deck profile is sketched in fig.(5.6). The study is concerned with an intermediate beam in a composite floor system.

A composite beam with a concrete flange, having a width equal to the steel beam spacing, is analysed using the layered finite element technique. The boundary conditions at the edges of the slab are assumed to be of zero rotation, θ_y , and zero displacement, u , in the direction perpendicular to the beam length. These boundary conditions are assumed

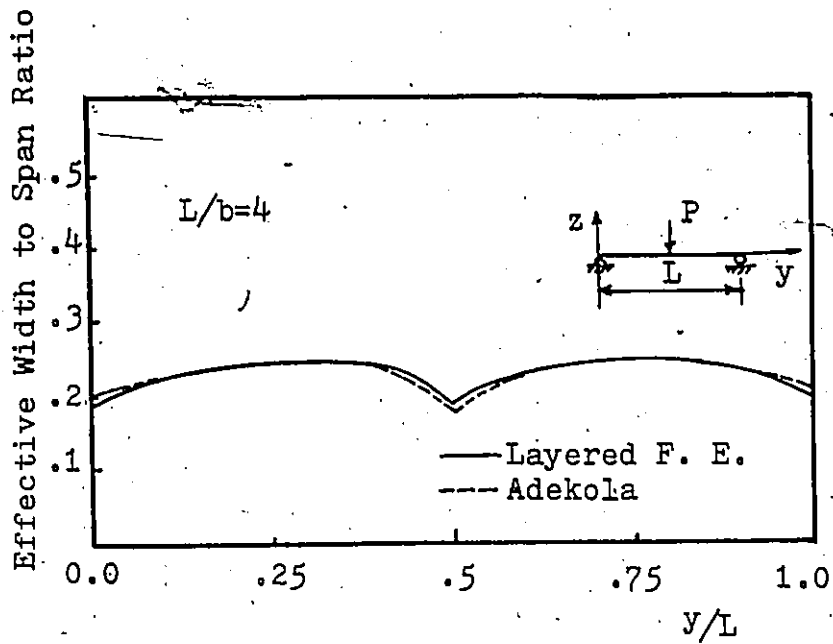


Fig.(5.3) Comparison with Adekola's⁽⁵⁾ Effective Width Distribution ($L/b=4$)

Effective Width to Width Ratio		
L/b	Adekola ⁽⁵⁾	Layered Finite Element Model
3	0.681	0.70
4	0.771	0.78

Table(5.1) Comparison with Adekola's⁽⁵⁾ Effective Width Ratios

to simulate the actual conditions for an intermediate beam in a composite floor system consisting of a large number of steel beams acting compositely with the floor slab.

Figure (5.4) and table (5.2) show the effective width to width ratio distribution along the intermediate composite beam in a 5-composite beams system and the beam analysed using the above mentioned boundary conditions. The results are in a very good agreement with a percentage difference of about one percent.

Tables(5.3&5.4) show the effect of the boundary conditions at the slab edges on the effective width ratio distribution along a composite beam with a ribbed concrete slab subjected to different loading conditions. Two different boundary conditions are considered:

- a. Free slab edges; to represent the boundary conditions in a laboratory test on a composite beam.
- b. Zero slope, θ_y , and zero displacement, u , at the slab edges; to represent the boundary conditions for an intermediate beam in a composite floor system.

Tables(5.3&5.4) show that the boundary conditions at the slab edges have a negligible effect on the effective width of composite beams with ribbed metal deck. The percentage difference is less than 2 percent when the beam is loaded with one point load at its mid-span and it is in the order of 4 percent when the slab is entirely loaded with a uniformly distributed load.

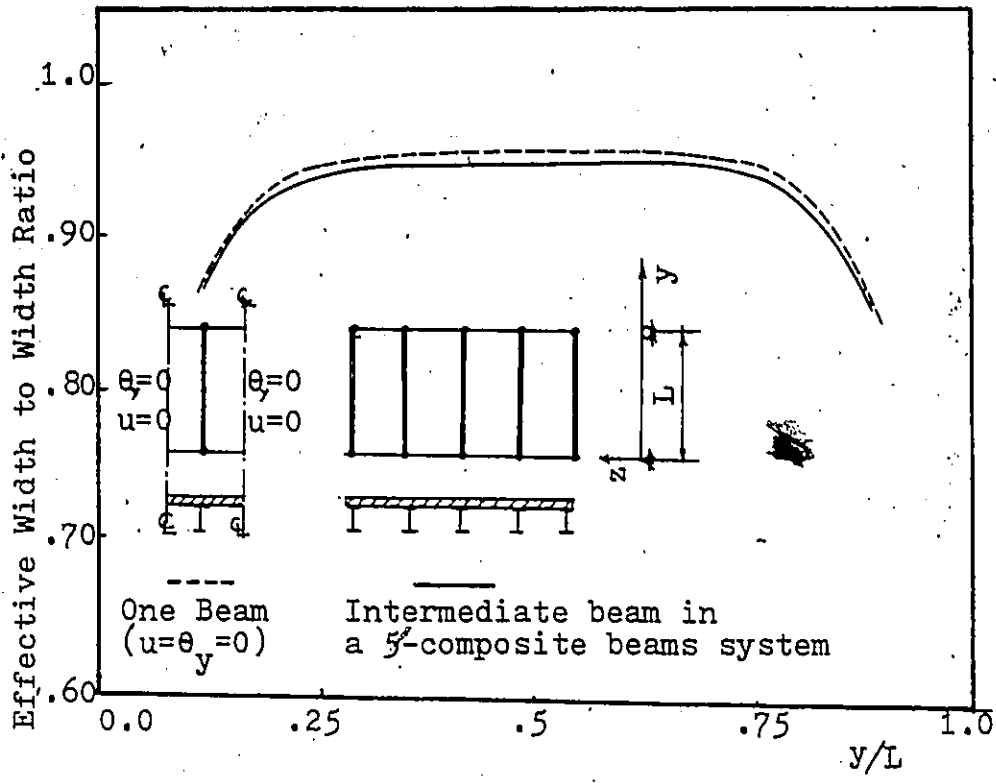


Fig.(5.4) Effective Width of an Intermediate Beam in a System of Composite Beams

y/L	0.10	0.20	0.30	0.40	0.50
One Composite Beam with Zero Slope, θ_y , and Zero Displacement u , at the Slab Edges	.840	.918	.948	.958	.961
Intermediate Beam in a System of 5-Composite Beams	.840	.918	.945	.952	.952

Table(5.2) Effective Width of an Intermediate Composite Beam

y/L	0.2	0.3	.35	.40	.45	.50
Composite Beam with Zero Slope, θ_y , and Zero Displ., u , at the Slab Edges	.98	1.0	.99	.97	.91	.76
Composite Beam with Free Slab Edges	.98	1.0	.99	.96	.90	.75

Table(5.3) Effect of Boundary Conditions on the effective Width of Composite Beams with Ribbed Metal Deck Subjected to one Point Load at the Mid-Span of the Beam ($L/b=4$)

y/L	0.2	0.3	.35	.40	.45	.50
Composite Beam with Zero Slope, θ_y , and Zero Displ., u , at the Slab Edges	.919	.953	.960	.964	.967	.967
Composite Beam with Free Slab Edges	.894	.922	.927	.930	.933	.934

Table(5.4) Effect of Boundary Conditions on the Effective Width of Composite Beams with Ribbed Metal Deck Subjected to UDL over the Slab Area($L/b=4$)

However, for the two loading conditions, the effective width ratio for the free slab edges was always smaller than that for the constrained slab edges ($u=\theta_y=0$). It may be concluded that the current method of testing composite beams, by considering free slab edges, can be used to estimate the effective slab width for a specific type of loading.

Figures (5.5 & 5.6) show the effective width ratios distribution along a composite beam with a solid and ribbed concrete slab under a uniformly distributed load over the slab area, for different beam span to slab width ratios, L/b . The solid and ribbed concrete slab are chosen to have an equal overall thickness of 4-in. The ribbed slab consists of 1-1/2-in ribbed metal deck and 2-1/2-in solid concrete part.

A study of the distribution of the effective width for different span to width ratios, shows that the effective width for any ratio is maximum at the centreline of the beam and it reduces toward the supports. It also shows that the effective width ratios could be assumed to be constant between the mid-span and the quarter-span positions especially for span to width ratios greater than 3.

Figures (5.5 & 5.6) show that the effective width increases with the increase of the span-to-width-ratios. In the case of a solid concrete slab, the effective width at mid-span is equal to the total width of the slab for span to width ratios equal to or greater than 5. However, for a ribbed slab the effective width is equal to the total width for ratios

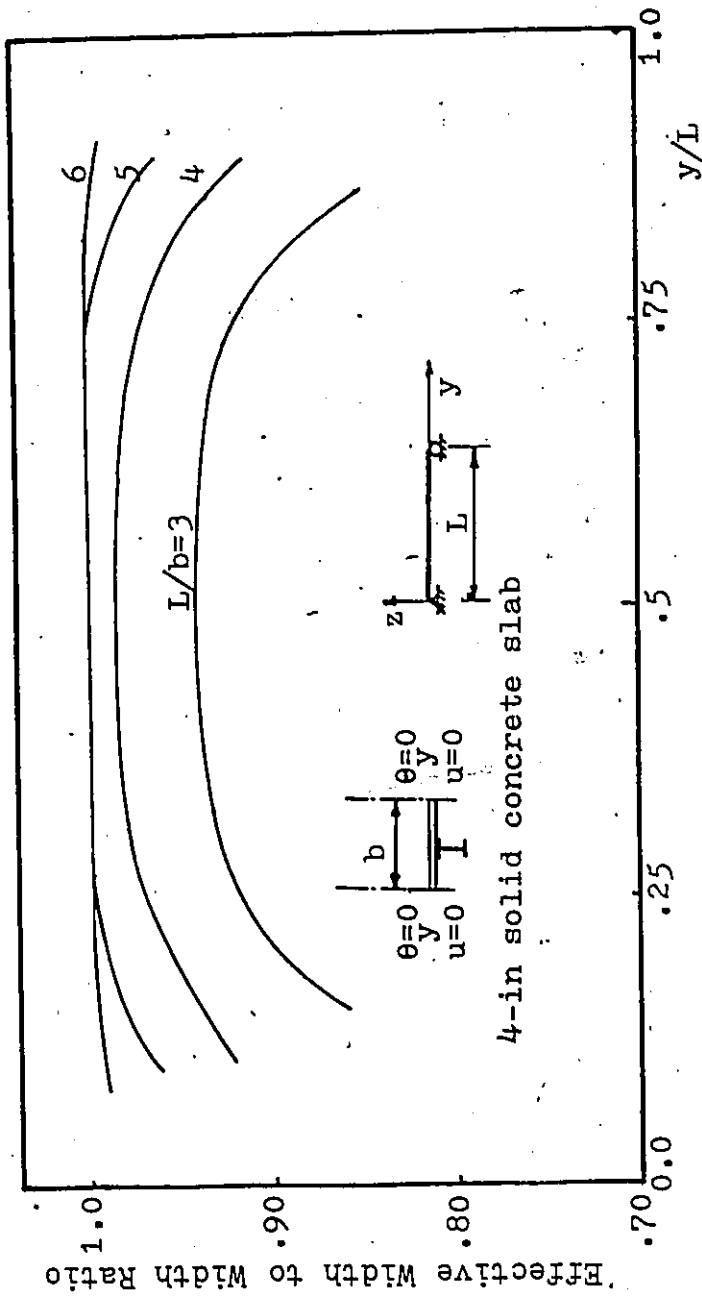


Fig.(5.5) Effective Width Ratio Distribution for a Composite Beam with a Solid Slab under a UDL over the Slab Area

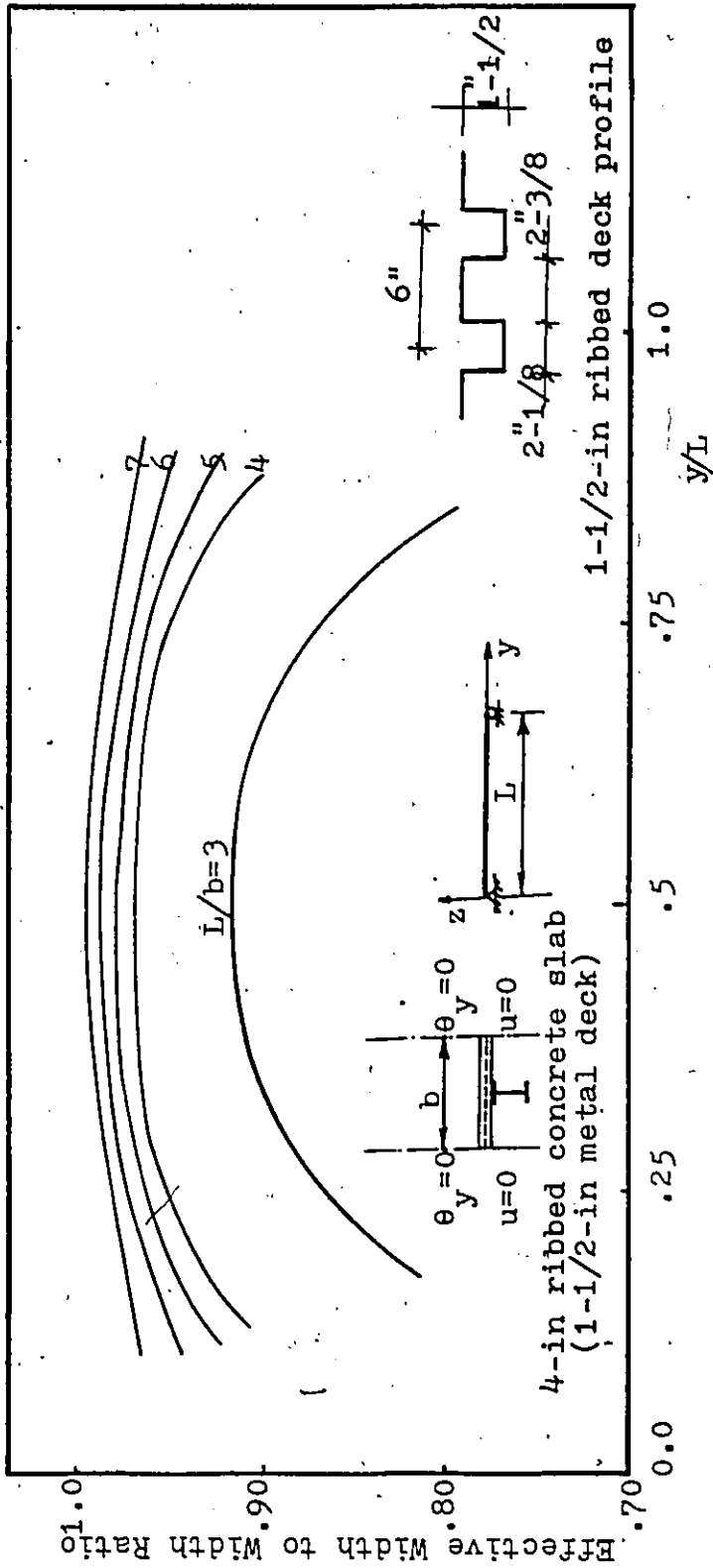


Fig.(5.6) Effective Width Ratio Distribution fo a Composite Beam with a Ribbed Metal Deck under a UDL over the Slab Area

greater than 7.50.

Figures (5.7 & 5.8) and tables (5.5 & 5.6) show a comparison of the effective width ratio distribution for a solid and a ribbed concrete slab for two different span to width ratios. This comparison shows that the percentage difference between the two cases, assuming that the overall thickness of the slab is the same, is in the order of 2 percent. It is also to be noticed that the effective width of a solid slab is always greater than that for a ribbed slab.

Table (5.7) shows that although the effective width in a composite beam with a ribbed slab is maximum at the centreline of the beam, when loaded with a uniformly distributed load over the slab area, it is still the most critical effective width when it is considered that it is the critical moment section.

5.5 Effective Width Variation with the Span to Width Ratio

Figure (5.9) shows the variation of the effective width ratio, at mid-span of the composite beam, with the span to width ratio. It shows that the effective width increases with the increase of the span to width ratio and equals the total width for ratios greater than 7.5.

Table (5.8) shows the distribution of the effective width ratio along two composite beams with different spans and slab widths, but having the same span to width ratio. It shows that the effective width to width ratio is almost constant for any specific span to width ratio.

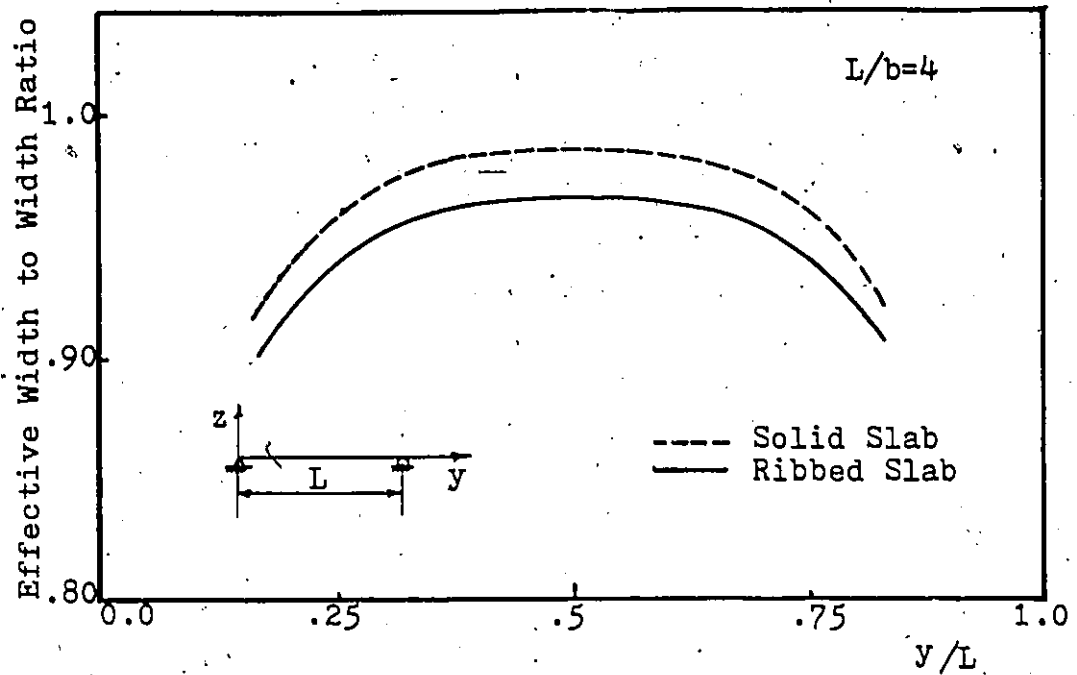


Fig.(5.7) Effective Width Ratio Distribution of a Solid and Ribbed Slab under UDL over Slab

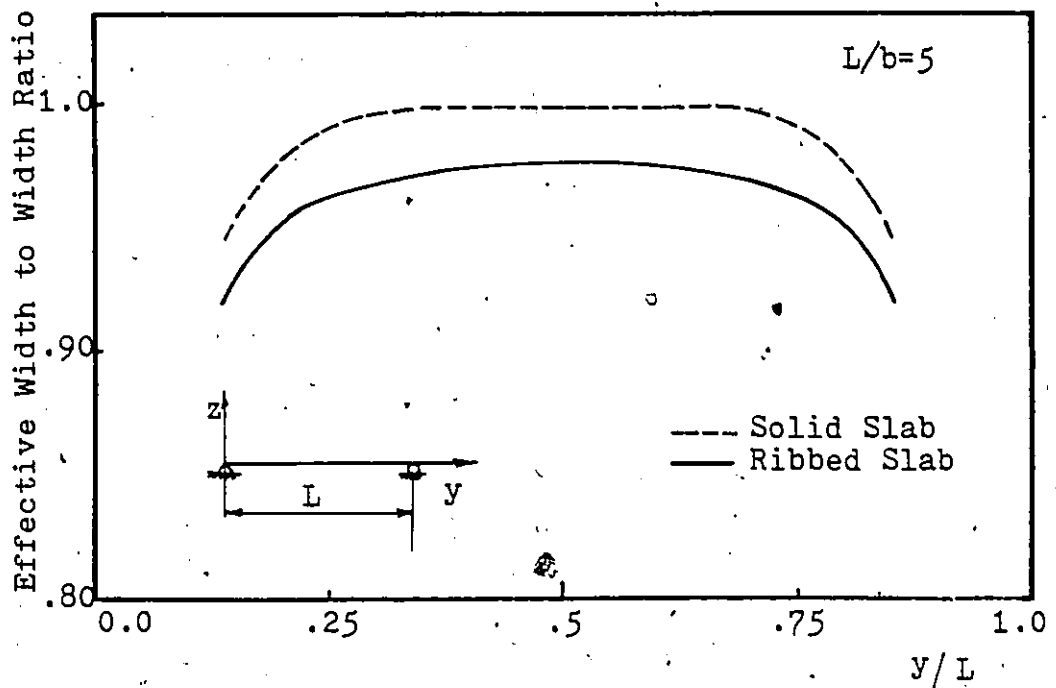


Fig.(5.8) Effective Width Ratio Distribution of a Solid and Ribbed Slab under UDL over Slab

y/L	0.20	0.25	0.30	0.35	0.40	0.45	0.50
Ribbed Concrete Slab	.919	.942	.953	.960	.964	.967	.967
Solid Slab	.937	.960	.972	.979	.983	.986	.986
Percentage difference	1.96	1.91	1.99	1.98	1.97	1.97	1.97

Table (5.5) Effective Width to Width Ratio Distribution for a Composite Beam with a Solid and Ribbed Slab under UDL over Slab Area ($L/b = 4$)

y/L	0.20	0.25	0.30	0.35	0.40	0.45	0.50
Ribbed Concrete Slab	.953	.966	.971	.974	.977	.979	.980
Solid Slab	.978	.992	.998	1.00	1.00	1.00	1.00
Percentage Difference	2.62	2.70	2.78	2.67	2.35	2.15	2.04

Table (5.6) Effective Width to Width Ratio Distribution for a Composite Beam with a Solid and Ribbed Slab under UDL over Slab Area ($L/b = 5$)

y/L	0.175	0.20	0.25	0.30	0.35	0.40	0.45	0.50
b _e /b	0.909	0.919	0.942	0.953	0.96	0.964	0.967	0.967
M in.kips	597.4	662.4	777.6	870.9	943.5	995.3	1026.	1037.
b _e (in)	65.45	66.17	67.82	68.62	69.12	69.41	69.62	69.62
M/b _e (Kips)	9.13	10.01	11.47	12.69	13.65	14.34	14.74	14.89

Table(5.7) Moment to Effective Width Ratio
 along a Composite Beam with a
 Ribbed Metal Deck under a UDL
 over the Slab Area (L/b=4)

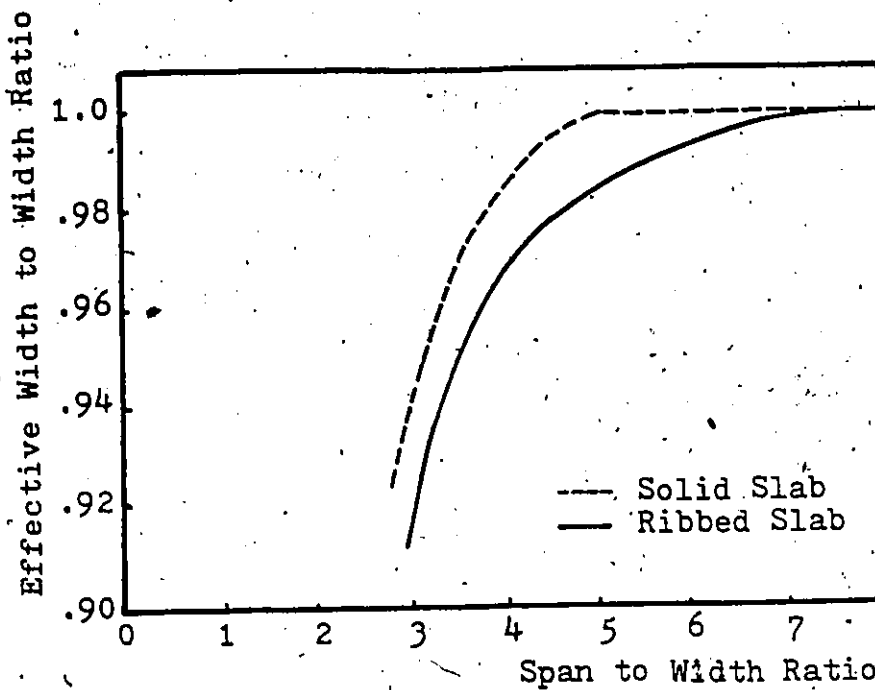


Fig.(5.9) Variation of Mid-Span Effective Width with Span to Width Ratio for a UDL over the Slab Area

y/L	0.25	0.30	0.35	0.40	0.45	0.50
Composite Beam (24' x 6' Slab)	0.942	0.953	0.960	0.964	0.967	0.967
Composite Beam (20' x 5' Slab)	0.942	0.953	0.961	0.964	0.966	0.967

Table (5.8) Effective Width to Width Ratio for Two Composite Beams having the Same L/b Ratio. (L/b=4)

5.6 Effect of the Concrete Compressive Strength on the Effective Width Ratio Distribution

Table (5.9) shows the effective width ratio distribution along a composite beam with a ribbed concrete slab, subjected to a uniformly distributed load over the slab area, for different concrete compressive strengths, f_c . It is to be noticed that the effective width variation due to the change in concrete strength is less than one percent. It may be concluded that the effect of the compressive strength of concrete on the effective width is of a minor importance.

5.7 Effect of Beam Size on the Effective Width Ratio Distribution

Table (5.10) shows the effective width ratio distribution for three-composite beams, having the same span to width ratio, but of different steel beam sizes. The variation in the effective width ratio is very small so that we may conclude that the beam size has a negligible effect on the effective width distribution of composite beams with ribbed slabs.

5.8 Effect of Type of Loading on the Effective Width Ratio Distribution

Figure (5.10) and table (5.11) show the drastic difference in the effective width ratio distribution along a composite beam with a ribbed slab for different types of loading. The critical effective width for the uniform load and the one point load is at the mid-span of the beam. However, the difference between these two effective width ratios is about 22 percent. It may be concluded that the effective width

y/L	0.20	0.25	0.30	0.35	0.40	0.45	0.50
$f'_c = 5800$ psi	.919	.942	.953	.960	.964	.967	.967
$f'_c = 4000$ psi	.921	.942	.954	.960	.964	.966	.967
$f'_c = 3000$ psi	.922	.943	.954	.960	.964	.966	.967

Table(5.9) Effect of Concrete Strength on the Effective Width Ratio Distribution in a Composite Beam under a UDL over the Ribbed Slab Area ($L/b=4$)

y/L	0.20	0.25	0.30	0.35	0.40	0.45	0.50
W16x26	.922	.944	.954	.960	.964	.966	.967
W14x22	.921	.943	.954	.960	.964	.966	.967
W12x19	.923	.944	.955	.960	.963	.966	.967

Table(5.10) Effect of Beam Size on the Effective Width Ratio of a Composite Beam with a Ribbed Metal Deck ($L/b=4$)

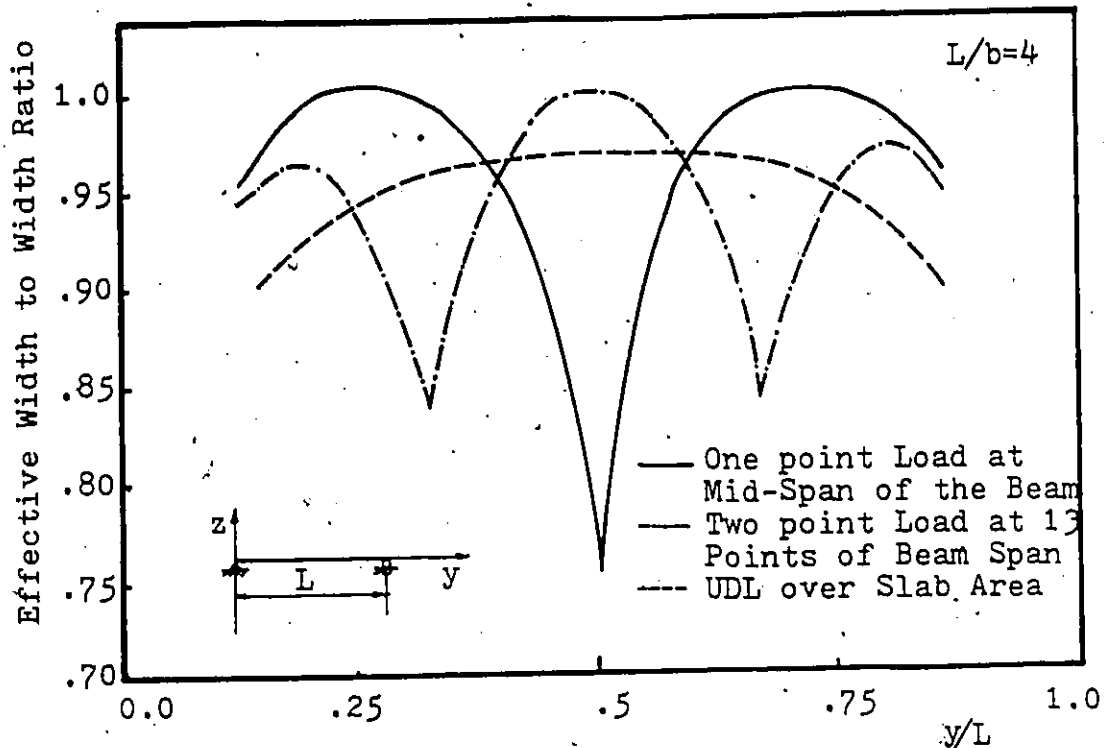


Fig.(5.10) Effect of Type of Loading on the Effective Width Ratio Distribution for a Composite Beam with a Ribbed Metal Deck

y/L	.20	.25	.30	.325	.33	.35	.40	.45	.475	.50
UDL over Slab	.92	.94	.95	.96	.96	.96	.96	.97	.97	.97
Two Point Load at 1/3 points of Beam Span	.96	.96	.92	.88	.83	.89	.96	.99	1.0	1.0
One Point Load at Mid-Span of the Beam	.98	1.0	1.0	1.0	.99	.99	.96	.90	.85	.75

Table(5.11) Effect of Type of Loading on the Effective Width Ratio of a Composite Beam with a Ribbed Metal Deck ($L/b = 4$)

used when designing a composite beam under a uniformly distributed load, which is the practical loading in most cases, should be different from that used for any other type of loading. It is conservative but wasteful of material to use the one-point load effective width in the design of composite beams subjected to a uniformly distributed load over the slab area.

5.9 Effective Width of Composite Beams with Ribbed Metal Deck in the Inelastic Stage

Figures (5.11 & 5.12) show the variation of the effective width to total width ratio of a composite beam with a ribbed concrete slab when loaded with a uniformly distributed load over the slab area in the different stages of loading until the ultimate capacity of the beam is reached.

It is noticed, as shown in figs.(5.11 & 5.12), that the effective width ratio is constant in the elastic stage. Once the bottom fibre of the steel beam yields, the effective width ratio starts to decrease. It keeps on decreasing until the concrete is no longer elastic and then it starts to increase again. The effective width keeps on increasing until it reaches or exceeds the elastic effective width. The length of this decreasing branch is a function of the compressive strength of concrete. The lower the compressive strength, the shorter this decreasing branch will be.

It may be concluded that the effective width at the

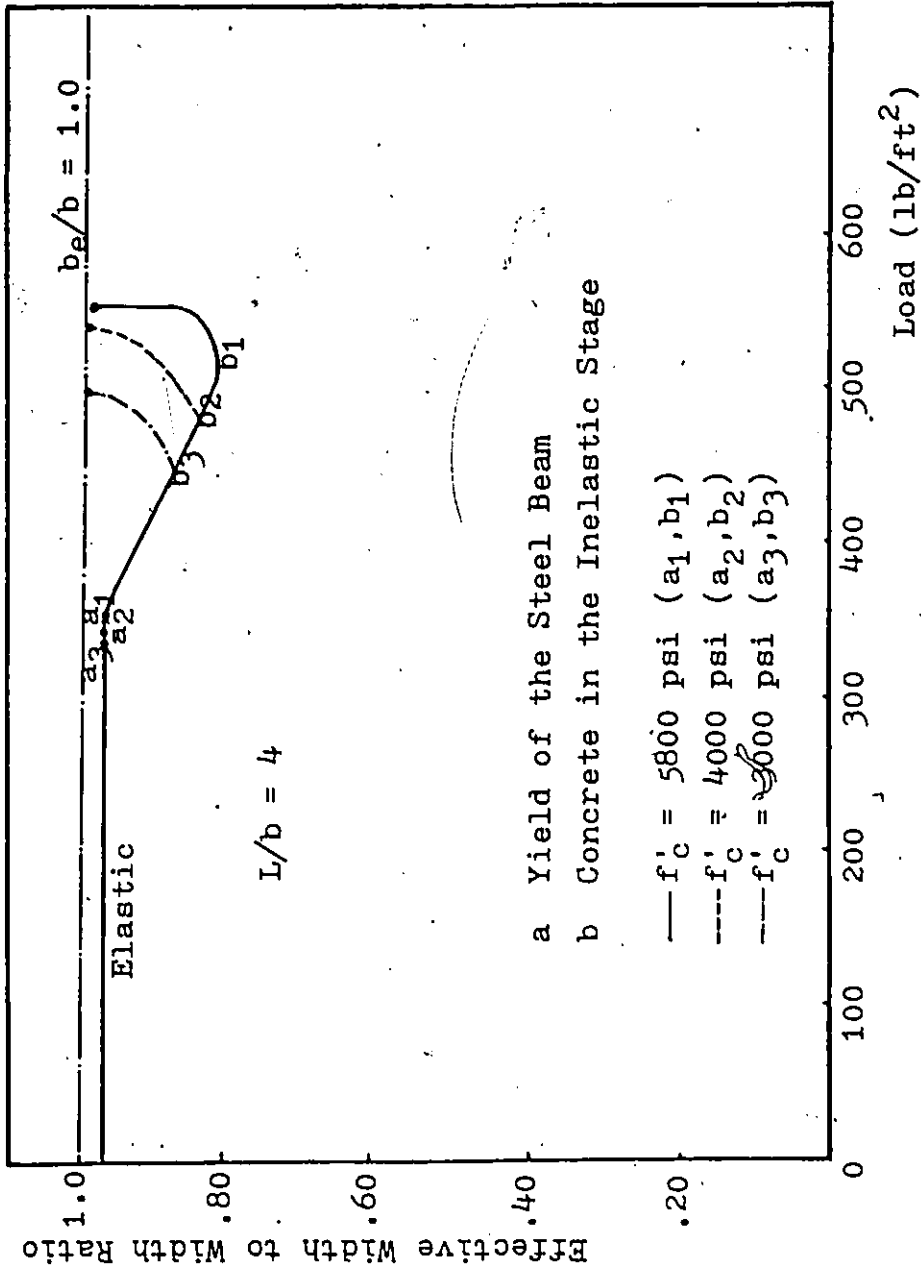


Fig.(5.11) Variation of the Effective Width of a Composite Beam with Ribbed Metal Deck with the Stage of Loading ($F_y = 38000$ psi , $L/b = 4$)

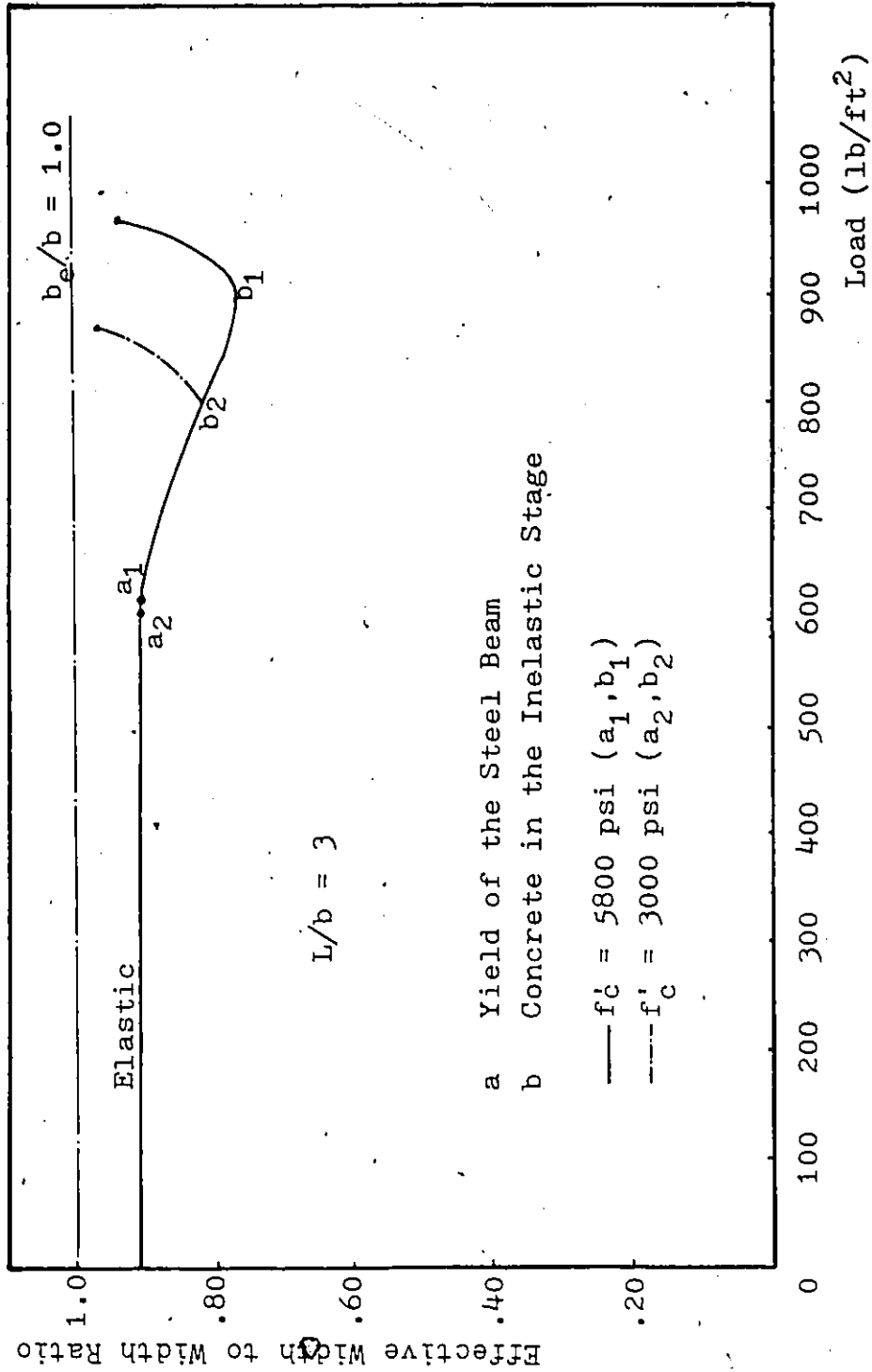


Fig.(5.12) Variation of the Effective Width of a Composite Beam with Ribbed Metal Deck with the Stage of Loading ($F_y = 38000$ psi, $L/b = 3$)

ultimate load is always greater than that in the elastic stage. The difference between the elastic effective width and the effective width at ultimate state is of the order of 4 percent. Thus, it is conservative and quite acceptable to use the effective width estimated in the elastic stage, in the calculation of the ultimate capacity of composite beams with ribbed concrete slabs.

5.10 Comparison with the CISC⁽³⁷⁾ and the AIJ⁽²⁹⁾ Specifications

The Canadian Institute of Steel Constructions (CISC)⁽³⁷⁾ specifications limit the value of the effective width, b_e , to the least of the following three values:

1. $b_e \geq 1/4$ beam span
i.e $b_e \leq L/4$
2. $b_e \leq$ Centreline to centreline distance between the adjacent beams.
i.e $b_e \leq b$
3. $b_e \leq 16t + b_f$

Where t is the total thickness of the slab and b_f is the flange width of the steel beam.

It is noticed that the CISC specifications with its different limits does not include the span to width ratio as a factor in the calculation of the effective width although it was shown in this study and by several other investigators^(3,21,46) that it is the most significant parameter influencing the effective width.

The Architectural Institute of Japan (AIJ)⁽²⁹⁾ specifications use an empirical formula to calculate the effective width of the composite beams with ribbed slabs. This formula takes into account the span to width ratio as an important parameter affecting the effective width.

$$b_e = b - 0.60(b-b_f)^2/L$$

Table (5.12) shows a comparison of the effective width ratio between the CISC specifications, the AIJ specifications and the results obtained from the layered finite element analysis of composite beams with ribbed slabs under uniformly distributed loading over the slab area. It shows that the CISC results are very close to the finite element model results for span to width ratios greater than or equal to 4. However, for ratios less than 4, the CISC is very conservative, fig.(5.13). The AIJ results are conservative for all span to width ratios with a difference of the order of 10 percent, fig.(5.13).

Table (5.13) gives the effective width ratios for different span to width ratios, for composite beams with 1-1/2 inch ribbed metal deck, subjected to a uniformly distributed load over the slab area, as calculated from the layered finite element analysis. Interpolation can be used

Composite Beam	L/b	Effective width to Width Ratio (b_e/b)			Layered Finite Element Model
		CISC	AIJ		
W14x22 (18'x6' Slab)	3	0.75	0.827	0.916	
W14x22 (24'x6' Slab)	4	0.958	0.870	0.967	
W14x22 (25'x5' Slab)	5	1.0	0.899	0.980	
W14x22 (30'x5' Slab)	6	1.0	0.916	0.989	
W14x22 (28'x4' Slab)	7	1.0	0.931	0.995	

Table(5.12) Comparison with the Effective Width of a Composite Beam with a Ribbed Metal Deck according to the Canadian and Japanese Specifications

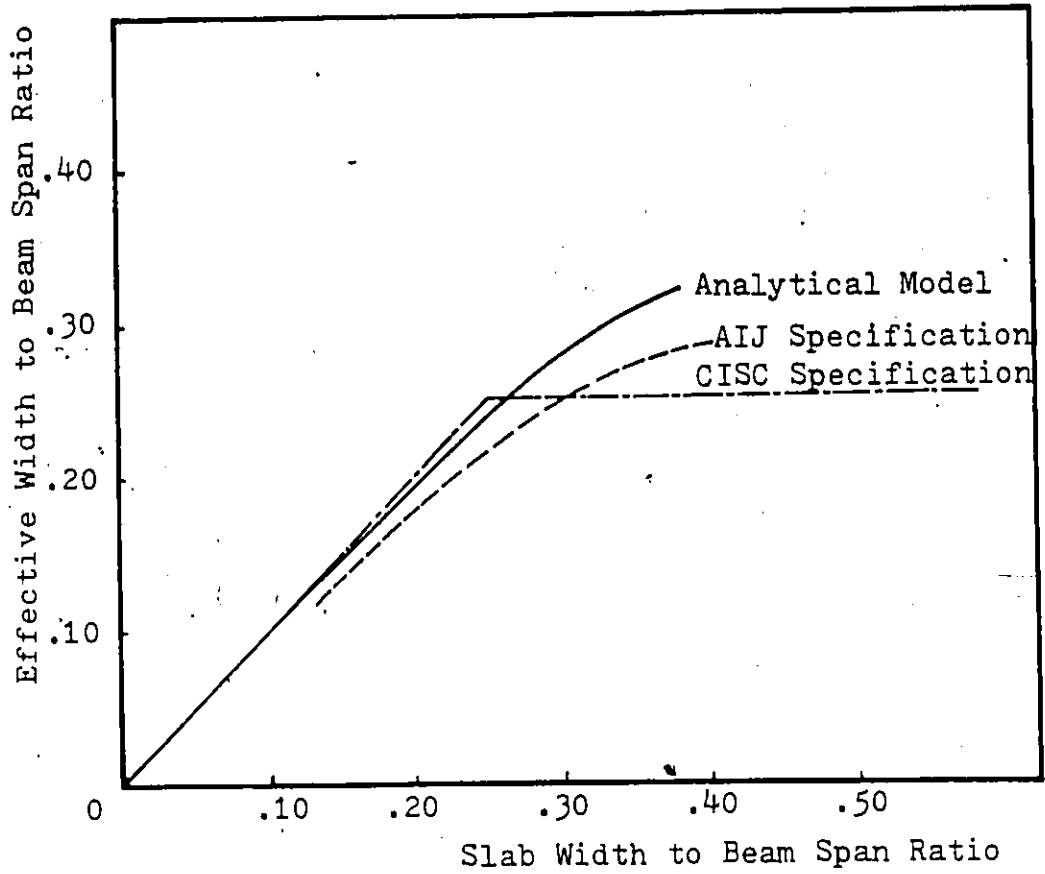


Fig.(5.13) Comparison between the Analytical Model and the CISC and the AIJ Specifications

L/b	3	4	5	6	7
b_e/b	.961	.967	.980	.989	.995

Table(5.13) Effective Width Ratios of a Composite Beam with 1-1/2 in Ribbed Metal Deck under a UDL over the Slab Area

to calculate the effective width ratio for any span to width ratio that does not exist in this table.

Tables (5.14 & 5.15) show a comparison of the effective width-to-width-ratio distribution for a 1-1/2-in ribbed metal deck and a 3-in deck, for two different span to width ratios. It is observed that the 3-in deck provides a slightly larger effective width than the 1-1/2-in deck, provided that both have equal depth for the solid part of the slab. It is also to be noticed that the difference in the effective width ratio due to the change in the depth of the ribbed metal deck, increases with the decrease of the span to width ratio.

5.11 Conclusions

1. Effective widths of slabs in simply supported composite beams, especially for span to width ratios greater than three, are practically constant along the beam lengths except near the ends.

2. The effective widths are significantly dependent on the plan dimensions of the composite beams. Within the practical range of composite beam members proportions, the size of the steel beam, the height of the ribbed metal deck and the strength of concrete play a negligible role.

3. The effective width increases with the increase of the span to width ratios. In the case of a solid slab, the effective width equals the total width when the span to width ratio is equal to or exceeds five. However, in the case of a ribbed slab, the effective width equals the total width when the span to width ratio is equal to or exceeds 7.5.

y/L	0.20	0.30	0.40	0.45	0.50
3-in metal deck +2-1/2-in solid slab	.862	.928	.951	.957	.961
1-1/2-in metal deck +2-1/2-in solid slab	.830	.886	.909	.914	.916
% Difference	3.71	4.53	4.42	4.49	4.68

Table (5.14) Effective Width to Width Ratio Distribution
for a 5-1/2-in and 4-in Ribbed Slabs (L/b=3)

y/L	0.20	0.30	0.40	0.45	0.50
3-in metal deck +2-1/2-in solid slab	.931	.970	.979	.982	.984
1-1/2-in metal deck +2-1/2-in solid slab	.921	.954	.964	.966	.967
% Difference	1.29	1.75	1.53	1.53	1.73

Table (5.15) Effective Width to Width Ratio Distribution
for a 5-1/2-in and 4-in Ribbed Slabs (L/b=4)

4. Effective width ratios for ribbed and solid slabs, having the same overall thickness, are very close to each other. Thus, it is possible to use the same effective width for the two types of slabs. However, it is conservative to use the effective width for the ribbed slab.

5. The effective width at the ultimate load reaches or exceeds the effective width in the elastic stage. For composite beams, it is on the conservative side to use the effective width based on the elastic theory at the ultimate state.

6. For composite beams with ribbed metal deck, the Canadian Code (CISC) gives quite good agreement, for span to width ratios greater than or equal to 4, with a difference of about 2 percent of the predicted analytical values. However, for span to width ratios smaller than 4, the Canadian Code (CISC) is very conservative with a difference of about 20 percent.

7. The Japanese Code (AIJ) seems to be conservative for all span to width ratios with a difference of about 10 percent of the predicted values presented in this investigation.

8. The effective width to width ratio is very sensitive to the type of loading. It is smallest in the case of a one-point load at mid-span of the beam and largest in the case of a uniformly distributed load over the slab area. Thus, the effective width should be specified according to the type of loading.

CHAPTER 6

LONGITUDINAL CRACKING OF COMPOSITE

BEAMS WITH RIBBED METAL DECKS

6.1 General

In composite beams with ribbed metal decks, the reinforced concrete slab, the metal deck and the steel beam on which the deck rests, all act as a unit. Composite action is achieved by means of shear connectors welded through the deck to the beam.

Each side of the shear connectors, the concrete slab is subjected to a longitudinal shearing force due to the composite action provided by these connectors. This longitudinal shearing force induces transverse tensile stresses in the slab that could create a longitudinal crack in the slab along the beam length.

However, slabs in composite beams are usually subjected to transverse negative moment over the beam length when loaded with a uniformly distributed load over the entire slab area, which is the most common type of loading. The transverse moment will create a tendency for the concrete slab to crack longitudinally over the beam length.

Generally, longitudinal cracking in composite beams is due to the combined action of transverse negative moments and the transverse tensile stresses induced by the composite action in the slab. However, for some specific cases, when the composite beam is loaded with point loads over the beam length, the longitudinal cracking, in the absence of the transverse moment, will be mainly due to the longitudinal shear effect.

The development of such a crack would result in the reduction of the ultimate capacity of the composite beam. Thus, it is desirable to ensure that the ultimate capacity of the composite beam is achieved before or simultaneously with the development of the longitudinal crack.

Very limited work has been reported on the study of the longitudinal cracking in composite beams with ribbed metal decks. However, some work was presented for the case of a composite beam with a solid concrete slab.

Davies⁽¹⁸⁾ tested a number of simply supported composite beams with solid concrete slabs to study the effect of the transverse reinforcement in resisting the longitudinal cracking of the slab. The composite beams were loaded at one point at mid-span of the beams. Davies^(17,18) explained the phenomenon of the development of the longitudinal cracking, in the absence of transverse moment, to be due to the longitudinal shear which is transmitted to the concrete near the underside of the slab. He concluded that longitudinal

cracking would most likely start at the bottom of the slab and then propagate to the upper surface to become visible.

Davies^(17,18) presented an empirical formula to estimate the amount of transverse reinforcement to be used to prevent longitudinal cracking of solid concrete slabs. He concluded that the amount of transverse reinforcement is dependent on the slab thickness, the concrete strength and the yield stress of the reinforcing steel. Davies' work was only concerned with the longitudinal cracking of composite beams with solid concrete slabs in the absence of transverse moment .

ElGhazzi^(19,20) presented an ultimate strength design method for the transverse reinforcement in the solid concrete slabs of composite beams. He presented a formula to estimate the amount of transverse reinforcement which permits a crack to develop longitudinally at the same time as the flexural capacity of the composite beam is attained. Again, ElGhazzi's work was only concerned with composite beams with solid concrete slabs loaded over the beam length without any consideration of any transverse moment .

Adekola⁽⁴⁾ tested a number of composite beams with solid concrete slabs under one point load at mid-span of the beams. He noticed that the failure load was reduced in the specimens that have no transverse reinforcement. The absence of transverse reinforcement allowed longitudinal cracking of the slabs at an early stage of loading.

Johnson^(31,32) has also recommended an ultimate strength design method for the transverse reinforcement in the solid slab of a composite beam. The total amount of steel reinforcement is mainly dependent on the strength of the concrete and the yield stress of the steel reinforcement. He concluded that the need for bottom transverse reinforcement is greatest where there is no negative transverse moment.

Azmi⁽⁸⁾ investigated the contribution of the ribbed metal deck to the transverse reinforcement of concrete slabs in composite beams with ribbed slabs loaded over the centerline of the beams. He tested a composite beam with a ribbed metal deck using 50 percent of the amount of transverse reinforcement calculated according to ElGhazzi's^(19,20) formula for solid slabs. He found that the composite beam achieved its ultimate capacity. Accordingly, he concluded that the ribbed metal deck contributes to the transverse reinforcement of the slab in resisting the longitudinal cracking.

Several investigators^(22,28,50,51) have tested composite beams with ribbed metal deck by loading over the beam length. They observed that the concrete slabs remained entirely intact according to visual inspection up to about 90 percent of the ultimate capacity. At this stage, the concrete slab began to show failure by longitudinal cracks extending from the load points to the ends of the beams. In these tests no provisions were made for the inclusion of the transverse moment effect.

The object of the parametric study presented in this chapter is to investigate the effect of the metal deck, the transverse reinforcement, the beam-span-to-slab-width ratio and the compressive strength of concrete on the resistance to longitudinal cracking in simply supported composite beams with 1-1/2-in ribbed metal deck subjected to uniformly distributed loading over the slab area. The combined composite action and transverse moment effect on longitudinal cracking is included in this study. A study of the effect of the type of loading, the steel beam size and the thickness of the solid part of the ribbed concrete slab on the longitudinal cracking is also presented in this chapter.

In fact, this study is mainly aimed at answering some practical questions concerning the longitudinal cracking of composite beams with ribbed metal decks subjected to uniformly distributed loading over the slab area. Such questions are: where do the cracks start? how much transverse reinforcement is required? and what are the factors that affect the longitudinal cracking of composite beams with ribbed metal decks?

At the end of the chapter, some design recommendations and rules are presented concerning the amount of transverse reinforcement and the quality of concrete used for composite beams with ribbed metal decks subjected to uniformly distributed loading over the entire slab.

6.2 Effect of the Type of Loading

Three identical composite beams with ribbed metal decks were studied under different types of loading to study the effect of the type of loading on the longitudinal cracking of the concrete slabs. The beams were simply supported over a 24-ft span and were loaded with one point load at mid-span of the beam, two point load at 1/3-points of beam length and a uniformly distributed load over the slab area, respectively. The beams consisted of W14x22 lb per ft steel sections and 4-in ribbed concrete slabs with 6-ft width. Tables (6.1 & 6.2) summarize the results for these cases of loading using two different types of concrete.

Loading over the beam length eliminates the transverse moment effect and the creation of the longitudinal cracking will be mainly owing to the composite action between the beam and the slab. In this case, the crack always starts near the bottom fibre of the concrete ribs, where the longitudinal shear is transmitted by the connectors. The crack is initiated near the load points and then it extends longitudinally toward the ends of the beam while it is propagating vertically through the depth of the slab.

In the case of a uniformly distributed load over the entire slab, the first occurrence of a longitudinal crack occurs along the top of the slab over the beam and is due to transverse moment. For that kind of loading, the concrete slab is subjected to the combined effect of transverse

Type of Loading	M _y (in-kips)	M _{Lc} (in-kips)		M _u (in-kips)	M _{Lc} /M _u
		Top Crack	Bottom Crack		
One Point Load at Beam Mid-Span	1825	----	2690	2865	0.94
Two Point Load at 1/3 Points of Beam	1780	----	Tendency near Bottom	2870	-----
U D L over Slab	1795	Tendency near Top	----	2870	-----

Table(6.1) Effect of Type of Loading on the Longitudinal Cracking(f'_c=5800 psi)

Type of Loading	M_y (in-kips)	M_{Lc} (in-kips)		M_u (in-kips)	M_{Lc}/M_u
		Top Crack	Bottom Crack		
One Point Load at Beam Mid-Span	1795	-----	2370	2765	0.86
Two Point Load at 1/3 Points of Beam	1750	-----	2760	2775	0.99
U D L over Slab	1760	2400	-----	2780	0.86

Table(6.2) Effect of Type of Loading on the Longitudinal Cracking($f'_c=3000$ psi)

moment and longitudinal shear. The longitudinal shear effect tends to initiate the cracking at the bottom fibre of the concrete ribs, while the transverse negative moment effect tends to initiate the cracking at the top fibre of the slab. However, the transverse moment effect seems to govern such that for a beam loaded with a uniformly distributed load over the entire slab area, the longitudinal crack usually starts at the top fibre in the non-ribbed parts of the slab near the mid-span section. Then, the crack extends downwards through the depth of the slab and longitudinally toward the ends of the beam.

It may be concluded that the transverse negative moment, due to the uniformly distributed load over the slab area, creates a tendency to suppress the longitudinal crack due to the longitudinal shear at the bottom of the slab. Thus, the need for transverse reinforcement at the lower face of the slab to resist the longitudinal cracking due to the longitudinal shear effect is greatest when there is no transverse negative moment. However, the existence of the transverse moment can eliminate the need for any bottom transverse reinforcement as it suppresses the longitudinal shear effect. On the other hand, there could be a need for some top transverse reinforcement to resist the longitudinal cracking due to the transverse moment depending on the beam span to slab width ratio of the composite beam and the compressive strength of the concrete slab.

6.3 Effect of the Compressive Strength of Concrete

A composite beam with ribbed metal deck is studied under two-point load at 1/3-points of the beam length, for two different values of the compressive strength of concrete, f'_c . Table (6.3) shows the effect of the compressive strength of concrete on the longitudinal cracking moment and the cracking moment to ultimate moment ratio. It is clear that the increase of the concrete compressive strength improves the longitudinal cracking phenomenon in the composite beam.

Table (6.4) shows the effect of the compressive strength of concrete on the longitudinal cracking moment of a composite beam with a 1-1/2-in ribbed metal deck subjected to a uniformly distributed load over the entire slab. It is noticed that the increase of the compressive strength of concrete, for a specific beam span to slab width ratio, increases the longitudinal cracking moment with respect to the ultimate capacity. It is also noticed that the greater the longitudinal cracking moment the larger the ultimate moment of the composite beam.

Table (6.5) shows a comparison between two composite beams loaded with a uniformly distributed load and having different concrete strengths and steel beam yield stresses but equal steel yield stress to concrete compressive strength ratio, F_y/f'_c . It shows that the longitudinal cracking moment to ultimate moment ratio is almost constant for any specific steel yield stress to concrete compressive

Strength of Concrete (psi)	M_y (in-kips)	M_{Lc} (in-kips)	M_u (in-kips)	M_{Lc}/M_u
5800	1780	-----	2870	-----
3000	1750	2760	2775	0.99

Table(6.3) Effect of Concrete Strength on the Longitudinal Cracking of Composite Beams Loaded with 2-Point Load at 1/3 Points of Beam Span ($L/b=4$)

Strength of Concrete (psi)	M_y (in-kips)	M_{Lc} (in-kips)	M_u (in-kips)	M_{Lc}/M_u
5800	1795	-----	2870	-----
4000	1780	2720	2825	0.96
3000	1760	2400	2780	0.86

Table(6.4) Effect of Concrete Strength on the Longitudinal Cracking of Composite Beams Loaded with a UDL over the Slab ($L/b=4$)

Steel Yield Stress to Concrete Strength Ratio	L (ft)	b (ft)	F _y (psi)	f' _c (psi)	M _y (in-kips)	M _{Lc} (in-kips)	M _u (in-kips)	M _{Lc} /M _u
9.5	18	6	38000	4000	1770	1530	2620	0.585
	18	6	44000	4600	2050	1750	3000	0.584
12.7	18	6	38000	3000	1750	1310	2545	0.515
	18	6	50000	3950	2315	1655	3315	0.500

Table(6.5) Longitudinal Cracking of Composite Beams Having
Equal Yield Stress to Concrete Strength Ratios

strength ratio.

Thus, it may be concluded that for a composite beam, with a specific span to width ratio, it is possible to increase the longitudinal cracking moment and correspondingly the ultimate moment by the proper selection of the concrete compressive strength, f'_c . In other words, the proper selection of the material properties of the composite beam, such as the steel beam yield stress to the concrete compressive strength ratio, F_y/f'_c , is very important in improving the behaviour of the composite beam with respect to longitudinal cracking.

It is also to be mentioned that the concrete strength, f'_c , required to improve the longitudinal cracking moment of the composite beam depends on the beam span to slab width ratio, L/b . In other words, as it will be shown in the next section, the larger the span to width ratio, L/b , the lower the required concrete compressive strength, f'_c .

6.4 Effect of the Beam Span to Slab Width Ratio

Two composite beams with ribbed metal deck, having different beam span to slab width ratios, are studied under one point load at the mid-span of the beam length. The beams were selected to have close ultimate moment capacities by keeping the slab width equal in the two beams and changing the span. All the other properties are kept the same. The results of this comparison are shown in table (6.6). It may

Beam Span to Slab width Ratio	L (ft)	b (ft)	M_y (in-kips)	M_{Lc} (in-kips)	M_u (in-kips)	M_{Lc}/M_u
3	18	6	1815	2540	2860	0.89
4	24	6	1825	2690	2865	0.94

Table(6.6) Effect of L/b Ratio on the Longitudinal Cracking of Composite Beams Loaded with One Point Load at Mid-Span of the Beam ($f'_c = 5800$ psi)

Beam Span to Slab Width Ratio	L (ft)	b (ft)	M_y (in-kips)	M_{Lc} (in-kips)	M_u (in-kips)	M_{Lc}/M_u
3	18	6	1770	1530	2615	0.59
4	24	6	1780	2720	2825	0.96

Table(6.7) Effect of L/b Ratio on the Longitudinal Cracking of Composite Beams Loaded with a UDL over the Slab Area ($f'_c = 4000$ psi)

be noticed that the increase of the span to width ratio, increases the longitudinal cracking moment with respect to the ultimate moment capacity of the composite beam.

Table (6.7) shows the effect of the span to width ratio, L/b , on the longitudinal cracking moments of composite beams with 1-1/2-in ribbed metal decks subjected to a uniformly distributed load over the entire slab. In this comparison, the beams have equal widths but different spans with all the other properties remaining constant. It may be noticed that the increase of the span to width ratio increases the longitudinal cracking moment with respect to the ultimate moment capacity. It also may be noticed that the greater the longitudinal cracking moment is the larger the ultimate moment of the composite beam.

Table (6.8) shows a comparison between two composite beams loaded with a uniformly distributed load and having different spans and widths but equal span to width ratio, $L/b = 3$. It shows that the longitudinal cracking moment to ultimate moment ratio is almost constant for any specific span to width ratio. The same conclusion can be drawn from table (6.9) in which a similar comparison is presented but for a different span to width ratio, $L/b = 4$. It is also possible to say, according to table (6.8) in which two concrete compressive strengths were used, that the previous conclusion is independent of the concrete strength.

Thus, it may be concluded that the beam span to slab

f'_c (psi)	L (ft)	b (ft)	L/b	M_y (in-kips)	M_{Lc} (in-kips)	M_u (in-kips)	M_{Lc}/M_u
3000	21	7	3	1810	1330	2565	0.519
	18	6	3	1750	1310	2545	0.515
4000	21	7	3	1825	1535	2635	0.583
	18	6	3	1770	1530	2620	0.597

Table(6.8) Longitudinal Cracking of Composite Beams
having the Same Span to Width Ratio (3)

f'_c (psi)	L (ft)	b (ft)	L/b	M_y (in-kips)	M_{Lc} (in-kips)	M_u (in-kips)	M_{Lc}/M_u
2000	20	5	4	1685	1945	2545	0.764
	24	6	4	1735	1945	2590	0.750

Table(6.9) Longitudinal Cracking of Composite Beams
having the Same Span to Width Ratio (4)

width ratio is a very important factor affecting the longitudinal cracking of composite beams with ribbed metal decks. The longitudinal cracking moment to ultimate moment ratio is almost constant for any specific span to width ratio.

6.5 Effect of the Metal Deck

Table (6.10) shows a comparison between two composite beams with ribbed metal decks in which the metal deck was removed in one of the two beams. The beams were loaded with one point load at mid-span of the beams and the slabs were not provided with any transverse reinforcement. The results, table (6.10), shows that the metal deck contributes to the resistance of the longitudinal cracking by increasing the cracking load by about 14 percent.

Table (6.11) shows a similar comparison for two composite beams loaded with a uniformly distributed load over the entire slab. It shows that the metal deck does not contribute to the resistance of the longitudinal cracking when the composite beams are subjected to uniformly distributed load over the slab area. This is mainly because the crack tends to start at the top fibre of the slab while the metal deck is near the bottom surface of the slab.

6.6 Effect of Beam Size

Table (6.12) shows the longitudinal cracking moment for three composite beams having the same span to width ratio,

	f'_c (psi)	L/b	M_y (in-kips)	M_{Lc} (in-kips)	M_u (in-kips)	M_{Lc}/M_u
With Metal Deck	3000	4	1795	2370	2765	0.857
Metal Deck Removed	3000	4	1795	2070	2735	0.756

Table(6.10) Effect of the Metal Deck on the Longitudinal Cracking of Composite Beams under One Point Load at Mid-Span of the Beam

	f'_c (psi)	L/b	M_y (in-kips)	M_{Lc} (in-kips)	M_u (in-kips)	M_{Lc}/M_u
With Metal Deck	3000	3	1750	1310	2545	0.515
Metal Deck Removed	3000	3	1755	1295	2545	0.506

Table(6.11) Effect of the Metal Deck on the Longitudinal Cracking of Composite Beams under a UDL over the Slab Area

Steel Beam Size	L/b	M_y (in-kips)	M_{Lc} (in-kips)	M_u (in-kips)	M_{Lc}/M_u
W12x19	4	1400	1050	2050	0.512
W14x22	4	1750	1310	2545	0.515
W16x26	4	2255	1580	3250	0.486

Table(6.12) Effect of the Steel Beam Size
on the Longitudinal Cracking($f'_c=3000$)

Overall Slab Thickness	f'_c (psi)	L/b	M_y (in-kips)	M_{Lc} (in-kips)	M_u (in-kips)	M_{Lc}/M_u
4	3000	3	1750	1310	2545	0.515
5		3	1920	2040	2860	0.713
4	4000	3	1770	1530	2620	0.585
5		3	1950	2550	3000	0.851
4	5000	3	1780	1870	2690	0.696
5		3	1970	-----	3060	-----

Table(6.13) Effect of the Thickness of the Solid Part of the Slab on the Longitudinal Cracking

but of different steel beam sizes. The beams were loaded with a uniformly distributed load over the slab area. The variation in the longitudinal cracking moment to ultimate moment ratio is very small so that we may conclude that the beam size has a negligible effect on the longitudinal cracking of composite beams with ribbed metal decks subjected to uniformly distributed load.

6.7 Effect of the Thickness of the Solid Part of the Slab

Table (6.13) shows a comparison between two composite beams with 1-1/2-in ribbed metal deck having an overall slab thickness of 4-in and 5-in, respectively. The beams were loaded with a uniformly distributed load over the slab area. This study was repeated for 3 different concrete compressive strengths.

It may be concluded from this study, table (6.13), that the increase of the thickness of the solid part of the slab can improve the behaviour of the composite beams with respect to the longitudinal cracking of the slabs.

6.8 Effect of the Transverse Reinforcement

Tables (6.14, 6.15 & 6.16) show the effect of the transverse steel reinforcement on the longitudinal cracking of composite beams with 1-1/2-in ribbed metal deck subjected to uniformly distributed load over the slab area. The reinforcing steel was placed 3/4-in below the top surface of

Percentage of Reinforcement	F_y/f'_c	M_y (in-kips)	M_{Lc} (in-kips)	M_u (in-kips)	M_{Lc}/M_u
0.0	9.5	1770	1530	2620	0.585
0.5	9.5	1760	1780	2635	0.676
1.0	9.5	1760	1925	2640	0.730

Table(6.14) Effect of the Transverse Reinforcement on the longitudinal Cracking of Composite Beams under UDL over the Slab Area($L/b=3$)

Percentage of Reinforcement	F_y/f'_c	M_y (in-kips)	M_{Lc} (in-kips)	M_u (in-kips)	M_{Lc}/M_u
0.0	12.7	1760	2400	2780	0.863
0.5	12.7	1760	2510	2785	0.901
1.0	12.7	1755	2590	2785	0.930

Table(6.15) Effect of the Transverse Reinforcement on the Longitudinal Cracking of Composite Beams under UDL over the Slab Area($L/b=4$)

Percentage of Reinforcement	F_y/f'_c	M_y (in-kips)	M_{Lc} (in-kips)	M_u (in-kips)	M_{Lc}/M_u
0.0	19	1715	2245	2540	0.884
0.5	19	1710	2360	2565	0.920
1.0	19	1710	2460	2575	0.955

Table(6.16) Effect of the Transverse Reinforcement on the Longitudinal Cracking of Composite Beams under UDL over the Slab Area($L/b=5$)

Percentage of Reinforcement	F_y/f'_c	M_y (in-kips)	M_{Lc} (in-kips)	M_u (in-kips)	M_{Lc}/M_u
0.0	12.7	1750	1310	2545	0.515
6x6/10x10 Welded Wire Mesh	12.7	1755	1330	2545	0.523

Table(6.17) Effect of the 6x6/10x10 Welded Wire Mesh on the Longitudinal Cracking of Composite Beams under UDL over the Slab Area($L/b=3$)

the concrete slab. The percentage of reinforcement was varied between zero and one percent.

The comparison shows that the increase of the amount of top transverse reinforcement increases the longitudinal cracking moment to ultimate moment ratio. It also shows that the need for transverse reinforcement decreases with the increase of the beam span to slab width ratio. For a span to width ratio equal to 3, a 0.50 percent reinforcement area in the transverse direction improves the longitudinal cracking moment by about 14 percent. However, for span to width ratios equal to or greater than 4, an increase in the longitudinal cracking moment can be only in the order of about 5 percent. It is to be noted that the rate of increase of the longitudinal cracking moment to the ultimate moment ratio decreases as the percentage of transverse reinforcement increases. It may be concluded that for span to width ratios greater or equal to 4, where the effect of transverse reinforcement on longitudinal cracking is small, the lower bound for this reinforcement would be dictated by the practical requirement for shrinkage.

Table (6.17) shows the effect of the 6 x 6/10 x 10 welded wire mesh, on the longitudinal cracking of composite beams with ribbed slabs. It shows that the welded wire mesh plays a negligible role in the resistance to longitudinal cracking. This is mainly so because this wire mesh constitutes a very small percentage of the total reinforcement (about .10%).

6.9 Design Recommendations and Conclusions

From the above parametric study it is possible to draw the following conclusions for a composite beam with a ribbed metal deck subjected to a uniformly distributed load over the slab area:

1. The beam-span-to-slab-width ratio is one of the main factors affecting the longitudinal cracking of composite beams with ribbed metal decks. The longitudinal cracking moment to ultimate moment ratio, M_{Lc}/M_u , increases with the increase of the span to width ratio, L/b .

2. The concrete strength and the steel beam yield stress have quite noticeable effect on the longitudinal cracking moment of composite beams. The decrease of the beam yield stress to concrete slab compressive strength ratio, F_y/f'_c , increases the longitudinal cracking moment to the ultimate moment ratio.

3. The percentage of top transverse reinforcement, P_T , affects the longitudinal cracking moment, M_{Lc} . However, the transverse reinforcement effect is not very appreciable especially for span to width ratios greater than 3. For a span to width ratio equal to 3, a .50 percent amount in the transverse reinforcement increases the longitudinal cracking moment to ultimate moment ratio by about 14 percent. However, for span to width ratios equal to or greater than 4, the increase in the longitudinal cracking moment to ultimate moment ratio is only in the order of about 5 percent.

4. The thickness of the solid part of the slab plays a considerable role in increasing the longitudinal cracking moment

to the ultimate moment ratio. However, increasing the thickness is not recommended from an economic point of view.

Making use of the conclusions above, a number of composite beams with ribbed metal decks, loaded with a uniformly distributed load over the entire slab, were studied considering different span to width ratios, beam yield stress to concrete strength ratios, percentages of top transverse reinforcement and slab thicknesses.

In this study, the slab to width ratio was considered to vary between 3 and 6. The ratio between the beam yield stress and the concrete compressive strength was considered to vary between 8 and 22. For the top transverse reinforcement, three cases were considered; no transverse reinforcement, .50 percent transverse reinforcement and 1.0 percent transverse reinforcement as an upper limit. Finally, for the slab thickness, the study was mainly concerned with the 4-in overall thickness. However, some examples were presented to study the effect of the increase of the thickness of the solid part of the slab so that the overall thickness would be 5-in.

Figure (6.1) shows the relationship between the longitudinal cracking moment to ultimate moment ratio, M_{LC}/M_u , and the beam yield stress to concrete compressive strength ratio, for different span to width ratios, L/b , and different percentages of top transverse reinforcement, p_T . The overall thickness of the slab was 4-in.

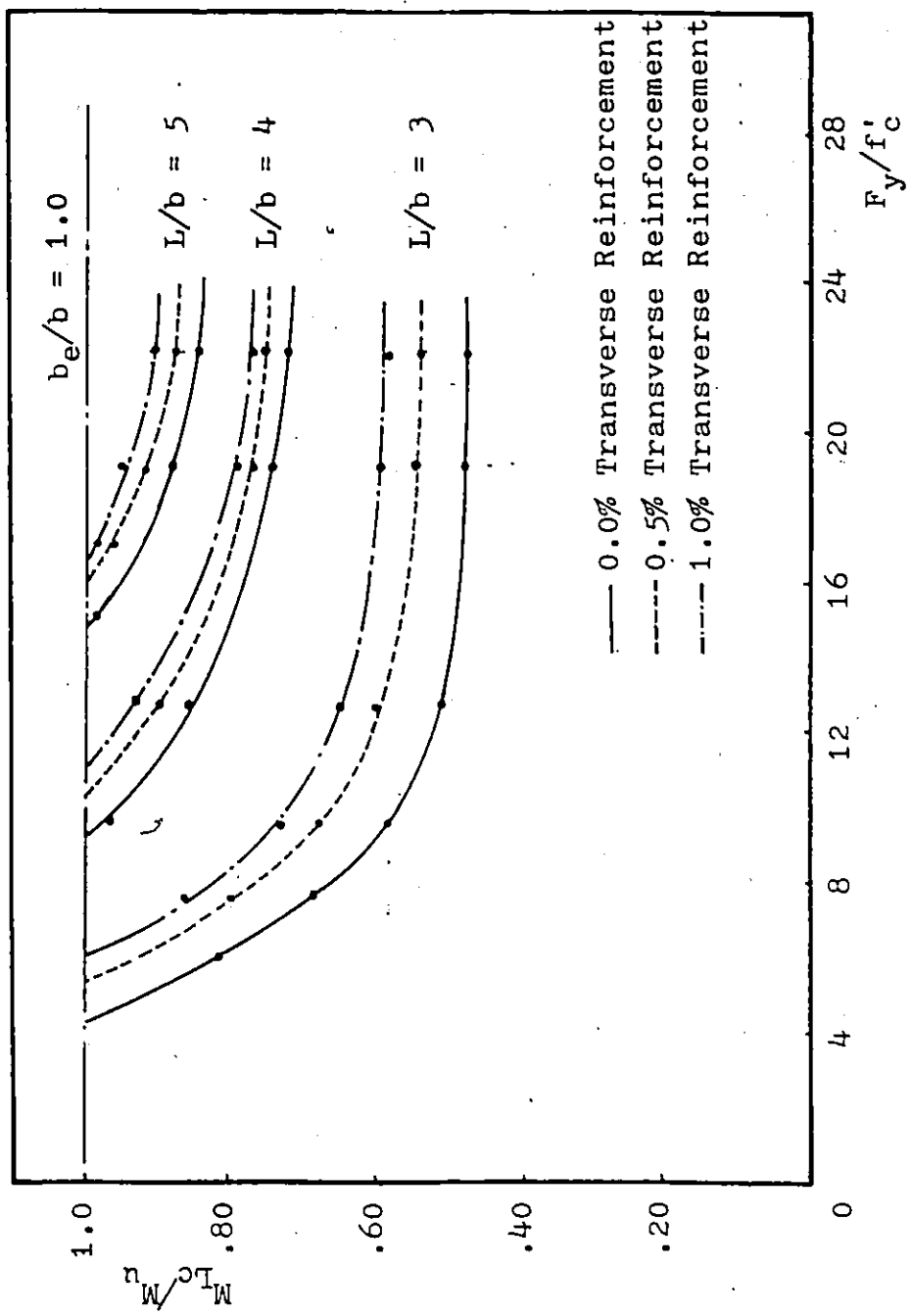


Fig.(6.1) Relationship between the Longitudinal Cracking Moment and the Properties of the Composite Beam

One can use fig.(6.1) to select the appropriate properties of the composite beam to achieve any required longitudinal cracking moment to ultimate moment ratio, for a specific beam span to slab width ratio. Thus, for a composite beam, knowing the beam span and the slab width, it is possible to select the concrete compressive strength, f'_c , the yield stress of the steel beam, F_y , and the percentage of the top transverse reinforcement, P_T , to ensure that the longitudinal cracking would occur as close as possible to the ultimate moment of the beam. Interpolation can be used to calculate the appropriate properties for a composite beam with a span to width ratio that does not exist in this figure. It should be noticed that the values of ultimate moments used in fig.(6.1) are those determined from the computer program considering the biaxial state of stress.

Figure(6.2) shows similar design curves considering the longitudinal cracking moment determined from the computer program and the ultimate moment calculated according to the ultimate stress block method⁽³⁸⁾. This can be used to select the concrete compressive strength, the steel beam yield stress and the percentage of the top transverse reinforcement required to ensure that the longitudinal cracking would occur close enough to the ultimate moment of the beam as calculated from the ultimate stress block method⁽³⁸⁾ which is the practical method of design of composite beams.

Figure (6.3) shows the relationship between the

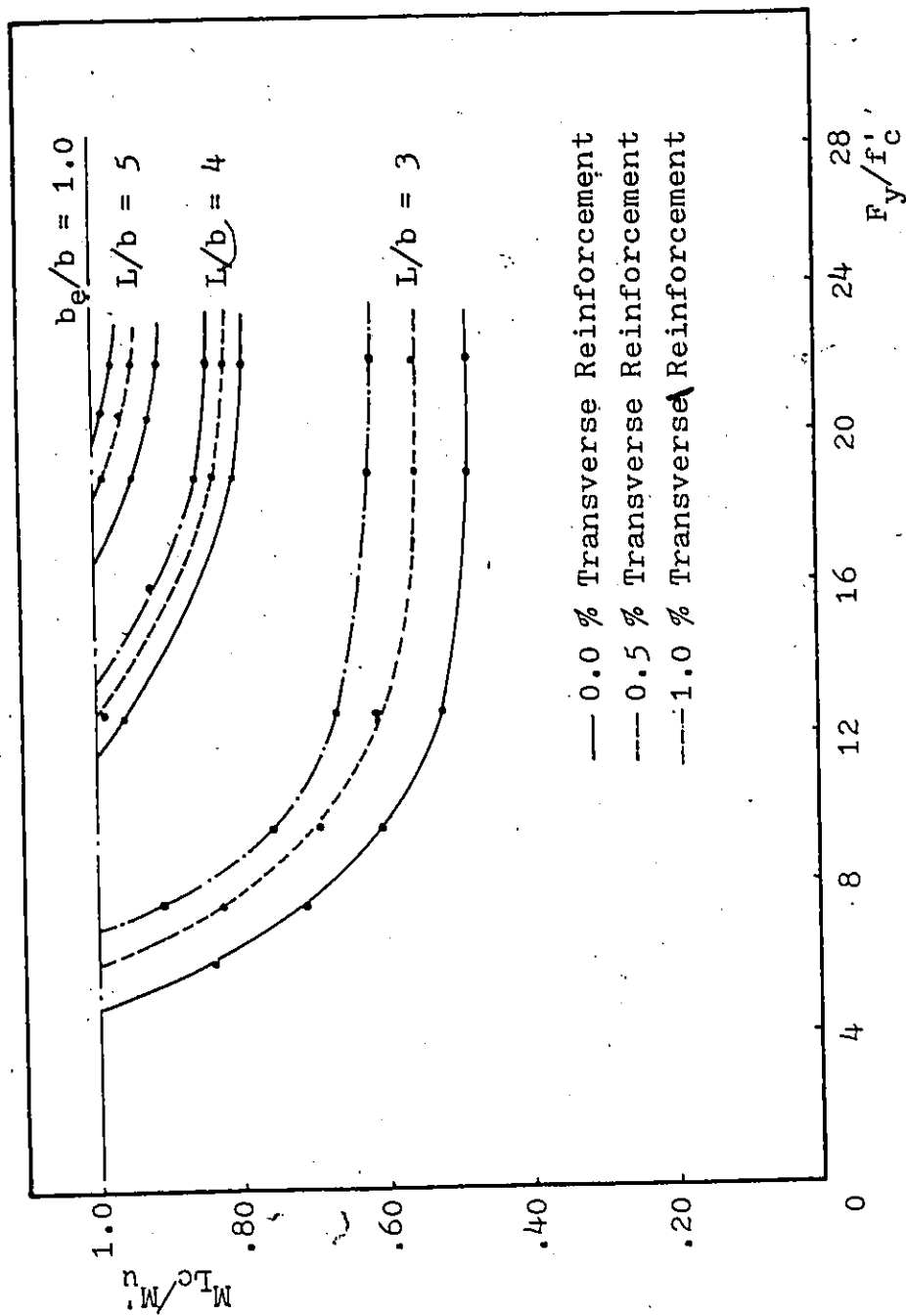


Fig.(6.2) Relationship between the Longitudinal Cracking Moment and the Properties of the Composite Beam (Using the Ultimate Stress Block Method)

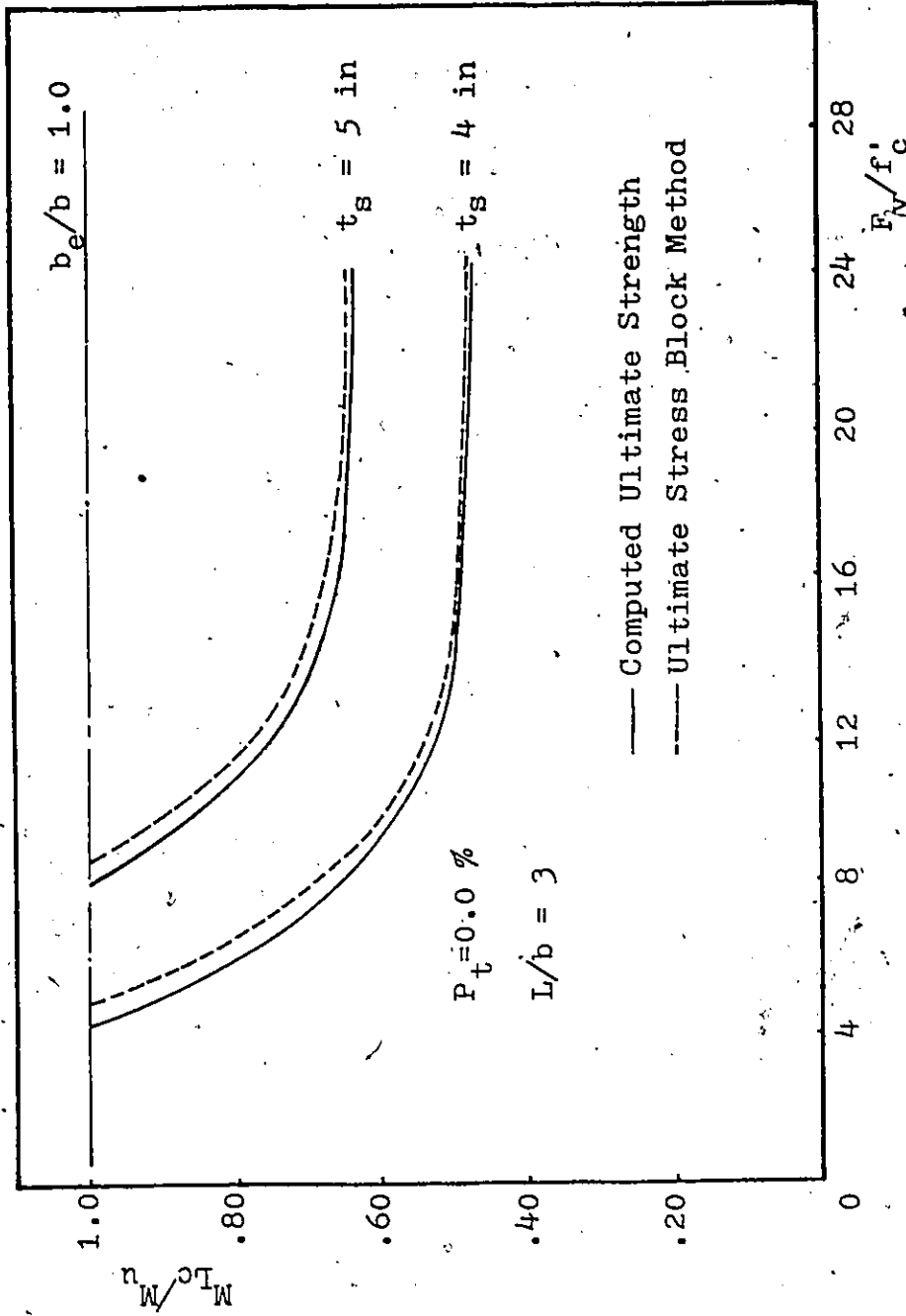


Fig.(6.3) Effect of the Thickness of the Solid Part of the Slab on the Longitudinal Cracking of Composite Beams with Ribbed Metal Deck

longitudinal cracking moment to the ultimate moment ratio, M_{Lc}/M_u , and the beam yield stress to concrete compressive strength ratio, F_y/f'_c , for a span to width ratio equal to 3. It shows a comparison between two different overall thicknesses of the slab. The two slabs have the same 1-1/2-in ribbed metal deck but the thickness of the solid parts is different. This comparison shows that the increase of the thickness of the solid part of the slab has a considerable effect on the increase of the longitudinal cracking moment. However, this solution could be considered as an uneconomic solution.

The data presented in fig.(6.2) is used to plot a set of design curves, fig.(6.4), that can be used to select directly the proper material properties and percentage of transverse reinforcement for any specific composite beam with ribbed metal deck such that the longitudinal cracking would occur simultaneously with the ultimate capacity of the beam. These curves are plotted using the ultimate moment calculated according to the ultimate stress block method which is the practical design method.

For any composite beam with a specific span-to-width ratio, use can be made of fig.(6.4) to determine the percentage of top transverse reinforcement and the steel yield stress to concrete strength ratio required to ensure the achievement of the ultimate capacity before or simultaneously with the occurrence of the longitudinal cracking. Now, if the yield stress of the steel beam is

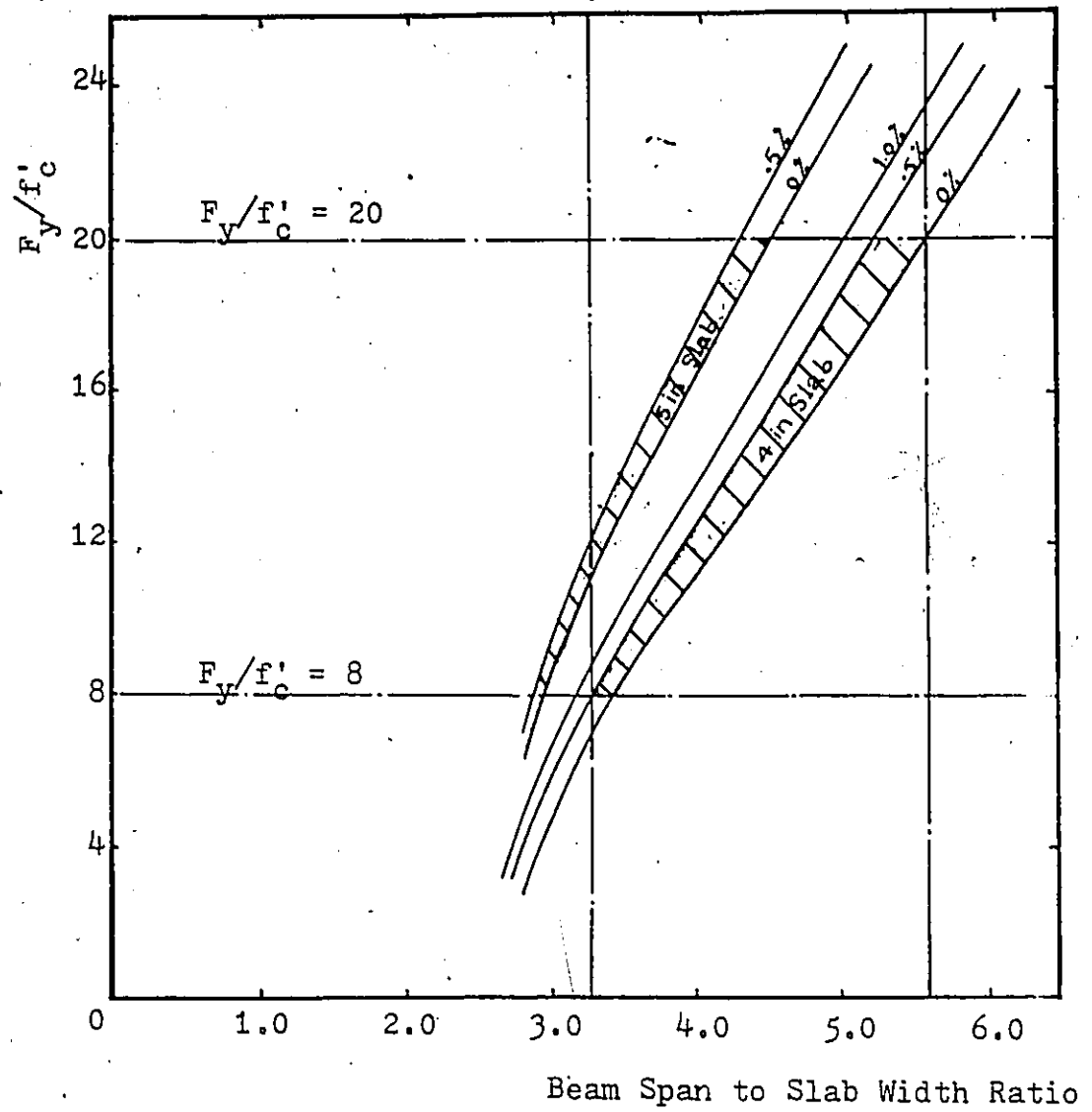


Fig.(6.4) Composite Beam Properties to Achieve the Ultimate Capacity Simultaneously with the Longitudinal Cracking

known, it is possible to estimate the compressive strength of concrete required. Generally, it is usually possible to make more than one choice for the same composite beam, like a small yield stress to concrete strength ratio with small percentage of transverse reinforcement or a larger yield stress to concrete strength ratio with greater amount of reinforcement. The final choice is to be governed by the economic points of view. However, it is to be mentioned that the transverse reinforcement effect is small compared to the effect of the compressive strength of concrete. Interpolation can be used for percentages of transverse reinforcement that do not exist in fig.(6.4).

If we put some practical limits for the steel beam yield stress to the concrete compressive strength ratio, as shown in fig.(6.4), it will be possible to draw the following conclusions:

1. For $L/b \geq 5.60$, there is no longitudinal cracking problem even without any top transverse reinforcement. In such a case, the slab will be reinforced with a 6 x 6/10 x 10 welded wire mesh which is the common practice to account for shrinkage in concrete.

2. For $3.25 \leq L/b < 5.60$, there is a longitudinal cracking problem before the ultimate capacity of the composite beam is achieved. However, this longitudinal cracking problem can be solved by means of the appropriate selection of the concrete strength and the percentage of the top

transverse reinforcement, fig.(6.4), to ensure that the ultimate capacity would be achieved before or simultaneously with the occurrence of the longitudinal cracking.

3. For $L/b < 3.25$, there is a longitudinal cracking problem that needs an excessive amount of transverse reinforcement and/or a very small steel yield stress to concrete strength ratio, which is impractical. In such a case, we are left with one of two alternatives:

- a. To go to the uneconomic solution of increasing the thickness of the solid part of the slab, fig.(6.4)
- b. To accept the occurrence of the longitudinal crack at an earlier stage but to try to select the percentage of transverse reinforcement, the steel beam yield stress and the concrete compressive strength, fig.(6.2), such that the crack would occur as close as possible to the ultimate state.

CHAPTER 7

SUMMARY AND CONCLUSIONS

7.1 Summary

The inelastic behaviour of composite beams with ribbed metal deck, subjected to uniformly distributed load over the slab area, was investigated.

A biaxial failure criteria was adopted for the concrete slab to account for the biaxial state of stress in the slab. Cracking and crushing of the concrete slab and yielding of the steel beam and the steel reinforcement were included in the analysis.

A layered finite element model was used to permit analysis of any variation in material properties through the depth of the slab. Thus, it was possible to represent separately the longitudinal and transverse reinforcement and the metal deck in the analysis. For the nonlinear solution, an incremental and iterative technique using the tangent modulus stiffness approach, was adopted in this investigation.

Some experimental results, obtained from testing composite beams with solid and ribbed slabs, were used for comparison to demonstrate the applicability of the model in predicting the inelastic behaviour of composite beams.

A study of the effect of the type of loading and the transverse moment in the slab on the load-deformation behaviour and the ultimate capacity of composite beams with ribbed metal deck was presented.

The effective width of composite beams with ribbed metal deck subjected to uniformly distributed load, was investigated. The variation of the effective width in the inelastic stage as well as the effective slab width at the ultimate load were also studied.

A study of the longitudinal cracking of composite beams with ribbed metal deck, subjected to uniformly distributed load over the slab area, was presented. A parametric study of the different factors affecting the longitudinal cracking of composite beams, such as the transverse moment in the slab, the beam span to slab width ratio, the compressive strength of concrete, the transverse reinforcement and the thickness of the solid part of the slab, was also presented. Some design recommendations in the form of design curves were proposed to compensate for early longitudinal cracking of composite beams with ribbed metal deck subjected to uniformly distributed load over the entire slab.

7.2 Conclusions

Some general conclusions that have been drawn from the overall study, concerning the behaviour characteristics of

composite beams with ribbed metal deck, are presented below:

1. The current methods of testing composite beams with ribbed metal deck, by loading over the steel beams and considering free slab edges, can give satisfactory results with respect to the ultimate capacity and the deflection of an intermediate composite beam in a composite floor system. The results obtained for a uniformly distributed load over the entire slab with constrained boundary conditions at its edges ($u=\theta_y=0$) and for a third point loading over the beam with free slab edges are almost identical.

2. The effective width of composite beams with ribbed metal deck is affected by the beam-span-to-slab-width ratio. The effective width increases with increase of the span-to-width ratio. For a uniformly distributed load over the slab area, the effective width to actual width ratio varies between 0.92 and 1.0, for span to width ratios of 3 to about 7.

3. The effective widths of composite beams with solid and ribbed slabs, subjected to uniformly distributed load over the slab area, are almost identical with about 2 percent difference, provided the two slabs have the same overall thickness. For a composite beam with a 4-in solid slab, the effective width equals the total width of the slab if the beam span to slab width ratio is equal to or greater than 5. However for a composite beam with a 1-1/2-in ribbed metal deck and a 2-1/2-in solid concrete part, the slab effective width equals the total width if the span to width ratio is equal to or greater than 7.5.

4. The effective width at the ultimate load of a composite beam with ribbed metal deck, subjected to uniformly distributed load over the slab area, always reaches or exceeds the effective width in the elastic stage, with a maximum difference of about 4 percent. Thus, it is conservative and quite satisfactory to use the effective width based on an elastic analysis, at the ultimate state.

5. The type of loading affects the effective width to a great extent. The one point load at mid-span of the beam may give an effective width about 20 percent smaller than if the slab were loaded with a uniformly distributed load over its entire area. Thus, the effective slab width should be specified according to the type of loading. However, a general specification should be prepared for a uniformly distributed load, which is the most common type of loading. Some special recommendations should be prepared for any other type of load in the form of effective width reduction factors with respect to the case of the uniformly distributed load (e.g., in the case of one point load and for $L/b=4$, this reduction factor is in the order of about 20 percent).

6. It is important to delay the occurrence of the longitudinal cracking in the concrete slab such that the theoretical ultimate capacity of the composite beam can be achieved before or simultaneously with the crack occurrence.

7. The type of loading affects the longitudinal cracking of composite beams with ribbed metal deck to a great extent.

If the composite beam is loaded by point loads over the steel beam, the longitudinal crack starts near the bottom fibre of the slab due to the longitudinal shear effect, in the absence of any transverse moment. In this case, if any transverse reinforcement is needed, it should be placed in the ribs near the bottom fibre of the slab. However, if the slab is loaded, it seems that the transverse negative moment effect suppresses the longitudinal shear effect such that the crack usually starts near the top fibre of the slab. In this latter case, if any transverse reinforcement is required, it should be placed near the top fibre of the slab.

8. The metal deck plays a negligible role in improving the longitudinal cracking load of composite beams loaded with uniformly distributed load over the slab area. However, if the composite beam is loaded by point loads over the steel beam, the metal deck increases the longitudinal cracking moment by about 15 percent, depending on the beam span to slab width ratio.

9. The properties of the materials used in a composite beam, especially the concrete compressive strength and the steel beam yield stress, have a considerable effect on the longitudinal cracking of composite beams with ribbed metal deck subjected to uniformly distributed load over the slab area. The decrease of the beam yield stress to concrete compressive strength ratio, increases the longitudinal

cracking moment to ultimate moment ratio.

10. The thickness of the solid part of the slab plays a considerable role in increasing the longitudinal cracking moment of composite beams with ribbed metal deck. One inch increase in the slab thickness may increase the longitudinal cracking moment to ultimate moment ratio by about 20 percent. However, increasing the slab thickness is not recommended from an economic point of view.

11. The increase of the top transverse reinforcement, increases the longitudinal cracking load. However, the effect of the transverse reinforcement is not very appreciable for beam span to slab width ratios greater than 3. For span to width ratio equal to 3, a 0.50 percent increase in the transverse reinforcement increases the longitudinal cracking moment to ultimate moment ratio by about 14 percent. But, for span to width ratios equal to or greater than 4, the increase in the longitudinal cracking moment to ultimate moment ratio is only of the order of about 5 percent.

12. The beam-span-to-slab-width ratio is one of the main factors affecting the longitudinal cracking of composite beams with ribbed metal deck, subjected to uniformly distributed load over the slab area. The longitudinal cracking moment increases with the increase of this ratio. Generally, composite beams with ribbed metal deck may be classified according to the span to width ratio as follows:

- a. If the span to width ratio is equal to or greater than 5.60, there is no longitudinal cracking problem. The ultimate capacity of the composite beam will be attained before or simultaneously with the occurrence of the longitudinal crack. In this case, no transverse reinforcement is required and only a 6x6/10x10 welded wire mesh will be needed to account for shrinkage in the concrete slab.
- b. If the span to width ratio is smaller than 5.6 but greater than or equal to 3.25, longitudinal cracking may occur before the ultimate capacity is reached. However, this problem can be solved by the proper selection of the concrete and steel properties and the percentage of the transverse reinforcement, fig.(6.4), such that the ultimate capacity of the composite beam can be reached before or simultaneously with the crack occurrence. It should also be mentioned that the effect of the increase of the concrete compressive strength in increasing the cracking moment is considerably greater than the effect of the increase of the percentage of the transverse reinforcement.
- c. If the span to width ratio is smaller than 3.25, longitudinal cracking would occur before the ultimate capacity is achieved. However, a proper selection of the steel and concrete properties

together with a practical increase of the percentage of transverse reinforcement can improve the longitudinal cracking moment such that the crack would occur in the neighbourhood of about 90 percent of the ultimate capacity. Increasing the thickness of the solid part of the slab may be considered as another alternative to increasing the longitudinal cracking moment, if it is accepted from the economic point of view.

APPENDIX A

FINITE ELEMENT APPROACH

A.1 Introduction

Recent progress in the application of the finite element technique to non-linear problems has been reported in a large number of papers, for e.g. (34,39,48,55,56,60).

The reliability of the layered finite element tangent stiffness approach in the study of elastic and inelastic reinforced concrete slabs has been reported by several investigators (25,26,34,39,53). They have demonstrated the advantages of the layered approach in following the variation in material properties, such as cracking or crushing of concrete or yielding of the steel beam, through the different stages of loading.

It has been demonstrated⁽⁶⁴⁾ how the stiffness matrix of a plate can be combined with that of other elements such as beams. This can be quite useful in the determination of the structural response of composite beams.

A finite element analysis was presented⁽²³⁾ to study the elastic behaviour of skewed composite girder bridges. The use of a combined plate element, for the solid concrete

slab, and beam element, for the steel beam, was demonstrated in this analysis.

Recent progress in the application of the finite element technique has led to a reliable approach for finding the inelastic response of eccentrically stiffened plates^(60,61,62). This approach has shown that a stiffened plate structure can adequately be discretized using plate and eccentrically attached beam elements. Furthermore, the use of the layering concept has allowed the inclusion of the cracking and crushing of the solid concrete slab and the yielding of the steel beam.

In this study, the application of the layered finite element approach in the inelastic analysis of composite beams with ribbed metal deck is described. The particular finite element approach taken is the displacement formulation.

The first step is to discretize the structure into a suitable number of finite plate and beam elements. In order to arrive at a simple formulation for this analysis, it is necessary that the beams are attached along the mesh lines of the plate elements. As shown in fig.(A.1), rectangular elements involving the four nodal points I, J, K and L are used to discretize the slab and beam straight line elements involving the two nodal points I and J are used to discretize the beam.

The beam and slab elements are subdivided into a suitably chosen number of layers in order to describe the process of cracking and crushing in the slab, and the yielding

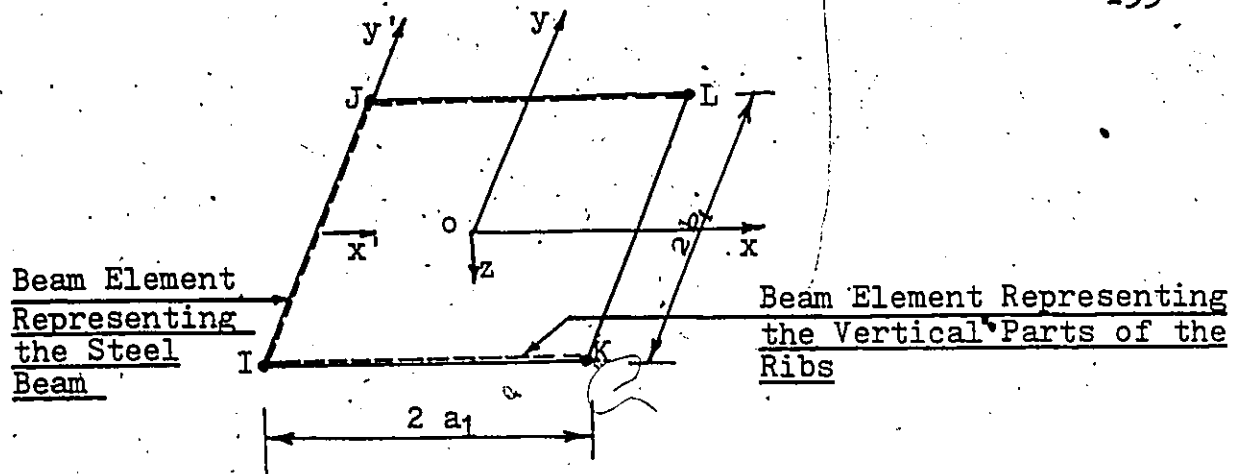


Fig.(A.1) Plate and Beam Nodal Numbering System and Elements Local Coordinate System

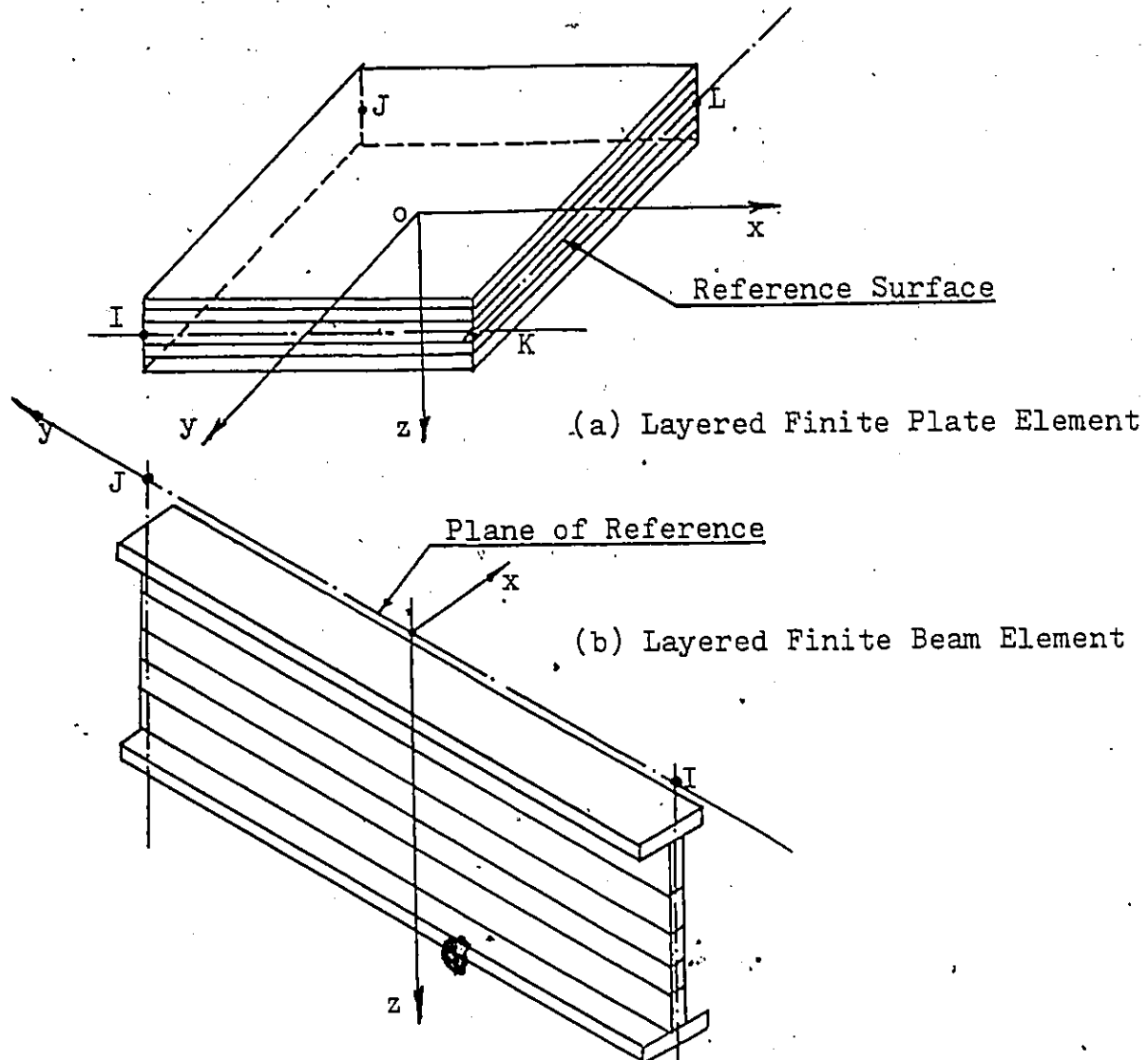


Fig.(A.2) Layered Beam and Plate Finite Elements

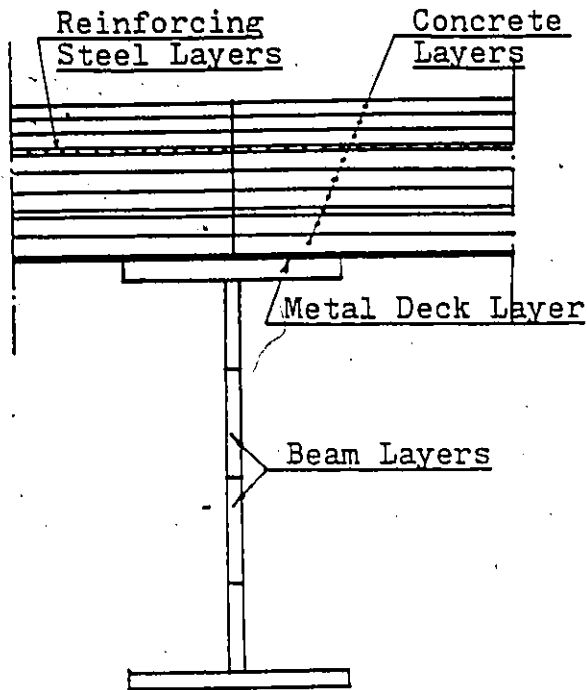
in the beam, fig.(A.2).

By introducing the layering concept, it is possible to have a variation in material properties across the thickness while avoiding a three dimensional finite element analysis. The total number of degrees of freedom depends solely on the number of nodal points and not on the number of layers introduced.

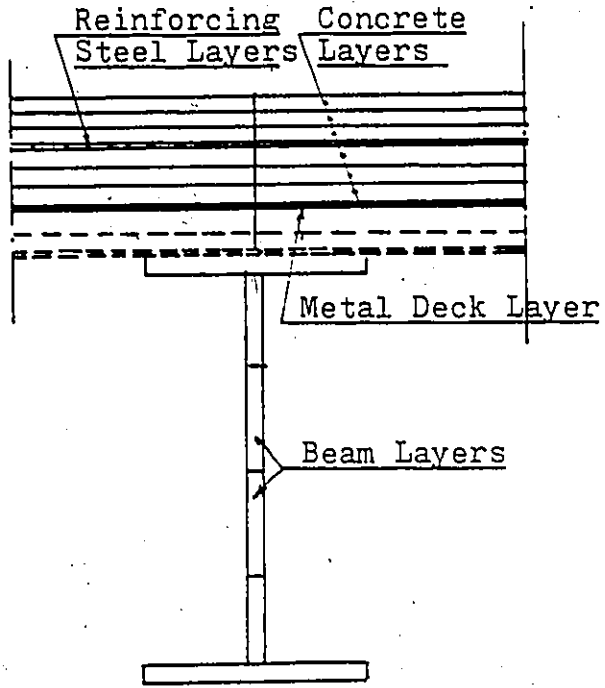
The reinforced concrete ribbed slab is modeled as an assemblage of plain concrete layers, reinforcing steel layers and metal deck layers, fig.(A.3). Each layer is assumed to be in a state of plane stress, and that the state of stress at the geometric centroid of the layer is taken as representative for the entire layer.

The reinforcing steel is replaced by an equivalent uniformly distributed steel layer, fig.(A.3), with stiffness only in the direction of the reinforcement. The equivalent thickness of the steel layer is determined such that the corresponding area of reinforcement in the layer remains unchanged. There could be one or more of these reinforcing steel layers at any depth and in any direction in the slab. Perfect bond is assumed to exist between the reinforcing steel and the surrounding concrete.

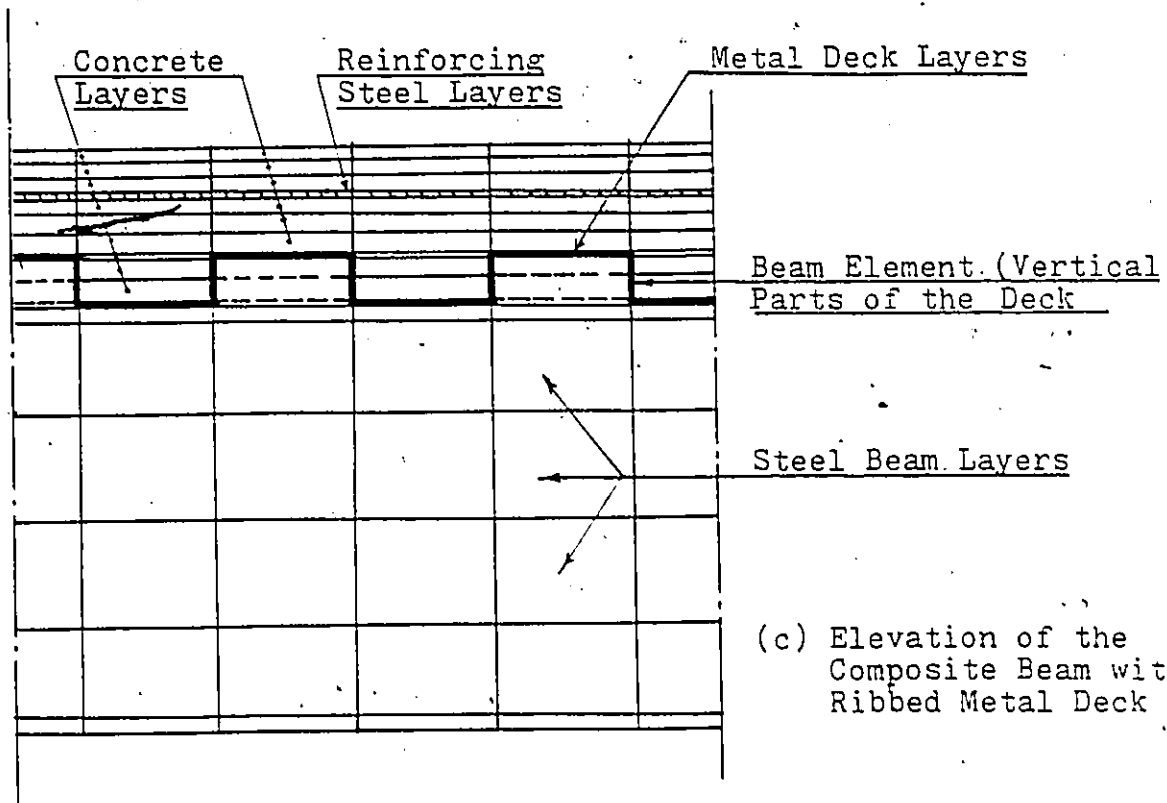
The horizontal parts of the ribbed metal deck are represented by discrete steel layers with stiffness only in the direction perpendicular to the steel beam, fig.(A.3). The vertical parts of the ribbed metal deck are represented



(a) Cross Section of the Composite Beam in the Ribbed Part of the Slab



(b) Cross Section of the Composite Beam in the Non-Ribbed Part of the Slab



(c) Elevation of the Composite Beam with Ribbed Metal Deck

Fig.(A.3) Composite Beam Modelling

by beam line elements attached along the mesh lines of the slab rectangular elements in the direction perpendicular to the steel beam, fig.(A.3-c). Perfect bond is assumed to exist between the metal deck and the surrounding concrete.

All nodal points are defined in a common plane. This plane will be called the plane of reference and is assumed to coincide with the middle plane of the solid part of the ribbed slab. The response of the composite beam must first be found with respect to this plane.

Five displacement components are introduced as unknowns at each nodal point (u , v , w , θ_x and θ_y). These five deformation components enable the description of the state of deformation in a plate and beam element. Compatibility of deformation must be enforced along the juncture lines between the beam and the slab since complete interaction is assumed.

An incremental and iterative technique, using the tangent stiffness approach, is adopted in this research work.

A.2 Derivation of Bending and Inplane Plate Stiffness Matrix

For the present analysis, the rectangular element originally proposed by Melosh⁽⁴⁴⁾ and described in detail by Zienkiewicz^(63,64) is used. Figure (A.4) shows the element nodal numbering system and the positive directions of the

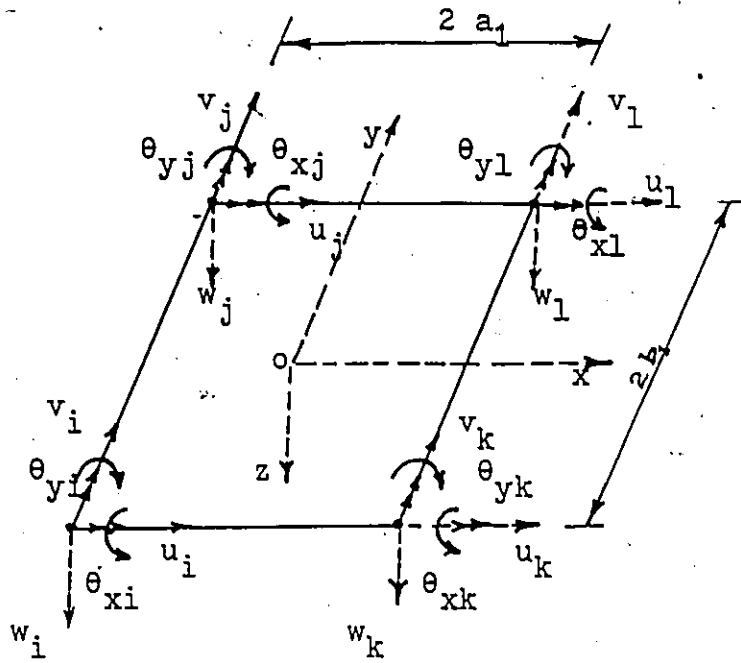


Fig.(A.4) Positive Orientation of the Nodal Degrees of Freedom

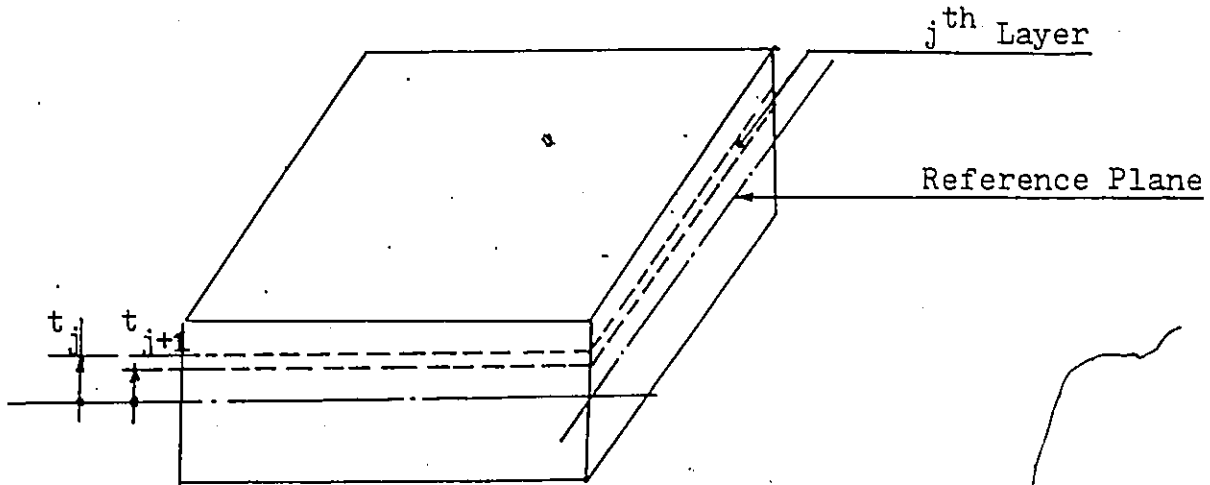


Fig.(A.5) Position of the j^{th} Layer

nodal degrees of freedom.

An incomplete fourth-order polynomial is used for representation of the lateral deflection of the plate. Three degrees of freedom are associated with the out-of-plane behaviour at each point, i.e., the lateral deflection, w , and the two slopes, θ_x and θ_y , of the deflected plate surface. Two more degrees of freedom per nodal point are associated with the in-plane behaviour: namely, u , the in-plane displacement in the x -direction, and v , the in-plane displacement in the y -direction.

The displacement functions of the element and the nodal displacements are written at a reference plane which is parallel to, but at an arbitrary distance from the beam, fig.(A.2). This plane of reference is chosen to coincide with the middle plane of the solid part of the ribbed slab.

$$\left. \begin{aligned} u &= \alpha_1 + \alpha_2 x + \alpha_3 y + \alpha_4 xy \\ v &= \alpha_5 + \alpha_6 x + \alpha_7 y + \alpha_8 xy \\ w &= \alpha_9 + \alpha_{10} x + \alpha_{11} y + \alpha_{12} xy + \alpha_{13} x^2 + \alpha_{14} y^2 \\ &\quad + \alpha_{15} x^3 + \alpha_{16} x^2 y + \alpha_{17} xy^2 + \alpha_{18} y^3 + \alpha_{19} x^3 y \\ &\quad + \alpha_{20} xy^3 \end{aligned} \right\} \quad (A.1)$$

The strain-displacement relations used are,

$$\left. \begin{aligned}
 \epsilon_{x_0} &= \partial u / \partial x \\
 \epsilon_{y_0} &= \partial v / \partial y \\
 \epsilon_{xy_0} &= \partial u / \partial y + \partial v / \partial x \\
 \chi_x &= -\partial^2 w / \partial x^2 \\
 \chi_y &= -\partial^2 w / \partial y^2 \\
 2\chi_{xy} &= 2(\partial^2 w / \partial x \partial y)
 \end{aligned} \right] \quad (A.2)$$

These relations include the following assumptions:

1. The normal to the undeformed surface remains straight and normal to the deformed surface.

2. Normals will undergo no extension when the plate is deformed.

3. The strains and deformations of the plate are small compared to the thickness of the plate.

Assumption one implies that there is no deformation due to transverse shear. The error involved in this assumption is small provided the plate is thin. This assumption enables the strains at a positive distance z from the reference surface to be expressed as:

$$\left. \begin{aligned}
 \epsilon_x &= \epsilon_{x_0} + z \cdot \chi_x \\
 \epsilon_y &= \epsilon_{y_0} + z \cdot \chi_y \\
 \epsilon_{xy} &= \epsilon_{xy_0} + 2z \cdot \chi_{xy}
 \end{aligned} \right] \quad (A.3)$$

Assumption three implies the use of the small deflection theory.

The nodal degrees of freedom defined at the reference surface can be written as,

$$\{\bar{U}\}_{5 \times 1} = \begin{Bmatrix} u \\ v \\ w \\ \theta_y \\ \theta_x \end{Bmatrix} = \begin{Bmatrix} u \\ v \\ w \\ \partial w / \partial x \\ \partial w / \partial y \end{Bmatrix}$$

The displacement at one node expressed in terms of the generalized displacement coefficients α are

$$\{\bar{U}\}_{5 \times 1} = [M]_{5 \times 20} \{\alpha\}_{20 \times 1} \quad (\text{A.4})$$

Where

$$[M] = \begin{bmatrix} 1 & x & y & xy & \dots & \dots & \dots & \dots & \dots & \dots & \dots & \dots & \dots & \dots & \dots & \dots & \dots & \dots & \dots & \dots \\ \dots & \dots & \dots & 1 & x & y & xy & \dots & \dots & \dots & \dots & \dots & \dots & \dots & \dots & \dots & \dots & \dots & \dots & \dots \\ \dots & \dots & \dots & \dots & \dots & \dots & 1 & x & y & xy & x^2 & y^2 & x^3 & x^2 y & xy^2 & y^3 & x^3 y & xy^3 & \dots & \dots \\ \dots & \dots & \dots & \dots & \dots & \dots & \dots & 1 & y & 2x & 3x^2 & 2xy & y^2 & \dots & 3x^2 y & y^3 & \dots & \dots & \dots & \dots \\ \dots & \dots & \dots & \dots & \dots & \dots & \dots & \dots & -1 & -x & -2y & \dots & -x^2 & -2xy & -3y^2 & -x^3 & -3xy^2 & \dots & \dots & \dots \end{bmatrix}$$

Using the element nodal numbering system, fig.(A.4), a vector of element nodal displacements may be expressed as,

$$\{U\}_{20 \times 1} = \begin{Bmatrix} \bar{U}_i \\ \bar{U}_j \\ \bar{U}_k \\ \bar{U}_l \end{Bmatrix}_{20 \times 1} = \begin{Bmatrix} [M_i] \\ [M_j] \\ [M_k] \\ [M_l] \end{Bmatrix}_{20 \times 20} \{\alpha\}_{20 \times 1}$$

i.e.,

$$\{U\}_{20 \times 1} = [A]_{20 \times 20} \{\alpha\}_{20 \times 1}$$

Where

$$[A] = \begin{Bmatrix} M_i \\ M_j \\ M_k \\ M_l \end{Bmatrix}$$

The inverse of this relationship, which will be desired later, is

$$\{\alpha\}_{20 \times 1} = [A^{-1}]_{20 \times 20} \{U\}_{20 \times 1} \quad (A.5)$$

The strain-displacement relations, eqn.(A.2), may be written as

$$\{\bar{\epsilon}\}_{6 \times 1} = \begin{Bmatrix} \epsilon \\ \chi \end{Bmatrix}_{6 \times 1} = \{D\}_{6 \times 5} \{\bar{U}\}_{5 \times 1} \quad (A.6)$$

Where

$\{\epsilon\}_{3 \times 1}$ = Vector of reference surface strains

$\{\chi\}_{3 \times 1}$ = Vector of Curvatures

$$\begin{bmatrix} \epsilon \\ \chi \end{bmatrix} = \begin{bmatrix} \epsilon_{x_0} \\ \epsilon_{y_0} \\ \epsilon_{xy_0} \\ \chi_x \\ \chi_y \\ 2\chi_{xy} \end{bmatrix}$$

$[D]_{6 \times 5}$ = Matrix of differential operators

$$= \begin{bmatrix} \partial/\partial x & . & . & . & . \\ . & \partial/\partial y & . & . & . \\ \partial/\partial y & \partial/\partial x & . & . & . \\ . & . & . & -\partial/\partial x & . \\ . & . & . & . & \partial/\partial y \\ . & . & . & \partial/\partial y & -\partial/\partial x \end{bmatrix}$$

Substitution of eqn. (A.4) into eqn. (A.6), yields

$$\{\bar{\epsilon}\}_{6 \times 1} = [D]_{6 \times 5} [M]_{5 \times 20} \{\alpha\}_{20 \times 1}$$

i.e.

$$\{\bar{\epsilon}\}_{6 \times 1} = [B]_{6 \times 20} \{\alpha\}_{20 \times 1} \quad (A.7)$$

Which relates the reference surface strains and curvatures to the unknown coefficients.

Where

$$[B] = \begin{bmatrix} \cdot & 1 & \cdot & y & \cdot & \cdot & \cdot & \cdot & \cdot & \cdot & \cdot & \cdot & \cdot & \cdot & \cdot & \cdot \\ \cdot & \cdot & \cdot & \cdot & \cdot & \cdot & 1 & x & \cdot & \cdot & \cdot & \cdot & \cdot & \cdot & \cdot & \cdot \\ \cdot & \cdot & 1 & x & \cdot & 1 & \cdot & y & \cdot & \cdot & \cdot & \cdot & \cdot & \cdot & \cdot & \cdot \\ \cdot & \cdot & \cdot & \cdot & \cdot & \cdot & \cdot & \cdot & \cdot & \cdot & -2 & \cdot & -6x & -2y & \cdot & \cdot & -6xy & \cdot \\ \cdot & \cdot & \cdot & \cdot & \cdot & \cdot & \cdot & \cdot & \cdot & \cdot & -2 & \cdot & \cdot & -2x & -6y & \cdot & -6xy & \cdot \\ \cdot & \cdot & \cdot & \cdot & \cdot & \cdot & \cdot & \cdot & \cdot & \cdot & \cdot & 2 & \cdot & \cdot & \cdot & 4x & 4y & \cdot & 6x^2 & 6y^2 \end{bmatrix}$$

Expressing strains at any depth as a function of middle surface deformation according to Kirchoff hypothesis, yields

$$\{\epsilon\}_{3 \times 1} = [G]_{3 \times 6} \left\{ \frac{\epsilon}{\chi} \right\}_{6 \times 1} \quad (A.8)$$

Where

$$[G]_{3 \times 6} = \begin{bmatrix} 1 & 0 & 0 & z & 0 & 0 \\ 0 & 1 & 0 & 0 & z & 0 \\ 0 & 0 & 1 & 0 & 0 & z \end{bmatrix}$$

The last expression required is to relate stress to strain, namely

$$\{f\}_{3 \times 1} = [C]_{3 \times 3} \{\epsilon\}_{3 \times 1} \quad (A.9)$$

Where $[C]$ is the material properties matrix

From the internal work expression,

$$W_{int} = \int_V \frac{1}{2} \{\epsilon\}^T \{f\} dv$$

which is integrated over the volume of the element, after substituting from eqns. (A.9, A.8, A.7 & A.5) obtains

$$W_{int} = \int_V \frac{1}{2} \{U\}^T [A^{-1}]^T [B]^T [G]^T [C] [G] [B] [A^{-1}] \{U\} dv$$

From the internal work expression, the internal virtual work is obtained by performing a variation on $\{U\}$. Thus,

$$\delta W_{int} = \int_V \{\delta U\}^T [A^{-1}]^T [B]^T [G]^T [C] [G] [B] [A^{-1}] \{U\} dv$$

But, since $[A^{-1}]$ and $\{U\}$ are independent of x , y and z , and $[B]$ is independent of z ,

$$\delta W_{int} = \{\delta U\}^T [A^{-1}]^T \int_A [B]^T \int_z [G]^T [C] [G] dz [B] dA [A^{-1}] \{U\}$$

Where

$$[K]_{20 \times 20} = [A^{-1}]^T \int_A [B]^T \int_Z [G]^T [C] [G] dz [B] dA [A^{-1}] \quad (A.10)$$

is the desired element stiffness matrix.

Performing the matrix multiplication for $[G]^T [C] [G]$ and calling the product $[\bar{D}]$ yields,

$$[\bar{D}]_{6 \times 6} = \begin{bmatrix} C_{3 \times 3} & z C_{3 \times 3} \\ z C_{3 \times 3} & z^2 C_{3 \times 3} \end{bmatrix} \quad (A.11)$$

Substituting of $[D]$ into eqn.(A.10), yields

$$[K]_{20 \times 20} = [A^{-1}]^T_{20 \times 20} \int_A [B]^T_{20 \times 6} \int_Z [\bar{D}]_{6 \times 6} dz [B]_{6 \times 20} dA [A^{-1}]_{20 \times 20} \quad (A.12)$$

In evaluating the element stiffness matrix, the mechanics of the layering concept only require that the innermost integral of eqn.(A.12) be integrated for each layer individually rather than as one integration over the total thickness. If the element thickness is divided into layers as shown in fig.(A.5), then this requires that,

$$\int_Z [\bar{D}] dz = \int_{t_1}^{t_2} [\bar{D}_1] dz + \int_{t_2}^{t_3} [\bar{D}_2] dz + \dots + \int_{t_j}^{t_{j+1}} [\bar{D}_i] dz + \dots + \int_{t_N}^{t_{N+1}} [\bar{D}_N] dz \quad (A.13)$$

Where

t_j and t_{j+1} = The distance from the reference surface to the top and bottom surface of the j^{th} layer respectively.

$[\bar{D}_j]$ = Expression (A.11) with the material properties for the j^{th} layer incorporated.

N = Number of layers.

This is simply a step-wise evaluation of a total integral. The integrated form of one of the right hand side integrals in eqn.(A.13) is

$$\int_{t_j}^{t_{j+1}} [\bar{D}_j] dz = \left[\begin{array}{c|c} (t_{j+1}-t_j) [C_j] & 1/2 (t_{j+1}^2-t_j^2) [C_j] \\ \hline 1/2 (t_{j+1}^2-t_j^2) [C_j] & 1/3 (t_{j+1}^3-t_j^3) [C_j] \end{array} \right] \quad (\text{A.14})$$

This equation together with eqn.(A.13) is the very heart of the layering concept.

To begin the actual evaluation of an element, let the three submatrices in eqn.(A.14) be denoted as $[D_j]$, $[H_j]$ and $[F_j]$, where

$$\int_{t_j}^{t_{j+1}} [\bar{D}_j] dz = \left[\begin{array}{c|c} [D_j] & [H_j] \\ \hline [H_j] & [F_j] \end{array} \right]_{6 \times 6}$$

and let,

$$\int_z [D] dz = \begin{bmatrix} [D] & [H] \\ [H] & [F] \end{bmatrix} \quad (\text{A.15})$$

Where the j^{th} subscript implies the j^{th} layer only and no subscript implies the subintegrals over all the layers.

When eqn.(A.14) is evaluated for each layer and summed, the result is eqn.(A.15). Equation(A.15) may then be substituted in eqn.(A.12) to yield,

$$[K]_{20 \times 20} = [A^{-1}]^T \int_{xy} [B]^T \begin{bmatrix} D & H \\ H & F \end{bmatrix} [B] dx dy [A^{-1}]$$

If $[B]$ is partitioned to separate the membrane effects, $[B_\epsilon]$, from the bending effects, $[B_\chi]$, then eqn.(A.12) may be expressed as,

$$\begin{aligned} [K]_{20 \times 20} &= [A^{-1}]^T \int_{-a_1}^{a_1} \int_{-b_1}^{b_1} \begin{bmatrix} B_\epsilon \\ B_\chi \end{bmatrix} \begin{bmatrix} D & H \\ H & F \end{bmatrix} \begin{bmatrix} B_\epsilon \\ B_\chi \end{bmatrix} dx dy [A^{-1}] \quad (\text{A.16}) \\ &= [A^{-1}]^T [K^*] [A^{-1}] \end{aligned}$$

Where

$$[K^*] = \int_{-a_1}^{a_1} \int_{-b_1}^{b_1} \begin{bmatrix} B_\epsilon \\ B_\chi \end{bmatrix} \begin{bmatrix} D & H \\ H & F \end{bmatrix} \begin{bmatrix} B_\epsilon \\ B_\chi \end{bmatrix} dx dy$$

A.3. Determination of the Reference Surface Strains

From the equations in the previous section, it is possible to express the strains and curvatures of the reference surface in terms of the nodal displacements.

$$\begin{aligned}
 \begin{Bmatrix} \epsilon \\ \chi \end{Bmatrix}_{6 \times 1} &= [D][M]\{\alpha\} \\
 &= [B]\{\alpha\} \\
 &= [B][A^{-1}]\{U\} \qquad (A.17)
 \end{aligned}$$

This expression defines the distribution of strains and curvatures over the element based on the nodal displacements. It is used to calculate the reference surface strains and curvatures at the centroid of the element ($x=y=0$).

A.4. Determination of the Layer Stresses

In order to determine the layer stresses it is necessary to first determine the layer strains. The j^{th} layer strains at the mid-depth of the layer are,

$$\epsilon_x = \epsilon_{x_0} + 1/2(t_{j+1} + t_j) \cdot \chi_x$$

$$\epsilon_y = \epsilon_{y_0} + 1/2(t_{j+1} + t_j) \cdot \chi_y$$

$$\epsilon_{xy} = \epsilon_{xy_0} + 1/2(t_{j+1} + t_j)(2\chi_{xy})$$

Where $1/2(t_{j+1} + t_j)$ is the distance from the middle surface to the mid-depth of the j^{th} layer. These mid-depth layer strains are assumed to be representative of the strains in the layer.

Based on the representative layer strain, some representative component layer stresses are obtained through the use of the component material properties, as follows

$$\begin{bmatrix} f_x \\ f_y \\ f_{xy} \end{bmatrix} = [C]_{3 \times 3} \begin{bmatrix} \epsilon_x \\ \epsilon_y \\ \epsilon_{xy} \end{bmatrix}$$

A.5 Determination of the Excess Nodal Forces

Excess layer stresses are converted to excess element nodal forces by considering the individual terms in the basic equation,

$$\{F\}_{20 \times 1} = [A^{-1}]^T \int_x \int_y [B]^T \int_z [\bar{D}] dz [B] dx dy [A^{-1}] \{U\} \quad (A.18)$$

Using eqns. (A.5 & A.7), one can write

$$\begin{bmatrix} \epsilon_x \\ \epsilon_y \\ \epsilon_{xy} \end{bmatrix} = [B] [A^{-1}] \{U\} \quad (A.19)$$

The stress resultants in the j^{th} layer may be expressed as,

$$\begin{bmatrix} N \\ M \end{bmatrix}_j = \int_z [\bar{D}]_j dz \begin{bmatrix} \epsilon_x \\ \epsilon_y \\ \epsilon_{xy} \end{bmatrix} \quad (A.20)$$

Substitution of eqn.(A.19) in eqn.(A.20), yields

$$\begin{Bmatrix} N \\ M \end{Bmatrix}_j = \int_z [\bar{D}_j] dz [B][A^{-1}]\{U\} \quad (A.21)$$

Substitution of eqn.(A.21) in eqn.(A.18), yields

$$\{F\}_{20 \times 1} = [A^{-1}] \int_x \int_y [B]^T dx dy \begin{Bmatrix} N \\ M \end{Bmatrix}_j$$

If $\begin{Bmatrix} N \\ M \end{Bmatrix}_j^{ex}$ are the excess stress resultants, where

$$\begin{Bmatrix} N \\ M \end{Bmatrix}_j^{ex} = \int_{t_j}^{t_{j+1}} [G]^T \{f\}^{ex} dz$$

and $\{f\}^{ex}$ is the excess layer stress, then

$$\{F_j\}^{ex} = [A^{-1}] \int_x \int_y [B]^T dx dy \begin{Bmatrix} N \\ M \end{Bmatrix}_j^{ex} \quad (A.22)$$

are the excess nodal forces that result from layer j due to the excess stresses in that layer.

A.6 Derivation of Bending and Inplane Beam Stiffness Matrix

In order to be able to study the process of yielding in the beam element, a subdivision into a number of layers as shown in fig.(A.2-b), is performed. It is assumed that the beam

is symmetric about its local z-axis and negligible in bending about this axis. Thus, a beam layer is assumed to be in a state of uniaxial stress for consideration of yielding.

Stresses in beam layers are computed on the basis of a linear distribution of strains extending to the bottom fibre of the beam element. The state of stress at the centroid of each layer is again taken as representative for consideration of yielding. Any layer is identified by its width, thickness and distance to the plane of reference.

A beam element is bounded by two nodal points, I and J, lying in the reference plane of the plate, as shown in fig.(A.2-b). The beam is assumed to be integrally attached to the plate and thus, compatibility of deformation must be enforced along the juncture line between the beam and the slab. Therefore, the same displacement functions chosen to represent the inplane and out-of-plane behaviour of the plate elements must be taken for the beam elements in order to satisfy this requirement. Only three of the five displacement components introduced at each nodal point of the reference surface are used to describe the behaviour of the beam element.

$$\begin{aligned} v &= \alpha_1 + \alpha_2 y \\ w &= \alpha_3 + \alpha_4 y + \alpha_5 y^2 + \alpha_6 y^3 \end{aligned} \quad (\text{A.23})$$

Introducing the nodal displacement vector for node I of

the beam element associated with its bending and inplane behaviour,

$$\{\bar{U}_i\}_{3 \times 1} = \begin{Bmatrix} v \\ w \\ \theta_x \end{Bmatrix} = \begin{Bmatrix} v \\ w \\ -\frac{d^2w}{dy^2} \end{Bmatrix} \quad (\text{A.24})$$

The displacements at one node expressed in terms of the coefficients α are

$$\{\bar{U}_i\}_{3 \times 1} = [M]_{3 \times 6} \{\alpha\}_{6 \times 1} \quad (\text{A.25})$$

Where

$$[M]_{3 \times 6} = \begin{bmatrix} 1 & y & \cdot & \cdot & \cdot & \cdot \\ \cdot & \cdot & 1 & y & y^2 & y^3 \\ \cdot & \cdot & \cdot & -1 & -2y & -3y^2 \end{bmatrix}$$

Using eqn.(A.24), one can write the element nodal displacements vector as

$$\{U\}_{6 \times 1} = \begin{Bmatrix} \bar{U}_i \\ \bar{U}_j \end{Bmatrix}_{6 \times 1} = \begin{Bmatrix} [M_i] \\ [M_j] \end{Bmatrix}_{6 \times 6} \{\alpha\}_{6 \times 1}$$

or as

$$\{U\}_{6 \times 1} = [A]_{6 \times 6} \{\alpha\}_{6 \times 1}$$

Where

$$[A] = \begin{Bmatrix} [M_i] \\ [M_j] \end{Bmatrix}$$

The inverse of this relationship is,

$$\{\alpha\} = [A^{-1}] \{U\} \quad (A.26)$$

The strain-displacement relations may be written as

$$\{\bar{\epsilon}\}_{2 \times 1} = \begin{Bmatrix} \epsilon_y \\ \chi_y \end{Bmatrix} = [D]_{2 \times 3} \{\bar{u}\}_{3 \times 1} \quad (A.27)$$

Where

$$[D]_{2 \times 3} = \begin{bmatrix} \partial/\partial y & \cdot & \cdot \\ \cdot & \cdot & \partial/\partial y \end{bmatrix}$$

Substitution of eqn.(A.25) into eqn.(A.27), yields

$$\{\bar{\epsilon}\}_{2 \times 1} = [D]_{2 \times 3} [M]_{3 \times 6} \{\alpha\}_{6 \times 1}$$

i.e.;

$$\{\bar{\epsilon}\}_{2 \times 1} = [B]_{2 \times 6} \{\alpha\}_{6 \times 1} \quad (A.28)$$

which relates the reference surface strains and curvatures to the unknown coefficients.

Where

$$[B]_{2 \times 6} = \begin{bmatrix} \cdot & 1 & \cdot & \cdot & \cdot & \cdot \\ \cdot & \cdot & \cdot & \cdot & -2 & -6y \end{bmatrix}$$

Expressing the strain at any depth to the reference surface quantities, yields

$$\epsilon_y = \epsilon_{y_0} + z\chi_y \quad (A.29)$$

The last expression required is to relate stress to strain, namely

$$f_y = E_s \cdot \epsilon_y \quad (A.30)$$

Following the same steps performed over the plate element and integrating over the depth of the beam, yields

$$[K] = [A^{-1}]^T \begin{bmatrix} b_1 \\ -b_1 \end{bmatrix} [B]^T \int_z \begin{bmatrix} E_s & E_s \cdot z \\ E_s \cdot z & E_s \cdot z^2 \end{bmatrix} dz [B] dy [A^{-1}]$$

i.e.;

$$[K] = [A^{-1}]^T \begin{bmatrix} b_1 \\ -b_1 \end{bmatrix} [B]^T \sum_{j=1}^{NB} \begin{bmatrix} E_s A_s & E_s S_s \\ E_s S_s & E_s I_s \end{bmatrix} [B] dy [A^{-1}] \quad (A.31)$$

Where

E_s = Modulus of elasticity of the beam j^{th} layer.

A_s = Area of the beam j^{th} layer

S_s = First moment of the beam j^{th} layer with respect to the plane of reference.

I_s = Moment of inertia of the beam j^{th} layer with respect to the plane of reference.

A.7 Stiffness Matrices of the Beam Elements Representing the Vertical Parts of the Metal Deck

To determine the contribution of the vertical parts of the ribbed metal deck and its response with respect to the plane of reference, it is assumed that these vertical parts of the deck, as shown in fig.(A.1), are attached to the plate along the transverse boundaries of the rectangular plate elements.

A beam element bounded by two nodal points I and K, fig.(A.1), lying in the reference plane of the plate, is assumed to be representing the vertical part of the metal deck. It is also assumed that these vertical parts are integrally attached to the plate and thus the same displacement functions chosen to represent the plate elements must be taken for the beam elements representing the vertical parts of the ribbed deck. Three of the five displacement components introduced at each nodal point of the reference surface are used to describe the behaviour of these beam elements.

$$\begin{aligned} u &= \alpha_1 + \alpha_2 x \\ w &= \alpha_3 + \alpha_4 x + \alpha_5 x^2 + \alpha_6 x^3 \end{aligned} \tag{A.32}$$

The formulation of the beam element stiffness matrix representing the vertical parts of the ribs is quite similar to that used for the elements representing the steel beam, except that these vertical parts of the ribs are running in the transverse direction with respect to the steel beam.

Following the same steps performed over the steel beam elements, yields

$$[K] = [A^{-1}]^T \int_{-a_1}^{a_1} [B]^T \begin{bmatrix} E_s A_s & E_s S_s \\ E_s S_s & E_s I_s \end{bmatrix} [B] dx [A^{-1}] \quad (A.33)$$

Where

E_s = Modulus of elasticity of the metal deck.

A_s = Area of the vertical part of the deck.

S_s = First moment of the vertical part of the deck with respect to the reference plane.

I_s = Moment of inertia of the vertical part of the deck with respect to the reference plane.

A.8 Assembly of the elements Stiffness Matrices:

The stiffness matrices of the individual elements can be assembled to form a single stiffness matrix called the system stiffness matrix of the entire structure. The establishment of this stiffness matrix entails the following steps:

1. The stiffness matrices of the rectangular plate elements representing the ribbed concrete slab

are formed.

2. The stiffness matrices of the beam elements representing the steel beam are formed.
3. The stiffness matrices of the beam elements representing the vertical parts of the ribbed metal deck are formed.
4. The stiffness matrices of the beam and plate elements are combined together according to the elements numbering topology.
5. The total system stiffness matrix is then assembled from the elements stiffness matrices resulting from step 4. During the assemblage of the structure stiffness matrix, each layer is constantly tested as to its state of stress, then its stiffness is evaluated and updated accordingly.

A.9 Displacement Compatibility

The compatibility of displacements across element boundaries depends on the assumed displacement functions and the nodal degrees of freedom. To see if an element is conforming, equality must exist for the displacements of two adjacent elements along their common edge.

First the in-plane displacement, u , from eqn.(A.1), is linear in y . Thus, two boundary conditions are required; two are available, the u displacements at each end of the common edge. Hence, the in-plane displacements are compatible.

A similar situation exists for the v-displacements.

Second, the w displacement, from eqn.(A.1), is cubic in y. Thus, four boundary conditions are required; four are available, w and $\partial w / \partial y$ at each end. Hence, the w displacements and the slope along the edge $\partial w / \partial y$ are compatible.

Third, the slope across the common edge, $\partial w / \partial x$ is cubic in y. Again four boundary conditions are required; only two exist, $\partial w / \partial x$ at each end. Thus, the transverse slope is not compatible.

Since the other edges could be treated likewise, the element conforms with respect to the in-plane displacements u and v, the out-of-plane displacement w and the slope $\partial w / \partial y$ along the edge.

APPENDIX B
COMPUTER PROGRAM

B.1 General Description

This program is designed to handle reinforced concrete slabs and beams, and composite beams with solid and ribbed reinforced concrete slabs under any type of loading.

The program can be used to study the load-deformation response of composite beams with ribbed metal deck through the elastic and inelastic stages up to the ultimate load. It provides a complete listing of stresses and strains in the concrete slab, the steel reinforcement, the metal deck and the steel beam at any stage of loading. It can also be used to determine the yield load of the steel beam and the cracking load of the concrete slab.

The program is written in Fortran IV language and has been developed and tested on a CDC 6400 system.

B.2 Program Subroutines

This program uses the subroutines DATA, DISP, WIDTH, STIFF, LOAD1, CONSTIT, CRITERI, STRESS, BAND, RSTIFF, BSTIFF, BSTRESS, BCONST.

B.2.1 SUBROUTINE DATA

It is used to read the input data of the problem, such as the number of beam and slab layers, the dimensions of the beam and the slab, the properties of steel and concrete and the loads applied on the structure.

B.2.2 SUBROUTINE DISP

It is mainly used to generate the total stiffness matrix of the composite beam. Thus, it assembles the elements stiffness matrices into one structural stiffness matrix.

B.2.3 SUBROUTINE WIDTH

It is used to determine the band width of the elements stiffness matrices.

B.2.4 SUBROUTINE STIFF

It generates the stiffness matrices of the slab elements and then combines them with the stiffness matrices of the beam elements representing the steel beam and the vertical parts of the ribbed metal deck.

B.2.5 SUBROUTINE LOAD1

It is used to generate the load vector which is recalled from subroutine DISP.

B.2.6 SUBROUTINE CONSTIT

It is used to determine the constitutive relation for any layer of an element in the concrete slab. The constitutive relation is determined according to the state of stress and the adopted failure criteria.

B.2.7 SUBROUTINE CRITERI

It is used to classify any layer of an element in the concrete slab according to its state of stress and the adopted transition criterion. Concrete could be elastic, inelastic, singly cracked, doubly cracked or crushed. Steel reinforcement and metal deck could be elastic or yielded. This classification is used in subroutine CONSTIT to determine the appropriate constitutive relation.

B.2.8 SUBROUTINE STRESS

It is used to calculate the reference surface strains and the strains and stresses of any layer of an element in the reinforced concrete slab. It is also used to calculate the excess forces due to the cracking or crushing of the slab.

B.2.9 SUBROUTINE BAND

It is used for the determination of the unknown nodal displacements.

B.2.10 SUBROUTINE RSTIFF

It determines the contribution of the stiffness of the vertical parts of the ribbed metal deck, in the total stiffness of the structure.

B.2.11 SUBROUTINE BSTIFF

It is used to calculate the stiffness matrices of the beam elements representing the steel beam.

B.2.12 SUBROUTINE BSTRESS

It is used to calculate the strains and stresses of any layer in the beam elements representing the steel beam.

B.2.13 SUBROUTINE BCONST

It is used to determine the constitutive relation for any layer of an element in the steel beam. The constitutive relation is determined according to the state of stress and the stress-strain curve used for the steel beam.

b.3 Notations

- A2 - Half the element dimension in the x-direction (across the slab width)
- B2 - Half the element dimension in the y-direction (along the beam length)
- BAS, BAS2 - Areas of beam layers

- BES, BES2 - Tangent modulus of the steel beam layers
- BIS, BIS2 - Moment of inertia of beam layers about the plane of reference.
- Breadth - Width of the concrete slab
- BSK - Stiffness matrix of the steel beam or the vertical parts of the ribbed metal deck elements
- BSS, BSS2 - First moment of area of beam layers about the plane of reference
- Bw, Bw2 - Widths of the beam layers
- C - Constitutive relation for the different layers of the reinforced concrete slab
- CURXO - Curvature in the x-direction
- CURYO - Curvature in the y-direction
- CURBYO - Curvature of the steel beam
- ECO - Modulus of elasticity of concrete
- EC1 - Tangent modulus of concrete in the second linear region
- EC2 - Tangent modulus of concrete in the third linear region
- ESO - Modulus of elasticity of the steel beam
- ES1 - Tangent modulus of the steel beam after yielding
- ES2 - Tangent modulus of steel in the strain hardening region
- MMMMM - Number of load increments

NB	- Half the band width for the rectangular elements
NBL	- Number of beam layers
NCRI,NCRIO	- A numbering system defining the criteria transition zone for the reinforced concrete slab.
NE	- Number of elements
NL	- Number of layers of the concrete slab
NLE	- Number of elements along the beam length
NP1	- Allowed displacements per element
NSL1,NSL2	- Longitudinal reinforcement layers numbering
NST1,NST2	- Transverse reinforcement layers numbering
NU	- Total number of unknown displacements
NW	- Number of the elements across the slab width
R1	- Load vector
R2	- Unknown displacement vector
RIBD	- Depth of the ribbed metal deck
RIBT	- Thickness of the ribbed metal deck
RIBZ	- Inertia of the ribbed metal deck about the reference plane
SB	- Displacement vector per element
SK	- Element stiffness matrix
SMAX,SMIN	- Layer principal stresses
Span	- Composite beam span
STRCM	- Concrete compressive strength in the

	third linear region
STRCO	- Concrete compressive strength in the elastic region
STRCT	- Concrete tensile strength
STRCU	- Concrete compressive strength in the second linear region
STRBY,STRBY2	- Strain in the steel beam layers
STREBY,STREBY2	- Stress in the steel beam layers
STREX	- Slab layer stress in the x-direction
STREXY	- Slab layer shear stress
STREY	- Slab layer stress in the y-direction
STRS	- Yield stress of the steel beam
STRX0,STRY0,STRXY0,STRXY0	-Reference surface element strains
T	- Thickness of the slab layers
TB,TB2	- Thickness of the beam layers
TSK	- Total stiffness matrix
UC	- Poisson's ratio for concrete

B.4 PROGRAM LISTING

The program is written in Fortran IV language and has been developed on a CDC 6400 system.

The program consists of a main program and 13 subroutines. It can handle composite beams with solid and ribbed reinforced concrete slabs under any type of loading.

The listing of the main program and its different subroutines is as follows:


```

PROGRAM TST ( INPUT=200, OUTPUT=200, TAPE5= INPUT, TAPE6=OUTPUT, TAPE1=
200, TAPE2=200, TAPE3=200, TAPE4=200)
COMMON R3(480)
COMMON NE, NL, NB, NNNN, MAX, NLE, NW
COMMON STRS, STRCO, STRCU, STRCM, STRCT, ECO, EC1, EC2, ESO, UC
COMMON A1(20,20), A2(84), B2(84), NP1(20), R1(480), SK(20,20), C(3,3)
COMMON T(15), STREX(84,14), STREY(84,14), STREXY(84,14)
COMMON SMAX, SMIN, ANCC(84,14), NCRI(84,14), NCRI0(84,14), TSK(18000)
COMMON NU, D(3,3), H(3,3), F(3,3), FX, FY, FXY, BMX, BMY, BMXY, R2(480)
COMMON ES1, NBL, TK, TK2, NLEB(25), NLEB2(25), BES(25,10), BES2(25,10)
COMMON BSK(6,6), BAS(10), BSS(10), BIS(10), BAS2(10), BSS2(10), BIS2(10)
COMMON SB(20), TB(11), BW(10), NSL1, NSL2, NST1, NST2
COMMON STRBY(25,10), STREBY(25,10), STRBY2(25,10), STREBY2(25,10)
COMMON BW2(10), TB2(10), RIBD, RIBT, RIBZ
NPRM=1
NNNN=1
NB=0
MAX=0
READ(5,*) NPRM
CALL DATA
CONTINUE
REWIND 1
REWIND 2
REWIND 3
REWIND 4
CALL DISP
CALL STRESS
NPRM=NPRM+1
IF(NPRM.LT.NNNND GO TO 1
STOP
END

SUBROUTINE DATA
COMMON R3(480)
COMMON NE, NL, NB, NNNN, MAX, NLE, NW
COMMON STRS, STRCO, STRCU, STRCM, STRCT, ECO, EC1, EC2, ESO, UC
COMMON A1(20,20), A2(84), B2(84), NP1(20), R1(480), SK(20,20), C(3,3)
COMMON T(15), STREX(84,14), STREY(84,14), STREXY(84,14)
COMMON SMAX, SMIN, ANCC(84,14), NCRI(84,14), NCRI0(84,14), TSK(18000)
COMMON NU, D(3,3), H(3,3), F(3,3), FX, FY, FXY, BMX, BMY, BMXY, R2(480)
COMMON ES1, NBL, TK, TK2, NLEB(25), NLEB2(25), BES(25,10), BES2(25,10)
COMMON BSK(6,6), BAS(10), BSS(10), BIS(10), BAS2(10), BSS2(10), BIS2(10)
COMMON SB(20), TB(11), BW(10), NSL1, NSL2, NST1, NST2
COMMON STRBY(25,10), STREBY(25,10), STRBY2(25,10), STREBY2(25,10)
COMMON BW2(10), TB2(10), RIBD, RIBT, RIBZ
READ(5,*) SPAN, BREADTH
WRITE(6,11) SPAN, BREADTH
FORMAT(2F15.7)
READ(5,*) NE, NL, NU, NW, NLE, NBL, NSL1, NSL2, NST1, NST2, TK, TK2, RIBD,
RIBT, RIBZ
READ(5,*) (NLEB(I), I=1, NLE)
READ(5,*) (NLEB2(I), I=1, NLE)
READ(5,*) (BW(I), I=1, NBL)
READ(5,*) (BW2(I), I=1, NBL)
NBL2=NBL+1
READ(5,*) (TB(I), I=1, NBL2)
READ(5,*) (TB2(I), I=1, NBL2)
DO 100 I=1, NBL
BAS2(I)=ABS((TB2(I+1)-TB2(I))*BW2(I))
BAS(I)=ABS((TB(I+1)-TB(I))*BW(I))
BSS2(I)=(BAS2(I)*.50*(TB2(I+1)+TB2(I)))
BIS2(I)=ABS(BAS2(I)*(.50*(TB(I+1)+TB(I))))**2.0)
BSS(I)=(BAS(I)*.50*(TB(I+1)+TB(I)))
BIS(I)=ABS(BAS(I)*(.50*(TB(I+1)+TB(I))))**2.0)
II=1
DO 10 I=1, NLE
READ(5,*) B2(II)
III=II+NW
II=1
III=NW

```

30	CONTINUE	750
	DO 20 I=II,III	760
20	B2(I)=B2(II)	770
	II=II+NW	780
	III=II+NW-1	790
	IF(III.GT.NE) GO TO 35	800
	GO TO 30	810
35	CONTINUE	820
	READ(5,*) (A2(I),I=1,NW)	830
	NLE1=NLE-1	840
	DO 40 I=1,NLE1	850
	DO 40 J=1,NW	860
	II=J+NW*I	870
40	A2(II)=A2(J)	880
	DO 1N=1,NE	890
	READ(5,*) (J,(NP1(I),I=1,20))	900
	WRITE(4) (NP1(I),I=1,20)	910
1	CONTINUE	920
	REWIND 4	930
	NL1=NL+1	940
	READ(5,*) (T(I),I=1,NL1)	950
	READ(5,*) ECO,EC1,EC2,ESO,ES1,UC	960
	READ(5,*) STRS,STRCO,STRCU,STRCM,STRCT	970
	RETURN	980
	END	990
		1000
		1010
		1020
		1030
		1040
		1050
		1060
		1070
		1080
		1090
		1100
		1110
		1120
		1130
		1140
		1150
		1160
		1170
		1180
		1190
1	CONTINUE	1200
	REWIND 4	1210
8	CONTINUE	1220
	DO 7 LL=1,18000	1230
7	TSK(LL)=0.0	1240
	DO 6 N=1,NE	1250
	IF(NNNN.EQ.1) GO TO 20	1260
	DO 9 LL=1,NLE	1270
	IF(N.EQ.NLEB(LL)) GO TO 23	1280
9	CONTINUE	1290
	DO 21 II=1,NL	1300
	IF(NCRI(N,II).NE.NCRIO(N,II)) GO TO 23	1310
21	CONTINUE	1320
	READ(1) ((SK(I,J),J=1,20),I=1,20)	1330
	WRITE(2) ((SK(I,J),J=1,20),I=1,20)	1340
	READ(3) ((A1(I,J),J=1,20),I=1,20)	1350
	GO TO 22	1360
23	CONTINUE	1370
	READ(1) ((SK(I,J),J=1,20),I=1,20)	1380
20	CONTINUE	1390
	CALL STIFF(N)	1400
	WRITE(2) ((SK(I,J),J=1,20),I=1,20)	1410
22	CONTINUE	1420
	READ(4) (NP1(I),I=1,20)	1430
	DO 2 J=1,20	1440
	IF(NP1(J).EQ.0) GO TO 2	1450
	DO 3 I=J,20	1460
	IF(NP1(I).EQ.0) GO TO 3	1470
	IF(NP1(J)-NP1(I))4,5,5	1480

5	K=(NP1(I)-1)*NB+NP1(J)	1490
	TSK(K)=TSK(K)+SK(J,I)	1500
	GO TO 3	1510
4	K=(NP1(J)-1)*NB+NP1(I)	1520
	TSK(K)=TSK(K)+SK(J,I)	1530
3	CONTINUE	1540
2	CONTINUE	1550
6	CONTINUE	1560
	REWIND 4	1570
	CALL LOAD1	1580
	DET=1.E-8	1590
	NB2=NB+1	1600
	CALL BAND (TSK,R1,MAX,NB2,1,DET)	1610
	RETURN	1620
	END	1630
		1640
		1650
		1660
		1670
		1680
	SUBROUTINE WIDTH	1690
	COMMON R3(480)	1700
	COMMON NE,NL,NB,NNNN,MAX,NLE,NW	1710
	COMMON STRS,STRCO,STRCU,STRCM,STRCT,ECO,EC1,EC2,ESO,UC	1720
	COMMON A1(20,20),A2(84),B2(84),NP1(20),R1(480),SK(20,20),C(3,3)	1730
	COMMON T(15),STREX(84,14),STREY(84,14),STREXY(84,14)	1740
	COMMON SMAX,SMIN,ANGC(84,14),NCRI(84,14),NCRIO(84,14),TSK(18000)	1750
	COMMON NU,D(3,3),H(3,3),F(3,3),FX,FY,FX,Y,BMX,BMY,BMXY,R2(480)	1760
	COMMON ES1,NBL,TK,TK2,NLEB(25),NLEB2(25),BES(25,10),BES2(25,10)	1770
	COMMON BSK(6,6),BAS(10),BSS(10),BIS(10),BAS2(10),BSS2(10),BIS2(10)	1780
	COMMON SB(20),TB(11),BW(10),NSL1,NSL2,NST1,NST2	1790
	COMMON STRBY(25,10),STREBY(25,10),STRBY2(25,10),STREBY2(25,10)	1800
	COMMON BW2(10),TB2(10),RIBD,RIBT,RIEZ	1810
	READ(4) (NP1(I),I=1,20)	1820
	MAXX=0	1830
	MINN=3000	1840
	DO 1 II=1,20	1850
	IF(NP1(II).EQ.0) GO TO 1	1860
	IF(NP1(II)-MAXX) 2,2,3	1870
3	MAXX=NP1(II)	1880
2	IF(NP1(II)-MINN) 4,1,1	1890
4	MINN=NP1(II)	1900
1	CONTINUE	1910
	NB1=MAXX-MINN	1920
	IF(NB1.GT.NB) NB=NB1	1930
	IF(MAXX.GT.MAX) MAX=MAXX	1940
	RETURN	1950
	END	1960
		1970
		1980
		1990
		2000
	SUBROUTINE STIFF(N)	2010
	COMMON R3(480)	2020
	COMMON NE,NL,NB,NNNN,MAX,NLE,NW	2030
	COMMON STRS,STRCO,STRCU,STRCM,STRCT,ECO,EC1,EC2,ESO,UC	2040
	COMMON A1(20,20),A2(84),B2(84),NP1(20),R1(480),SK(20,20),C(3,3)	2050
	COMMON T(15),STREX(84,14),STREY(84,14),STREXY(84,14)	2060
	COMMON SMAX,SMIN,ANGC(84,14),NCRI(84,14),NCRIO(84,14),TSK(18000)	2070
	COMMON NU,D(3,3),H(3,3),F(3,3),FX,FY,FX,Y,BMX,BMY,BMXY,R2(480)	2080
	COMMON ES1,NBL,TK,TK2,NLEB(25),NLEB2(25),BES(25,10),BES2(25,10)	2090
	COMMON BSK(6,6),BAS(10),BSS(10),BIS(10),BAS2(10),BSS2(10),BIS2(10)	2100
	COMMON SB(20),TB(11),BW(10),NSL1,NSL2,NST1,NST2	2110
	COMMON STRBY(25,10),STREBY(25,10),STRBY2(25,10),STREBY2(25,10)	2120
	COMMON BW2(10),TB2(10),RIBD,RIBT,RIBZ	2130
	DIMENSION B1(20,20)	2140
	A=A2(N)	2150
	B=B2(N)	2160
	DO 1 I=1,3	2170
	DO 1 J=1,3	2180
	D(I,J)=0.0	2190
	F(I,J)=0.0	2200
	H(I,J)=0.0	2210
1	CONTINUE	2220
	DO 2 I=1,NL	

	CALL CONSTIT (N, I)	2230
	DO 2 J=1,3	2240
	DO 2 K=1,3	2250
	F(J, K)=F(J, K)+C(J, K)*(T(I+1)**3.0-T(I)**3.0)/3.0	2260
	D(J, K)=D(J, K)+C(J, K)*(T(I+1)-T(I))	2270
	H(J, K)=H(J, K)+.5*C(J, K)*(T(I+1)**2.0-T(I)**2.0)	2280
2	CONTINUE	2290
	DO 3 I=1,20	2300
	DO 3 J=1,20	2310
	A1(I, J)=0.0	2320
3	SK(I, J)=0.0	2330
	SK(2, 2)=4.0*A*B*D(1, 1)	2340
	SK(2, 7)=4.0*A*B*D(1, 2)	2350
	SK(2, 13)=-8.0*A*B*H(1, 1)	2360
	SK(2, 14)=-8.0*A*B*H(1, 2)	2370
	DO 13 I=3,20	2380
13	SK(I, 2)=SK(2, I)	2390
	SK(3, 3)=4.0*A*B*D(3, 3)	2400
	SK(3, 6)=4.0*A*B*D(3, 3)	2410
	SK(3, 12)=8.0*A*B*H(3, 3)	2420
	SK(3, 19)=8.0*A*A*A*B*H(3, 3)	2430
	SK(3, 20)=8.0*A*B*B*B*H(3, 3)	2440
	DO 14 I=4,20	2450
14	SK(I, 3)=SK(3, I)	2460
	SK(4, 4)=(4.0*A*B*B*B*D(1, 1)+4.0*A*A*A*B*D(3, 3))/3.0	2470
	SK(4, 16)=(-8.0*A*B*B*B*H(1, 1)+16.0*A*A*A*B*H(3, 3))/3.0	2480
	SK(4, 18)=-8.0*A*B*B*B*H(1, 2)	2490
	DO 15 I=5,20	2500
15	SK(I, 4)=SK(4, I)	2510
	SK(6, 6)=4.0*A*B*D(3, 3)	2520
	SK(6, 12)=8.0*A*B*H(3, 3)	2530
	SK(6, 19)=8.0*A*A*A*B*H(3, 3)	2540
	SK(6, 20)=8.0*A*B*B*B*H(3, 3)	2550
	DO 17 I=7,20	2560
17	SK(I, 6)=SK(6, I)	2570
	SK(7, 7)=4.0*A*B*D(2, 2)	2580
	SK(7, 13)=-8.0*A*B*H(1, 2)	2590
	SK(7, 14)=-8.0*A*B*H(2, 2)	2600
	DO 18 I=8,20	2610
18	SK(I, 7)=SK(7, I)	2620
	SK(8, 8)=(4.0*A*A*A*B*D(2, 2)+4.0*A*B*B*B*D(3, 3))/3.0	2630
	SK(8, 15)=-8.0*A*A*A*B*H(1, 2)	2640
	SK(8, 17)=(-8.0*A*A*A*B*H(2, 2)+16.0*A*B*B*B*H(3, 3))/3.0	2650
	DO 19 I=9,20	2660
19	SK(I, 8)=SK(8, I)	2670
	SK(12, 12)=16.0*A*B*F(3, 3)	2680
	SK(12, 19)=16.0*A*A*A*B*F(3, 3)	2690
	SK(12, 20)=16.0*A*B*B*B*F(3, 3)	2700
	DO 20 I=13,20	2710
20	SK(I, 12)=SK(12, I)	2720
	SK(13, 13)=16.0*A*B*F(1, 1)	2730
	SK(13, 14)=16.0*A*B*F(1, 2)	2740
	DO 21 I=14,20	2750
21	SK(I, 13)=SK(13, I)	2760
	SK(14, 14)=16.0*A*B*F(2, 2)	2770
	SK(15, 15)=48.0*A*A*A*B*F(1, 1)	2780
	SK(15, 17)=16.0*A*A*A*B*F(1, 2)	2790
	DO 23 I=16,20	2800
23	SK(I, 15)=SK(15, I)	2810
	SK(16, 16)=(16.0*A*B*B*B*F(1, 1)+64.0*A*A*A*B*F(3, 3))/3.0	2820
	SK(16, 18)=16.0*A*B*B*B*F(1, 2)	2830
	DO 24 I=17,20	2840
24	SK(I, 16)=SK(16, I)	2850
	SK(17, 17)=(16.0*A*A*A*B*F(2, 2)+64.0*A*B*B*B*F(3, 3))/3.0	2860
	SK(19, 18)=48.0*A*B*D*B*F(2, 2)	2870
	SK(19, 19)=16.0*A*A*A*B*B*B*F(1, 1)+144.0*A*A*A*A*A*B*F(3, 3)/5.0	2880
	SK(19, 20)=16.0*A*A*A*B*B*B*F(1, 2)+16.0*A*A*A*B*B*B*F(3, 3)	2890
	SK(20, 19)=SK(19, 20)	2900
	SK(20, 20)=16.0*A*A*A*B*B*B*F(2, 2)+144.0*A*B*B*B*B*B*F(3, 3)/5.0	2910
	IF(NNNN.EQ.1) GO TO 25	2920
	READ(3) ((A1(I, J), J=1,20), I=1,20)	2930
	GO TO 26	2940
25	CONTINUE	2950
	A1(1, 1)=.25	2960

$A1(1,2) = -1.0/(4.0*A)$	2970
$A1(1,3) = -1.0/(4.0*B)$	2980
$A1(1,4) = 1.0/(4.0*A*B)$	2990
$A1(2,5) = .25$	3000
$A1(2,6) = A1(1,2)$	3010
$A1(2,7) = A1(1,3)$	3020
$A1(2,8) = A1(1,4)$	3030
$A1(3,9) = .25$	3040
$A1(3,10) = -3.0/(8.0*A)$	3050
$A1(3,11) = -3.0/(8.0*B)$	3060
$A1(3,12) = 2.0/(4.0*A*B)$	3070
$A1(3,15) = 1.0/(8.0*A*A*A)$	3080
$A1(3,18) = 1.0/(8.0*B*B*B)$	3090
$A1(3,19) = -1.0/(8.0*A*A*A*B)$	3100
$A1(3,20) = -1.0/(8.0*A*B*B*B)$	3110
$A1(4,9) = A/B.0$	3120
$A1(4,10) = -.125$	3130
$A1(4,11) = -A/(8.0*B)$	3140
$A1(4,12) = 1.0/(8.0*B)$	3150
$A1(4,13) = -1.0/(8.0*A)$	3160
$A1(4,15) = 1.0/(8.0*A*A)$	3170
$A1(4,16) = 1.0/(8.0*A*B)$	3180
$A1(4,19) = -1.0/(8.0*A*A*B)$	3190
$A1(5,9) = -.125*B$	3200
$A1(5,10) = .125*B/A$	3210
$A1(5,11) = .125$	3220
$A1(5,12) = -.125/A$	3230
$A1(5,14) = .125/B$	3240
$A1(5,17) = -.125/(A*B)$	3250
$A1(5,18) = -.125/(B*B)$	3260
$A1(5,20) = .125/(A*B*B)$	3270
$A1(6,1) = A1(1,1)$	3280
$A1(6,2) = A1(1,2)$	3290
$A1(6,3) = -A1(1,3)$	3300
$A1(6,4) = -A1(1,4)$	3310
$A1(7,5) = A1(2,5)$	3320
$A1(7,6) = A1(2,6)$	3330
$A1(7,7) = -A1(2,7)$	3340
$A1(7,8) = -A1(2,8)$	3350
$A1(8,9) = A1(3,9)$	3360
$A1(8,10) = A1(3,10)$	3370
$A1(8,11) = -A1(3,11)$	3380
$A1(8,12) = -A1(3,12)$	3390
$A1(8,15) = A1(3,15)$	3400
$A1(8,18) = -A1(3,18)$	3410
$A1(8,19) = -A1(3,19)$	3420
$A1(8,20) = -A1(3,20)$	3430
$A1(9,9) = A1(4,9)$	3440
$A1(9,10) = A1(4,10)$	3450
$A1(9,11) = -A1(4,11)$	3460
$A1(9,12) = -A1(4,12)$	3470
$A1(9,13) = A1(4,13)$	3480
$A1(9,15) = A1(4,15)$	3490
$A1(9,16) = -A1(4,16)$	3500
$A1(9,19) = -A1(4,19)$	3510
$A1(10,9) = -A1(5,9)$	3520
$A1(10,10) = -A1(5,10)$	3530
$A1(10,11) = A1(5,11)$	3540
$A1(10,12) = A1(5,12)$	3550
$A1(10,14) = -A1(5,14)$	3560
$A1(10,17) = -A1(5,17)$	3570
$A1(10,18) = A1(5,18)$	3580
$A1(10,20) = A1(5,20)$	3590
$A1(11,1) = A1(1,1)$	3600
$A1(11,2) = -A1(1,2)$	3610
$A1(11,3) = A1(1,3)$	3620
$A1(11,4) = -A1(1,4)$	3630
$A1(12,5) = A1(2,5)$	3640
$A1(12,6) = -A1(2,6)$	3650
$A1(12,7) = A1(2,7)$	3660
$A1(12,8) = -A1(2,8)$	3670
$A1(13,9) = A1(3,9)$	3680
$A1(13,10) = -A1(3,10)$	3690
$A1(13,11) = A1(3,11)$	3700

	A1(13,12)=-A1(3,12)	3710
	A1(13,15)=-A1(3,15)	3720
	A1(13,18)=A1(3,18)	3730
	A1(13,19)=-A1(3,19)	3740
	A1(13,20)=-A1(3,20)	3750
	A1(14,9)=-A1(4,9)	3760
	A1(14,10)=A1(4,10)	3770
	A1(14,11)=-A1(4,11)	3780
	A1(14,12)=A1(4,12)	3790
	A1(14,13)=-A1(4,13)	3800
	A1(14,15)=A1(4,15)	3810
	A1(14,16)=-A1(4,16)	3820
	A1(14,19)=A1(4,19)	3830
	A1(15,9)=A1(5,9)	3840
	A1(15,10)=-A1(5,10)	3850
	A1(15,11)=A1(5,11)	3860
	A1(15,12)=-A1(5,12)	3870
	A1(15,14)=A1(5,14)	3880
	A1(15,17)=-A1(5,17)	3890
	A1(15,18)=A1(5,18)	3900
	A1(15,20)=-A1(5,20)	3910
	A1(16,1)=A1(1,1)	3920
	A1(16,2)=-A1(1,2)	3930
	A1(16,3)=-A1(1,3)	3940
	A1(16,4)=A1(1,4)	3950
	A1(17,5)=A1(2,5)	3960
	A1(17,6)=-A1(2,6)	3970
	A1(17,7)=-A1(2,7)	3980
	A1(17,8)=A1(2,8)	3990
	A1(18,9)=A1(3,9)	4000
	A1(18,10)=-A1(3,10)	4010
	A1(18,11)=-A1(3,11)	4020
	A1(18,12)=A1(3,12)	4030
	A1(18,15)=-A1(3,15)	4040
	A1(18,18)=-A1(3,18)	4050
	A1(18,19)=A1(3,19)	4060
	A1(18,20)=A1(3,20)	4070
	A1(19,9)=-A1(4,9)	4080
	A1(19,10)=A1(4,10)	4090
	A1(19,11)=A1(4,11)	4100
	A1(19,12)=-A1(4,12)	4110
	A1(19,13)=-A1(4,13)	4120
	A1(19,15)=A1(4,15)	4130
	A1(19,16)=A1(4,16)	4140
	A1(19,19)=-A1(4,19)	4150
	A1(20,9)=-A1(5,9)	4160
	A1(20,10)=A1(5,10)	4170
	A1(20,11)=A1(5,11)	4180
	A1(20,12)=-A1(5,12)	4190
	A1(20,14)=-A1(5,14)	4200
	A1(20,17)=A1(5,17)	4210
	A1(20,18)=A1(5,18)	4220
	A1(20,20)=-A1(5,20)	4230
	WRITE(3)((A1(I,J),J=1,20),I=1,20)	4240
26	CONTINUE	4250
	DO 4I=1,20	4260
	DO 4J=1,20	4270
	B1(I,J)=0.0	4280
	DO 4K=1,20	4290
4	B1(I,J)=B1(I,J)+A1(I,K)*SK(K,J)	4300
	DO 7 I=1,20	4310
	DO 7 J=1,20	4320
	SK(I,J)=0.0	4330
	DO 7 K=1,20	4340
7	SK(I,J)=SK(I,J)+B1(I,K)*A1(J,K)	4350
	CALL RSTIFF(N)	4360
	CALL BSTIFF(N)	4370
	IF(MNNN.GT.1) GO TO 40	4380
	WRITE(1)((SK(I,J),J=1,20),I=1,20)	4390
40	CONTINUE	4400
	RETURN	4410
	END	4420
		4430
		4440

	SUBROUTINE LOAD1	4450
	COMMON R3(480)	4460
	COMMON NE,NL,NB,NNNN,MAX,NLE,NW	4470
	COMMON STRS,STRCO,STRCU,STRCM,STRCT,ECO,EC1,EC2,ESO,UC	4480
	COMMON A1(20,20),A2(84),B2(84),NP1(20),R1(480),SK(20,20),C(3,3)	4490
	COMMON T(15),STREX(84,14),STREY(84,14),STREXY(84,14)	4500
	COMMON SMAX,SMIN,ANGC(84,14),NCRI(84,14),NCRIO(84,14),TSK(18000)	4510
	COMMON NU,D(3,3),H(3,3),F(3,3),FX,FY,FX,Y,BMX,BMY,BMXY,R2(480)	4520
	COMMON ES1,NBL,TK,TK2,NLEB(25),NLEB2(25),BES(25,10),BES2(25,10)	4530
	COMMON BSK(6,6),BAS(10),BSS(10),BIS(10),BAS2(10),BSS2(10),BIS2(10)	4540
	COMMON SB(20),TB(11),BW(10),NSL1,NSL2,NST1,NST2	4550
	COMMON STRBY(25,10),STREBY(25,10),STRBY2(25,10),STREBY2(25,10)	4560
	COMMON BW2(10),TB2(10),RIBD,RIBT,RIBZ	4570
	IF(NNNN.GT.1) GO TO 1	4580
	DO 3 I=1,NU	4590
	R1(I)=0.0	4600
3	R2(I)=0.0	4610
C	THIS CARD SHOULD BE CHANGED EACH TIME DEPENDING ON THE NO) OF LOAD	4620
	READ(5,*)R2(1),R2(3),R2(6),R2(9),R2(11)	4630
	IJ1=13	4640
	IJ2=17	4650
	IJ3=22	4660
	IJ4=27	4670
	IJ5=31	4680
100	CONTINUE	4690
	READ(5,*) R2(IJ1),R2(IJ2),R2(IJ3),R2(IJ4),R2(IJ5)	4700
	IJ1=IJ1+21	4710
	IJ2=IJ2+21	4720
	IJ3=IJ3+21	4730
	IJ4=IJ4+21	4740
	IJ5=IJ5+21	4750
	IF(IJ1.GT.391) GO TO 200	4760
	GO TO 100	4770
200	READ(5,*) R2(415),R2(420),R2(425),R2(429)	4780
	DO 4 I=1,NU	4790
4	R1(I)=R1(I)+R2(I)	4800
	DO 5 I=1,NU	4810
5	R3(I)=R1(I)	4820
	GO TO 7	4830
1	CONTINUE	4840
	DO 6 I=1,NU	4850
	R1(I)=R3(I)	4860
6	CONTINUE	4870
7	CONTINUE	4880
	WRITE(6,10) R2(76),R2(223)	4890
10	FORMAT(2F13.7)	4900
	RETURN	4910
	END	4920
		4930
		4940
		4950
		4960
		4970
	SUBROUTINE CONSTIT (N,I)	4980
	COMMON R3(480)	4990
	COMMON NE,NL,NB,NNNN,MAX,NLE,NW	5000
	COMMON STRS,STRCO,STRCU,STRCM,STRCT,ECO,EC1,EC2,ESO,UC	5010
	COMMON A1(20,20),A2(84),B2(84),NP1(20),R1(480),SK(20,20),C(3,3)	5020
	COMMON T(15),STREX(84,14),STREY(84,14),STREXY(84,14)	5030
	COMMON SMAX,SMIN,ANGC(84,14),NCRI(84,14),NCRIO(84,14),TSK(18000)	5040
	COMMON NU,D(3,3),H(3,3),F(3,3),FX,FY,FX,Y,BMX,BMY,BMXY,R2(480)	5050
	COMMON ES1,NBL,TK,TK2,NLEB(25),NLEB2(25),BES(25,10),BES2(25,10)	5060
	COMMON BSK(6,6),BAS(10),BSS(10),BIS(10),BAS2(10),BSS2(10),BIS2(10)	5070
	COMMON SB(20),TB(11),BW(10),NSL1,NSL2,NST1,NST2	5080
	COMMON STRBY(25,10),STREBY(25,10),STRBY2(25,10),STREBY2(25,10)	5090
	COMMON BW2(10),TB2(10),RIBD,RIBT,RIBZ	5100
	DO 7 II=1,3	5110
	DO 7 JJ=1,3	5120
7	C(II,JJ)=0.0	5130
	IF(NNNN.GT.2) GO TO 8	5140
	IF(I.EQ.NST1.OR.I.EQ.NST2) GO TO 9	5150
	IF(I.EQ.11.OR.I.EQ.12.OR.I.EQ.13.OR.I.EQ.14) GO TO 16	5160
	IF(I.EQ.NSL1.OR.I.EQ.NSL2) GO TO 10	5170
	NCRI(N,I)=1	5180

	C(1,1)=ECO/(1.0-UC**2.0)	5190
	C(1,2)=UC*C(1,1)	5200
	C(2,1)=C(1,2)	5210
	C(2,2)=C(1,1)	5220
	C(3,3)=C(1,1)*(1.0-UC)/2.0	5230
	GO TO 100	5240
9	C(1,1)=ESO	5250
	NCRI(N,I)=5	5260
	GO TO 100	5270
10	C(2,2)=ESO	5280
	NCRI(N,I)=6	5290
	GO TO 100	5300
16	IJ1=1	5310
	IJ2=4	5320
	DO 17 JJJ=1,10	5330
	IF(N.GE.IJ1.AND.N.LE.IJ2) GO TO 18	5340
	IJ1=IJ1+8	5350
	IJ2=IJ2+8	5360
17	CONTINUE	5370
	IF(1.EQ.12.OR.1.EQ.13.OR.1.EQ.14) GO TO 19	5380
	C(1,1)=ESO	5390
	NCRI(N,I)=5	5400
	GO TO 100	5410
19	NCRI(N,I)=4	5420
	GO TO 100	5430
18	CONTINUE	5440
	IF(1.EQ.11.OR.1.EQ.12.OR.1.EQ.13) GO TO 20	5450
	C(1,1)=ESO	5460
	NCRI(N,I)=5	5470
	GO TO 100	5480
20	NCRI(N,I)=1	5490
	C(1,1)=ECO/(1.0-UC**2.0)	5500
	C(1,2)=UC*C(1,1)	5510
	C(2,1)=C(1,2)	5520
	C(2,2)=C(1,1)	5530
	C(3,3)=C(1,1)*(1.0-UC)/2.0	5540
	GO TO 100	5550
8	CONTINUE	5560
	IF(NCRI(N,I).EQ.1) GO TO 1	5570
	IF(NCRI(N,I).EQ.2) GO TO 2	5580
	IF(NCRI(N,I).EQ.3) GO TO 3	5590
	IF(NCRI(N,I).EQ.31) GO TO 31	5600
	IF(NCRI(N,I).EQ.41) GO TO 41	5610
	IF(NCRI(N,I).EQ.51) GO TO 51	5620
	IF(NCRI(N,I).EQ.32) GO TO 32	5630
	IF(NCRI(N,I).EQ.42) GO TO 42	5640
	IF(NCRI(N,I).EQ.52) GO TO 52	5650
	IF(NCRI(N,I).EQ.4) GO TO 4	5660
	IF(NCRI(N,I).EQ.5) GO TO 5	5670
	IF(NCRI(N,I).EQ.6) GO TO 6	5680
	IF(NCRI(N,I).EQ.7) GO TO 11	5690
	IF(NCRI(N,I).EQ.8) GO TO 12	5700
	IF(NCRI(N,I).EQ.9) GO TO 13	5710
1	C(1,1)=ECO/(1.0-UC**2.0)	5720
	C(1,2)=UC*C(1,1)	5730
	C(2,1)=C(1,2)	5740
	C(2,2)=C(1,1)	5750
	C(3,3)=C(1,1)*(1.0-UC)/2.0	5760
	GO TO 100	5770
2	C(1,1)=EC1/(1.0-UC**2.0)	5780
	C(1,2)=UC*C(1,1)	5790
	C(2,1)=C(1,2)	5800
	C(2,2)=C(1,1)	5810
	C(3,3)=C(1,1)*(1.0-UC)/2.0	5820
	GO TO 100	5830
3	CONTINUE	5840
	X=SIN(ANGC(N,I))	5850
	Y=COS(ANGC(N,I))	5860
	C(1,1)=ECO*Y*Y*Y*Y	5870
	C(1,2)=ECO*X*X*Y*Y	5880
	C(1,3)=ECO*X*Y*Y*Y	5890
	C(2,2)=ECO*X*X*X*X	5900
	C(2,3)=ECO*X*X*X*Y	5910
	C(3,3)=ECO*X*X*Y*Y	5920

	C(2,1)=C(1,2)	5930
	C(3,1)=C(1,3)	5940
	C(3,2)=C(2,3)	5950
	GO TO 100	5960
31	C(2,2)=ECO	5970
	STREX(N,1)=0.0	5980
	GO TO 100	5990
41	C(2,2)=EC1	6000
	STREX(N,1)=0.0	6010
	GO TO 100	6020
51	C(2,2)=EC2	6030
	STREX(N,1)=0.0	6040
	GO TO 100	6050
32	C(1,1)=ECO	6060
	STREY(N,1)=0.0	6070
	GO TO 100	6080
42	C(1,1)=EC1	6090
	STREY(N,1)=0.0	6100
	GO TO 100	6110
32	C(1,1)=EC2	6120
	STREY(N,1)=0.0	6130
	GO TO 100	6140
4	CONTINUE	6150
	GO TO 100	6160
11	C(1,1)=EC2/(1.0-UC**2.0)	6170
	C(1,2)=UC*C(1,1)	6180
	C(2,1)=C(1,2)	6190
	C(2,2)=C(1,1)	6200
	C(3,3)=C(1,1)*(1.0-UC)/2.0	6210
	GO TO 100	6220
5	C(1,1)=ESO	6230
	GO TO 100	6240
6	C(2,2)=ESO	6250
	GO TO 100	6260
12	C(1,1)=ES1	6270
	GO TO 100	6280
13	C(2,2)=ES1	6290
100	CONTINUE	6300
	RETURN	6310
	END	6320
		6330
		6340
		6350
		6360
		6370
		6380
		6390
	SUBROUTINE CRITERI(N,1)	6400
	COMMON R3(480)	6410
	COMMON NE,NL,NB,NNNN,MAX,NLE,NW	6420
	COMMON STRS,STRCO,STRCU,STRCM,STRCT,ECO,EG1,EC2,ESO,UC	6430
	COMMON A1(20,20),A2(84),B2(84),NP1(20),R1(480),SK(20,20),C(3,3)	6440
	COMMON T(15),STREX(84,14),STREY(84,14),STREXY(84,14)	6450
	COMMON SMAX,SMIN,ANGC(84,14),NCRI(84,14),NCRIO(84,14),TSK(18000)	6460
	COMMON NU,D(3,3),H(3,3),F(3,3),FX,FY,FX,Y,BMX,BMY,BMXY,R2(480)	6470
	COMMON ES1,NBL,TK,TK2,NLEB(25),NLEB2(25),BES(25,10),BES2(25,10)	6480
	COMMON BSK(6,6),BAS(10),BSS(10),BIS(10),BAS2(10),BSS2(10),BIS2(10)	6490
	COMMON SB(20),TB(11),BW(10),NSL1,NSL2,NST1,NST2	6500
	COMMON SURBY(25,10),STREBY(25,10),STRBY2(25,10),STREBY2(25,10)	6510
	COMMON BW2(10),TB2(10),RIBD,RIBT,RIBZ	6520
	IF(NNNN.EQ.2) GO TO 14	6530
	GO TO 15	6540
14	CONTINUE	6550
	NCRI(N,1)=1	6560
	IF(I.EQ.NSL1.OR.I.EQ.NSL2) NCRI(N,1)=6	6570
	IF(I.EQ.NST1.OR.I.EQ.NST2) NCRI(N,1)=5	6580
	IF(I.EQ.11.OR.I.EQ.12.OR.I.EQ.13.OR.I.EQ.14) GO TO 621	6590
	GO TO 15	6600
621	CONTINUE	6610
	IJ1=1	6620
	IJ2=4	6630
	DO 627 JJJ=1,10	6640
	IF(N.GE.IJ1.AND.N.LE.IJ2) GO TO 628	6650
	IJ1=IJ1+8	6660
	IJ2=IJ2+8	6670
627	CONTINUE	6680
	IF(I.EQ.12.OR.I.EQ.13.OR.I.EQ.14) GO TO 629	6690

	NCRI(N, I)=3	6670
	GO TO 15	6680
629	NCRI(N, I)=4	6690
	GO TO 15	6700
628	CONTINUE	6710
	IF(I.EQ.11.OR.I.EQ.12.OR.I.EQ.13) GO TO 630	6720
	NCRI(N, I)=5	6730
	GO TO 15	6740
630	NCRI(N, I)=1	6750
15	CONTINUE	6760
	NCRI(N, I)=NCRI(N, I)	6770
	IF(NCRI(N, I).EQ.31.OR.NCRI(N, I).EQ.41.OR.NCRI(N, I).EQ.51) GO TO150	6780
	IF(NCRI(N, I).EQ.3) GO TO 150	6790
	IF(NCRI(N, I).EQ.32.OR.NCRI(N, I).EQ.42.OR.NCRI(N, I).EQ.52) GO TO151	6800
	IF(NCRI(N, I).EQ.4) GO TO 160	6810
	IF(I.EQ.NSL1.OR.I.EQ.NSL2) GO TO 200	6820
	IF(I.EQ.NST1.OR.I.EQ.NST2) GO TO 400	6830
	IF(I.EQ.14.AND.NCRI(N, I).EQ.5) GO TO 400	6840
	IF(I.EQ.11.AND.NCRI(N, I).EQ.5) GO TO 400	6850
	IF(I.EQ.14.AND.NCRI(N, I).EQ.8) GO TO 410	6860
	IF(I.EQ.11.AND.NCRI(N, I).EQ.8) GO TO 410	6870
	IF(STREX(N, I).LT.0.0.AND.STREY(N, I).LT.0.0) GO TO 10	6880
	IF(STREX(N, I).GT.0.0.AND.STREY(N, I).GT.0.0) GO TO 50	6890
	IF(STREX(N, I).GT.0.0.AND.STREY(N, I).LT.0.0) GO TO 100	6900
	IF(STREY(N, I).GT.0.0.AND.STREX(N, I).LT.0.0) GO TO 101	6910
150	IF(STREY(N, I).GT.STRCT.OR.ABS(STREY(N, I)).GT.STRCM) GO TO 160	6920
	IF(ABS(STREY(N, I)).GT.STRCU) NCRI(N, I)=31	6930
	IF(ABS(STREY(N, I)).GT.STRCO) NCRI(N, I)=41	6940
	IF(STREY(N, I).LT.STRCT.AND.STREY(N, I).GT.(-STRCO)) NCRI(N, I)=31	6950
	NCRI(N, I)=3	6960
	GO TO 300	6970
151	IF(STREX(N, I).GT.STRCT.OR.ABS(STREX(N, I)).GT.STRCM) GO TO 160	6980
	IF(ABS(STREX(N, I)).GT.STRCU) NCRI(N, I)=52	6990
	IF(ABS(STREX(N, I)).GT.STRCO) NCRI(N, I)=42	7000
	IF(STREX(N, I).LT.STRCT.AND.STREX(N, I).GT.(-STRCO)) NCRI(N, I)=32	7010
	GO TO 300	7020
200	IF(ABS(STREY(N, I)).GT.STRS) GO TO 210	7030
	NCRI(N, I)=6	7040
	GO TO 300	7050
210	NCRI(N, I)=9	7060
	GO TO 300	7070
400	IF(ABS(STREX(N, I)).GT.STRS) GO TO 410	7080
	NCRI(N, I)=5	7090
	GO TO 300	7100
410	NCRI(N, I)=8	7110
	GO TO 300	7120
160	NCRI(N, I)=4	7130
	GO TO 300	7140
10	AX=STREX(N, I)/STREY(N, I)	7150
	AAA=SQRT(AX**2.0+1.0-AX)	7160
	AAA=-AAA+.12*(AX+1.0)	7170
	XXX=.88*STRCO/AAA	7180
	YYY=AX*XXX	7190
	IF(ABS(XXX).GE.ABS(STREY(N, I)).AND.ABS(YYY).GE.ABS(STREX(N, I))) GO	7200
	STO 20	7210
	XXX=.88*STRCU/AAA	7220
	YYY=AX*XXX	7230
	IF(ABS(XXX).GE.ABS(STREY(N, I)).AND.ABS(YYY).GE.ABS(STREX(N, I))) GO	7240
	STO 30	7250
	XXX=.88*STRCM/AAA	7260
	YYY=AX*XXX	7270
	IF(ABS(XXX).GE.ABS(STREY(N, I)).AND.ABS(YYY).GE.ABS(STREX(N, I))) GO	7280
	STO 70	7290
	NCRI(N, I)=4	7300
	GO TO 300	7310
70	NCRI(N, I)=7	7320
	GO TO 300	7330
30	NCRI(N, I)=2	7340
	GO TO 300	7350
20	NCRI(N, I)=1	7360
	GO TO 300	7370
50	IF(STREX(N, I).LE.STRCT.AND.STREY(N, I).LE.STRCT) GO TO 110	7380
	IF(STREX(N, I).GT.STRCT.AND.STREY(N, I).GT.STRCT) GO TO 160	7390
	IF(STREX(N, I).GT.STRCT) NCRI(N, I)=31	7400

	IF(STREY(N,1).GT.STRCT) NCRI(N,1)=32	7410
	GO TO 300	7420
110	NCRI(N,1)=1	7430
	GO TO 300	7440
100	AX=ABS(STREY(N,1)/STREX(N,1))	7450
	YYY=(STRCT*STRCU)/(AX*STRCT+STRCU)	7460
	XXX=AX*YYY	7470
	IF(ABS(XXX).GT.ABS(STREY(N,1)).AND.ABS(YYY).GT.ABS(STREX(N,1))) GO	7480
	STO 110	7490
	GO TO 150	7500
101	AX=ABS(STREX(N,1)/STREY(N,1))	7510
	YYY=(STRCT*STRCU)/(AX*STRCT+STRCU)	7520
	XXX=AX*YYY	7530
	IF(ABS(XXX).GT.ABS(STREX(N,1)).AND.ABS(YYY).GT.ABS(STREY(N,1))) GO	7540
	STO 110	7550
	GO TO 131	7560
300	CONTINUE	7570
	RETURN	7580
	END	7590
		7600
		7610
		7620
		7630
		7640
		7650
		7660
		7670
		7680
		7690
		7700
		7710
		7720
		7730
		7740
		7750
		7760
		7770
		7780
		7790
1002	FORMAT(7(F11.7,4X))	7800
	DO 7 I=1,NU	7810
	R2(I)=R1(I)	7820
7	R1(I)=0.0	7830
	IF(NNRN.GT.1) GO TO 5	7840
	DO 6 I=1,NE	7850
	DO 6 J=1,NL	7860
	STREX(I,J)=0.0	7870
	STREY(I,J)=0.0	7880
6	STREXY(I,J)=0.0	7890
5	CONTINUE	7900
	I=1	7910
	DO 1 KKK=1,NLE	7920
	DO 1 LLL=1,NW	7930
	NCR=1	7940
	FX=0.	7950
	FY=0.	7960
	FXY=0.	7970
	BMX=0.	7980
	BMY=0.	7990
	BMXY=0.	8000
	A=A2(I)	8010
	B=B2(I)	8020
	HEAD(4) (NP1(11),11=1,20)	8030
	DO 2 JJ=1,20	8040
	SB(JJ)=0.0	8050
	LL=NP1(JJ)	8060
	IF(LL.EQ.0) GO TO 2	8070
	SB(JJ)=R2(LL)	8080
2	CONTINUE	8090
	STRXO = (.25/A)*(-SB(1)-SB(6)+SB(11)+SB(16))	8100
	STRYO = (.25/B)*(-SB(2)+SB(7)-SB(12)+SB(17))	8110
	STRXYO = (.25/B)*(-SB(1)+SB(6)-SB(11)+SB(16)) + (.25/A)*(-SB(2)+SB(7)-SB(12)+SB(17)-SB(7))	8120
	CURXO = (+.25/A)*(SB(4)+SB(9)-SB(14)-SB(19))	8130
	CURYO = (-.25/B)*(SB(5)-SB(10)+SB(15)-SB(20))	8140

	CURXYO = (SB(3)-SB(8)-SB(13)+SB(18))/(A*B*2.0)	8150
	IF(LLL.NE.1) GO TO 10	8160
	STRXYO=CURXYO*0.0	8170
	STRYO1=(.5/B)*(-SB(2)+SB(7))	8180
	CURYO1=(-.5/B)*(SB(5)-SB(10))	8190
10	CONTINUE	8200
	DO 3 J=1,NL	8210
	STRX=STRXO +.5*(T(J+1)+T(J))*CURXO	8220
	STRY=STRYO +.5*(T(J+1)+T(J))*CURYO	8230
	STRXY=STRXYO +(T(J+1)+T(J))*CURXYO *.50	8240
	IF(LLL.EQ.1) STRY1=STRYO1+.5*(T(J+1)+T(J))*CURYO1	8250
	CALL CONSTIT(I,J)	8260
	IF(NCRI(I,J).EQ.4) GO TO 110	8270
	IF(NCRI(I,J).EQ.3) GO TO 120	8280
	STREX(I,J)=STREX(I,J)+C(1,1)*STRX+C(1,2)*STRY+C(1,3)*STRXY	8290
	STREY(I,J)=STREY(I,J)+C(2,1)*STRX+C(2,2)*STRY+C(2,3)*STRXY	8300
	STREXY(I,J)=STREXY(I,J)+C(3,1)*STRX+C(3,2)*STRY+C(3,3)*STRXY	8310
	CCC=(STREX(I,J)+STREY(I,J))/2.0	8320
	BBB=SQRT(((STREY(I,J)-STREX(I,J))/2.0)**2.0+(STREXY(I,J))**2.0)	8330
	SMAX=CCC+BBB	8340
	SMIN=CCC-BBB	8350
	ANG=.5*ATAN(2.0*STREXY(I,J)/(STREY(I,J)-STREX(I,J)))	8360
	IF(STREX(I,J).GT.STREY(I,J)) GO TO 50	8370
	ANCC(I,J)=ANG	8380
	GO TO 60	8390
50	ANCC(I,J)=ANG+3.141593/2.0	8400
60	IF(ANG(I,J).LT..0) ANCC(I,J)=ANCC(I,J)+3.141593	8410
	GO TO 100	8420
110	STREX(I,J)=0.0	8430
	STREY(I,J)=0.0	8440
	STREXY(I,J)=0.0	8450
	SMAX=0.0	8460
	SMIN=0.0	8470
	GO TO 100	8480
120	CONTINUE	8490
	IF(STREX(I,J).GT.STREY(I,J)) GO TO 300	8500
	STREY(I,J)=0.0	8510
	STREX(I,J)=STREX(I,J)+C(1,1)*STRX+C(1,2)*STRY+C(1,3)*STRXY	8520
	GO TO 100	8530
300	STREX(I,J)=0.0	8540
	STREY(I,J)=STREY(I,J)+C(2,1)*STRX+C(2,2)*STRY+C(2,3)*STRXY	8550
100	CONTINUE	8560
	IF(LLL.NE.1) GO TO 911	8570
	WRITE(6,4) J,STREX(I,J),STREY(I,J),STRX,STRY	8580
4	FORMAT(110,4(F15.8,5X))	8590
911	CONTINUE	8600
	CALL CRITERI(I,J)	8610
	IF(NNNH.LE.2) GO TO 3	8620
	IF(NCRI(I,J).EQ.1.OR.NCRI(I,J).EQ.2.OR.NCRI(I,J).EQ.5.OR.NCRI(I,J)	8630
	S.EQ.6.OR.NCRI(I,J).EQ.7.OR.NCRI(I,J).EQ.8.OR.NCRI(I,J).EQ.9) GO TO 3	8640
	IF(NCRI(I,J).EQ.3.OR.NCRI(I,J).EQ.4) GO TO 3	8650
	NCR=2	8660
	CALL INLOAD(I,J)	8670
3	CONTINUE	8680
	IF(NCR.EQ.1) GO TO 30	8690
	K1=NP1(1)	8700
	K2=NP1(2)	8710
	K3=NP1(3)	8720
	K4=NP1(4)	8730
	K5=NP1(5)	8740
	K6=NP1(6)	8750
	K7=NP1(7)	8760
	K8=NP1(8)	8770
	K9=NP1(9)	8780
	K10=NP1(10)	8790
	K11=NP1(11)	8800
	K12=NP1(12)	8810
	K13=NP1(13)	8820
	K14=NP1(14)	8830
	K15=NP1(15)	8840
	K16=NP1(16)	8850
	K17=NP1(17)	8860
	K18=NP1(18)	8870
	K19=NP1(19)	8880

	K20=NP1(20)	8896
	IF(K1.EQ.0) GO TO 11	8906
	R1(K1)=R1(K1)-B*FX-A*FX	8910
11	IF(K2.EQ.0) GO TO 12	8920
	R1(K2)=R1(K2)-B*FX-A*FY	8930
12	IF(K3.EQ.0) GO TO 13	8940
	R1(K3)=R1(K3)+2.0*BMDY	8950
13	IF(K4.EQ.0) GO TO 14	8960
	R1(K4)=R1(K4)-B*BMDX	8970
14	IF(K5.EQ.0) GO TO 15	8980
	R1(K5)=R1(K5)-A*BMY	8990
15	IF(K6.EQ.0) GO TO 16	9000
	R1(K6)=R1(K6)-B*FX+A*FX	9010
16	IF(K7.EQ.0) GO TO 17	9020
	R1(K7)=R1(K7)-B*FX+A*FY	9030
17	IF(K8.EQ.0) GO TO 18	9040
	R1(K8)=R1(K8)-2.0*BMDY	9050
18	IF(K9.EQ.0) GO TO 19	9060
	R1(K9)=R1(K9)-B*BMDX	9070
19	IF(K10.EQ.0) GO TO 20	9080
	R1(K10)=R1(K10)+A*BMY	9090
20	IF(K11.EQ.0) GO TO 21	9100
	R1(K11)=R1(K11)+B*FX-A*FX	9110
21	IF(K12.EQ.0) GO TO 22	9120
	R1(K12)=R1(K12)+B*FX-A*FY	9130
22	IF(K13.EQ.0) GO TO 23	9140
	R1(K13)=R1(K13)-2.0*BMDY	9150
23	IF(K14.EQ.0) GO TO 24	9160
	R1(K14)=R1(K14)+B*BMDX	9170
24	IF(K15.EQ.0) GO TO 25	9180
	R1(K15)=R1(K15)-A*BMY	9190
25	IF(K16.EQ.0) GO TO 26	9200
	R1(K16)=R1(K16)+B*FX+A*FX	9210
26	IF(K17.EQ.0) GO TO 27	9220
	R1(K17)=R1(K17)+B*FX+A*FY	9230
27	IF(K18.EQ.0) GO TO 28	9240
	R1(K18)=R1(K18)+2.0*BMDY	9250
28	IF(K19.EQ.0) GO TO 29	9260
	R1(K19)=R1(K19)+B*BMDX	9270
29	IF(K20.EQ.0) GO TO 30	9280
	R1(K20)=R1(K20)+A*BMY	9290
30	CONTINUE	9300
	WRITE(6,9) I	9310
9	FORMAT(15)	9320
	IF(LLL.EQ.1.OR.LLL.EQ.6) GO TO 31	9330
	GO TO 8	9340
31	CONTINUE	9350
	CALL BSTRESS (I, KKK, LLL)	9360
8	I=I+1	9370
1	CONTINUE	9380
	NNNN=NNNN+1	9390
	REWIND 1	9400
	REWIND 2	9410
	DO 90 II=1,NE	9420
	READ(2) ((SK(I,J),J=1,20),I=1,20)	9430
	WRITE(1) ((SK(I,J),J=1,20),I=1,20)	9440
90	CONTINUE	9450
	RETURN	9460
	END	9470
		9480
		9490
		9500
		9510
	SUBROUTINE BAND(A,B,N,M,LT,DET)	9520
	DIMENSION A(1),B(1)	9530
	MM=N-1	9540
	NM=N*M	9550
	NN1=MM-MM	9560
	IF (LT.NE.1) GO TO 55	9570
	NP=N+1	9580
	KK=2	9590
	FAC=DET	9600
	A(1)=1./SQRT(A(1))	9610
	BIGL=A(1)	9620

	SML=A(1)	9630
	A(2)=A(2)*A(1)	9640
	A(MP)=1./SQRT(A(MP)-A(2)*A(2))	9650
	IF(A(MP).GT.BIGL)BIGL=A(MP)	9660
	IF(A(MP).LT.SML)SML=A(MP)	9670
	NP=NP+M	9680
	DO 62 J=MP,MM1,M	9690
	JP=J-MM	9700
	MZC=0	9710
	IF(KK.GE.MD GO TO 1	9720
	KK=KK+1	9730
	II=1	9740
	JC=1	9750
	GO TO 2	9760
1	KK=KK+M	9770
	II=KK-MM	9780
	JC=KK-MM	9790
2	DO 65 I=KK,JP,MM	9800
	IF(A(I).EQ.0.)GO TO 64	9810
	GO TO 66	9820
64	JC=JC+M	9830
65	MZC=MZC+I	9840
	ASUM1=0.	9850
	GO TO 61	9860
66	MMZC=MM+MZC	9870
	II=II+MZC	9880
	KM=KK+MMZC	9890
	A(KM)=A(KM)*A(JC)	9900
	IF(KM.GE.JP)GO TO 6	9910
	KJ=KM+MM	9920
	DO 5 I=KJ,JP,MM	9930
	ASUM2=0.	9940
	IM=I-MM	9950
	II=II+1	9960
	KI=II+MMZC	9970
	DO 7 K=KM,IM,MM	9980
	ASUM2=ASUM2+A(KI)*A(K)	9990
7	KI=KI+MM	*****
5	A(I)=(A(I)-ASUM2)*A(KI)	*****
6	CONTINUE	*****
	ASUM1=0.	*****
	DO 4 K=KM,JP,MM	*****
4	ASUM1=ASUM1+A(K)*A(K)	*****
61	S=A(J)-ASUM1	*****
	IF(S.LT.0.)DET=S	*****
	IF(S.EQ.0.)DET=0.	*****
	IF(S.GT.0.)GO TO 63	*****
	NROW=(J+MD)/M	*****
	WRITE(6,99) NROW	*****
99	FORMAT(35H0ERROR CONDITION ENCOUNTERED IN ROW,16)	*****
	RETURN	*****
63	A(J)=1./SQRT(S)	*****
	IF(A(J).GT.BIGL)BIGL=A(J)	*****
	IF(A(J).LT.SML)SML=A(J)	*****
62	CONTINUE	*****
	IF(SML.LE.FAC*BIGL)GO TO 54	*****
	GO TO 53	*****
54	DET=0.	*****
	RETURN	*****
53	DET=SML/BIGL	*****
55	B(1)=B(1)*A(1)	*****
	KK=1	*****
	K1=1	*****
	J=1	*****
	DO 8 L=2,N	*****
	BSUM1=0.	*****
	LM=L-1	*****
	J=J+M	*****
	IF(KK.GE.MD GO TO 12	*****
	KK=KK+1	*****
	GO TO 13	*****
12	KK=KK+M	*****
	K1=K1+1	*****
13	JK=KK	*****


```

SK(14,14)=SK(14,14)+BSK(6,6)
SK(19,19)=SK(19,19)+BSK(6,6)
SK(1,3)=SK(3,1)=SK(1,3)+BSK(1,2)
SK(6,8)=SK(8,6)=SK(6,8)+BSK(1,2)
SK(1,4)=SK(4,1)=SK(1,4)+BSK(1,3)
SK(6,9)=SK(9,6)=SK(6,9)+BSK(1,3)
SK(1,11)=SK(11,1)=SK(1,11)+BSK(1,4)
SK(6,16)=SK(16,6)=SK(6,16)+BSK(1,4)
SK(1,13)=SK(13,1)=SK(1,13)+BSK(1,5)
SK(6,18)=SK(18,6)=SK(6,18)+BSK(1,5)
SK(1,14)=SK(14,1)=SK(1,14)+BSK(1,6)
SK(6,19)=SK(19,6)=SK(6,19)+BSK(1,6)
SK(3,4)=SK(4,3)=SK(3,4)+BSK(2,3)
SK(8,9)=SK(9,8)=SK(8,9)+BSK(2,3)
SK(3,11)=SK(11,3)=SK(3,11)+BSK(2,4)
SK(8,16)=SK(16,8)=SK(8,16)+BSK(2,4)
SK(3,13)=SK(13,3)=SK(3,13)+BSK(2,5)
SK(8,18)=SK(18,8)=SK(8,18)+BSK(2,5)
SK(3,14)=SK(14,3)=SK(3,14)+BSK(2,6)
SK(8,19)=SK(19,8)=SK(8,19)+BSK(2,6)
SK(4,11)=SK(11,4)=SK(4,11)+BSK(3,4)
SK(9,16)=SK(16,9)=SK(9,16)+BSK(3,4)
SK(4,13)=SK(13,4)=SK(4,13)+BSK(3,5)
SK(9,18)=SK(18,9)=SK(9,18)+BSK(3,5)
SK(4,14)=SK(14,4)=SK(4,14)+BSK(3,6)
SK(9,19)=SK(19,9)=SK(9,19)+BSK(3,6)
SK(11,13)=SK(13,11)=SK(11,13)+BSK(4,5)
SK(16,18)=SK(18,16)=SK(16,18)+BSK(4,5)
SK(11,14)=SK(14,11)=SK(11,14)+BSK(4,6)
SK(16,19)=SK(19,16)=SK(16,19)+BSK(4,6)
SK(13,14)=SK(14,13)=SK(13,14)+BSK(5,6)
SK(18,19)=SK(19,18)=SK(18,19)+BSK(5,6)
RETURN
END

```

```

SUBROUTINE BSTIFF (N)
COMMON R3(480)
COMMON NE, NL, NB, NNNN, MAX, NLE, NW
COMMON STRS, STRCO, STRCU, STRCM, STRCT, ECO, EC1, EC2, ESO, UC
COMMON A1(20,20), A2(84), B2(84), NP1(20), R1(480), SK(20,20), C(3,3)
COMMON T(15), STREX(84,14), STREY(84,14), STREXY(84,14)
COMMON SMAX, SMIN, ANGC(84,14), NCR1(84,14), NCR10(84,14), TSK(18000)
COMMON NU, D(3,3), H(3,3), F(3,3), FX, FY, FXY, BMX, BMY, BMXY, R2(480)
COMMON BSK(6,6), BAS(10), BSS(10), BIS(10), BAS2(10), BSS2(10), BIS2(10)
COMMON SB(20), TB(11), BW(10), NSL1, NSL2, NST1, NST2
COMMON STRBY(25,10), STREBY(25,10), STRBY2(25,10), STREBY2(25,10)
COMMON BW2(10), TB2(10), RIBD, RIBT, RIBZ
B=B2(N)
DO 10 II=1,NLE
IF(N.EQ.NLEB(II)) GO TO 20
IF(N.EQ.NLEB2(II)) GO TO 120
10 CONTINUE
GO TO 200
20 I=II
IF(NNNN.GT.1) GO TO 25
DO 26 K=1,NBL
26 BES(I,K)=ESO
25 CONTINUE
DO 30 IJ=1,6
DO 30 JJ=1,6
30 BSK(II,JJ)=0.0
DO 50 K=1,NBL
BSK(1,1)=BSK(1,1)+BES(I,K)*BAS(K)/(2.0*B)
BSK(1,3)=BSK(3,1)=BSK(1,3)+BES(I,K)*BSS(K)/(2.0*B)
BSK(1,4)=BSK(4,1)=-BSK(1,1)
BSK(1,6)=BSK(6,1)=-BSK(1,3)
ESK(2,2)=BSK(2,2)+12.0*BES(I,K)*BIS(K)/(B*B*B*8.0)
BSK(2,3)=BSK(3,2)=BSK(2,3)-6.0*BES(I,K)*BIS(K)/(4.0*B*B)
BSK(2,5)=BSK(3,2)=-BSK(2,2)
BSK(2,6)=BSK(6,2)=BSK(2,3)

```



```

BSK(3,3)=BSK(3,3)+4.0*BES(1,K)*BIS(K)/(2.0*B) *****
BSK(3,4)=BSK(4,3)*BSK(1,6) *****
BSK(3,5)=BSK(5,3)=-BSK(2,3) *****
BSK(3,6)=BSK(6,3)*BSK(3,6)+BES(1,K)*BIS(K)/B *****
BSK(4,4)=BSK(1,1) *****
BSK(4,6)=BSK(6,4)*BSK(1,3) *****
BSK(5,5)=BSK(2,2) *****
BSK(5,6)=BSK(6,5)=-BSK(2,3) *****
BSK(6,6)=BSK(3,3) *****
30 CONTINUE *****
SK(2,2)=SK(2,2)+BSK(1,1) *****
SK(3,3)=SK(3,3)+BSK(2,2) *****
SK(5,5)=SK(5,5)+BSK(3,3) *****
SK(7,7)=SK(7,7)+BSK(4,4) *****
SK(8,8)=SK(8,8)+BSK(5,5) *****
SK(10,10)=SK(10,10)+BSK(6,6) *****
SK(2,3)=SK(3,2)=SK(2,3)+BSK(1,2) *****
SK(2,5)=SK(5,2)=SK(2,5)+BSK(1,3) *****
SK(2,7)=SK(7,2)=SK(2,7)+BSK(1,4) *****
SK(2,8)=SK(8,2)=SK(2,8)+BSK(1,5) *****
SK(2,10)=SK(10,2)=SK(2,10)+BSK(1,6) *****
SK(3,5)=SK(5,3)=SK(3,5)+BSK(2,3) *****
SK(3,7)=SK(7,3)=SK(3,7)+BSK(2,4) *****
SK(3,8)=SK(8,3)=SK(3,8)+BSK(2,5) *****
SK(3,10)=SK(10,3)=SK(3,10)+BSK(2,6) *****
SK(5,7)=SK(7,5)=SK(5,7)+BSK(3,4) *****
SK(5,8)=SK(8,5)=SK(5,8)+BSK(3,5) *****
SK(5,10)=SK(10,5)=SK(5,10)+BSK(3,6) *****
SK(7,8)=SK(8,7)=SK(7,8)+BSK(4,5) *****
SK(7,10)=SK(10,7)=SK(7,10)+BSK(4,6) *****
SK(8,10)=SK(10,8)=SK(8,10)+BSK(5,6) *****
SK(4,4)*SK(4,4)+(ESO*TK)/(5.0*B) *****
SK(4,9)=SK(9,4)=SK(4,9)-(ESO*TK)/(5.0*B) *****
SK(9,9)=SK(9,9)+(ESO*TK)/(5.0*B) *****
GO TO 200 *****
120 I=11 *****
IF(BW2(1).EQ.0.0) GO TO 200 *****
IF(NNNN.GT.1) GO TO 125 *****
DO 126 K=1,NBL *****
126 BES2(1,K)=ESO *****
125 CONTINUE *****
DO 130 II=1,6 *****
DO 130 JJ=1,6 *****
130 BSK(II,JJ)=0.0 *****
DO 150 K=1,NBL *****
BSK(1,1)=BSK(1,1)+BES2(1,K)*BAS2(K)/(2.0*B) *****
BSK(1,3)=BSK(3,1)=BSK(1,3)-BES2(1,K)*BSS2(K)/(2.0*B) *****
BSK(1,4)=BSK(4,1)=-BSK(1,1) *****
BSK(1,6)=BSK(6,1)=-BSK(1,3) *****
BSK(2,2)=BSK(2,2)+12.0*BES2(1,K)*BIS2(K)/(B*B*B*8.0) *****
BSK(2,3)=BSK(3,2)=BSK(2,3)+6.0*BES2(1,K)*BIS2(K)/(4.0*B*B) *****
BSK(2,5)=BSK(5,2)=-BSK(2,2) *****
BSK(2,6)=BSK(6,2)=BSK(2,3) *****
BSK(3,3)=BSK(3,3)+4.0*BES2(1,K)*BIS2(K)/(2.0*B) *****
BSK(3,4)=BSK(4,3)=BSK(1,6) *****
BSK(3,5)=BSK(5,3)=-BSK(2,3) *****
BSK(3,6)=BSK(6,3)=BSK(3,6)+BES2(1,K)*BIS2(K)/B *****
BSK(4,4)=BSK(1,1) *****
BSK(4,6)=BSK(6,4)=BSK(1,3) *****
BSK(5,5)=BSK(2,2) *****
BSK(5,6)=BSK(6,5)=-BSK(2,3) *****
BSK(6,6)=BSK(3,3) *****
150 CONTINUE *****
SK(12,12)=SK(12,12)+BSK(1,1) *****
SK(13,13)=SK(13,13)+BSK(2,2) *****
SK(15,15)=SK(15,15)+BSK(3,3) *****
SK(17,17)=SK(17,17)+BSK(4,4) *****
SK(18,18)=SK(18,18)+BSK(5,5) *****
SK(20,20)=SK(20,20)+BSK(6,6) *****
SK(12,13)=SK(13,12)=SK(12,13)+BSK(1,2) *****
SK(20,20)=SK(20,20)+BSK(6,6) *****
SK(12,13)=SK(13,12)=SK(12,13)+BSK(1,2) *****
SK(12,15)=SK(15,12)=SK(12,15)+BSK(1,3) *****
SK(12,17)=SK(17,12)=SK(12,17)+BSK(1,4) *****

```

```

SK(12,18)=SK(18,12)+SK(12,18)+BSK(1,5) *****
SK(12,20)=SK(20,12)+SK(12,20)+BSK(1,6) *****
SK(13,15)=SK(15,13)+SK(13,15)+BSK(2,3) *****
SK(13,17)=SK(17,13)+SK(13,17)+BSK(2,4) *****
SK(13,18)=SK(18,13)+SK(13,18)+BSK(2,5) *****
SK(13,20)=SK(20,13)+SK(13,20)+BSK(2,6) *****
SK(15,17)=SK(17,15)+SK(15,17)+BSK(3,4) *****
SK(15,18)=SK(18,15)+SK(15,18)+BSK(3,5) *****
SK(15,20)=SK(20,15)+SK(15,20)+BSK(3,6) *****
SK(17,18)=SK(18,17)+SK(17,18)+BSK(4,5) *****
SK(17,20)=SK(20,17)+SK(17,20)+BSK(4,6) *****
SK(18,20)=SK(20,18)+SK(18,20)+BSK(5,6) *****
SK(14,14)=SK(14,14)+(ESO*TK2)/(5.0*B) *****
SK(14,19)=SK(19,14)+SK(14,19)-(ESO*TK2)/(5.0*B) *****
SK(19,19)=SK(19,19)+(ESO*TK2)/(3.0*B) *****
200 CONTINUE *****
RETURN *****
END *****

SUBROUTINE BSTRESS (I, KKK, LLL) *****
COMMON R3(480) *****
COMMON NE, NL, NB, NNN, MAX, NLE, NW *****
COMMON STRS, STRCO, STRCU, STRCM, STRCT, ECO, EC1, EC2, ESO, UC *****
COMMON A1(20,20), A2(84), B2(84), NP1(20), R1(480), SK(20,20), C(3,3) *****
COMMON T(15), STREX(84,14), STREY(84,14), STREXY(84,14) *****
COMMON SMAX, SMIN, ANCC(84,14), NCRI(84,14), NCRI0(84,14), TSK(18000) *****
COMMON NU, D(3,3), H(3,3), F(3,3), FX, FY, FXY, BMX, BMY, BMKY, R2(480) *****
COMMON ES1, NBL, TK, TK2, NLEB(25), NLEB2(25), BES(25,10), BES2(25,10) *****
COMMON BSK(6,6), BAS(10), BSS(10), BIS(10), BAS2(10), BSS2(10), BIS2(10) *****
COMMON SB(20), TB(11), BW(10), NSL1, NSL2, NST1, NST2 *****
COMMON STRBY(25,10), STREBY(25,10), STRBY2(25,10), STREBY2(25,10) *****
COMMON BW2(10), TB2(10), RIBD, RIBT, RIBZ *****
IF(NNN.GT.1) GO TO 2 *****
IF(LLL.EQ.6) GO TO 40 *****
DO 1 J=1,NBL *****
STRBY(KKK,J)=0.0 *****
STREBY(KKK,J)=0.0 *****
1 GO TO 2 *****
40 CONTINUE *****
DO 4 J=1,NBL *****
STRBY2(KKK,J)=0.0 *****
STREBY2(KKK,J)=0.0 *****
4 CONTINUE *****
2 B=B2(1) *****
IF(LLL.EQ.6) GO TO 10 *****
STRBYO=(.50/B)*(-SB(2)+SB(7)) *****
CURBYO=(-.50/B)*(SB(5)-SB(10)) *****
GO TO 15 *****
10 STRBYO=(.50/B)*(-SB(12)+SB(17)) *****
CURBYO=(-.50/B)*(SB(15)-SB(20)) *****
15 CONTINUE *****
DO 3 J=1,NBL *****
IF(LLL.EQ.6) GO TO 20 *****
STRBY(KKK,J)=STRBYO+.5*(TB(J+1)+TB(J))*CURBYO+STRBY(KKK,J) *****
STREBY(KKK,J)=STREBY(KKK,J)+(STRBYO+.3*(TB(J+1)+TB(J))*CURBYO)*BES *****
*(KKK,J) *****
GO TO 33 *****
20 CONTINUE *****
STRBY2(KKK,J)=STRBY2(KKK,J)+STRBYO+.5*(TB(J+1)+TB(J))*CURBYO *****
STREBY2(KKK,J)=STREBY2(KKK,J)+(STRBYO+CURBYO*(TB(J+1)+TB(J))*50)* *****
*BES2(KKK,J) *****
33 CALL BCONST(KKK,LLL,J) *****
3 CONTINUE *****
IF(LLL.EQ.6) GO TO 30 *****
WRITE(6,5) (STREBY(KKK,J),J=1,NBL) *****
5 FORMAT(8F10.2) *****
WRITE(6,6) (STRBY(KKK,J),J=1,NBL) *****
6 FORMAT(8F10.7) *****
GO TO 100 *****
30 CONTINUE *****
WRITE(6,5) (STREBY2(KKK,J),J=1,NBL) *****

```


REFERENCES

1. Abdel Sayed, G., "Effective Width of Steel Deck Plate in Bridges", Journal of the Structural Division, ASCE, Vol. 95, Oct. 69.
2. Adekola, A.o., "On the Influence Curves for Effective Widths in Non-Prismatic Composite Beams", Proceedings, Institute of Civil Engineering, Vol. 57, Part 2, March 74.
3. Adekola, A.o., "Effective Widths of Composite Beams of Steel and Concrete", The Structural Engineer, Vol. 46, No. 9, Sept. 68.
4. Adekola, A.o., "An Investigation into the Behaviour of Composite Steel Rib and Concrete Slab", Building Science, Vol. 1, Oct. 66.
5. Allen, D.N. de G. and Severn, R.T., "Composite Action Between Beams and Slabs under Transverse Load", The Structural Engineer, Vol. 39, May 61.
6. Ansourian, P., "An Investigation of the Method of Finite Element to the Analysis of Composite Floor Systems, Proceedings, Institute of Civil Engineering, Part 2, Vol. 59, Dec. 75.
7. Atan, Y. and Slate, F.o., "Structural Lightweight Concrete under Biaxial Compression, "ACI Journal, Vol. 70, No. 3, March 73.
8. Azmi, H., "Strength of Composite Beams Incorporating 3-inch Cellular Metal Deck", M.Eng. Project, McMaster Univ., Hamilton, Ontario, June 75.
9. Barnard, P.R. and Johnson, R.P., "Ultimate Strength of Composite Beams", Proceedings, Institution of Civil Engineers, Vol. 32, Oct. 65.
10. Barnard, P.R., "Series of Tests on Simply Supported Composite Beams", Journal of ACI, Vol. 62, April 65.

11. Brendel, G., "Strength of the Compression Slab of T. Beam Subject to Simple Bending", Journal of ACI, Vol. 61, Jan. 64.
12. Bresler, B. and Pister, K.S., "Strength of Concrete under Combined Stress", Journal of ACI, Vol. 55, No. 10, Sept. 58.
13. Buyukozturk, O., Nilson, A.H. and Slate, F.O., "Stress-Strain Response and Fracture of a Concrete Model in Biaxial Loading", Journal of ACI, Vol. 68, No. 8, Aug. 71.
14. Cheung, M.S. and Chan, M.Y.T., "Finite Strip Evaluation of Effective Flange Width of Bridge Girders", Canadian Journal of Civil Engineering, Vol. 5, No. 2, June 78.
15. Cook, J.P., "Composite Construction Methods", John Wiley & Sons, New York, 1977.
16. Dallaire, E.E., "Cellular Steel Floors Mature", Journal of the Structural Division, ASCE, July 71.
17. Davies, C., "Steel-Concrete Composite Beams for Buildings", John Wiley & Sons, New York, 75.
18. Davies, C., "Tests on Half-Scale Steel Concrete Composite Beams with Welded Stud Connectors", Journal of the Structural Engineering, Vol. 47, No. 1, Jan. 69.
19. ElGhazzi, M.N., Robinson, H. and Elkholy, I.A.S., "Longitudinal Shear Capacity of the Slabs of Composite Beams", Canadian Journal of Civil Engineering, Vol. 3, No. 4, 76.
20. ElGhazzi, M.N., "Longitudinal Shear Capacity of Slabs of Composite Beams", M.Eng. Thesis, McMaster Univ., Hamilton, Ontario, 72.
21. Fan, H.M. and Heins, C.P., "Effective Slab Width of Simple Span Composite Bridges at Ultimate Load", Civil Engineering Report No. 54, Univ. of Maryland, College Park, Md., June 74.
22. Fisher, J.W., Kim, S.W. and Slutter, R.G., "Tests of Lightweight Concrete Composite Beams and Pushout Specimens with Cellular Steel Deck", Fritz Engineering Laboratory, Report No. 200.67.438.1, Lehigh University, July 67.
23. Gustafson, W.C. and Wright, R.N., "Analysis of Skewed

- Composite Girder Bridges", Journal of the Structural Division, ASCE, Vol. 94, No. ST4, April 68.
24. Hagood, T.A., Guthrie, L. and Hoadley, P.G., "An Investigation of the Effective Concrete Slab Width for Composite Construction", American Institute of Steel Construction Engineering Journal, Jan. 68.
 25. Hand, F.R., Pecknold, D.A. and Schnobrich, W.C., "Nonlinear Layered Analysis of RC Plates and Shells", Journal of the Structural Division, ASCE, Vol. 99, No ST7, July 73.
 26. Hand, F., "Nonlinear Layered Finite Element Analysis of Reinforced Concrete Plates and Shells", PH.D. Thesis, The University of Illinois, Urbana-Champaign, 1972.
 27. Heins, C.P. and Fan, H.M., "Effective Composite Beam Width at Ultimate Load", Journal of the Structural Division, ASCE, Vol. 102, No. ST11, Nov. 76.
 28. Henderson, W.D., "Effect of Stud Height on Shear Connector Strength in Composite Beams with Lightweight Concrete in Three-Inch Metal Deck", M.SC. Thesis, The University of Texas, Austin, 1976.
 29. Iyengar, H.S., "State of the Art Report on Mixed Steel-Concrete Construction for Buildings", Report Published by the American Society of Civil Engineering, Section 3, 1977.
 30. Jofreit, J.C. and McNiece, G.M., "Finite Element Analysis of Reinforced Concrete Slabs", Journal of the Structural Division, ASCE, Vol. 97, No. ST3, March 71.
 31. Johnson, R.P., "Composite Structures of Steel and Concrete", Vol. 1, "Beams, Columns, Frames and Applications in Buildings", Crosby Lockwood Staples, London, 1975.
 32. Johnson, P., "Longitudinal Shear Strength of Composite Beams", ACI Journal, June 70.
 33. Johnson, R.P., "Research on Steel-Concrete Composite Beams", Journal of the Structural Division, ASCE, Vol. 96, No. ST3, March 1970.
 34. Kabir, A., "Nonlinear Analysis of Reinforced Concrete Pannels, Slabs and Shells for Time-Dependent Effects", PH.D. Thesis, The Univ. of California, Berkeley, 1977.

35. Kupfer, H.B. and Gerstle, K.H., "Behaviour of Concrete under Biaxial Stresses", Journal of the Engineering Mechanics Division, ASCE, Vol. 99, No. EM4, Aug. 73.
36. Kupfer, H. Hilsdorf, H.K. and Rusch, H., "Behaviour of Concrete under Biaxial Stresses", ACI journal, Vol. 66, No. 8, Aug. 69.
37. Lee, J.A.N., "Effective Width of Tee-Beams", The Structural Engineer, Vol. 40, Jan. 62.
38. "Limit State Design Steel Manual", Canadian Institute of Steel Construction, CISC, clause 17.3.2.1, First Edition, Jan. 77.
39. Lin, C.S. and Scordelis, A.C., "Nonlinear Analysis of RC Shells of General Form", Journal of the Structural Division, ASCE, Vol. 101, ST3, March 75.
40. Liu, T.C., Nilson, A.H. and Slate, F.O., "Stress-Strain Response and Fracture of Concrete in Uniaxial and Biaxial Compression", ACI Journal, Vol. 69, No. 5, May 72.
41. Liu, T.C., Nilson, A.H. and Slate, F.O., "Biaxial Stress-Strain Relations for Concrete", Journal of the Structural Division, ASCE, Vol. 98, No. ST5, May 72.
42. Ma, K.P., "Inelastic Analysis of Composite Beams with Partial Connection", M.Eng. Thesis, McMaster Univ., Hamilton, Ontario, 1974.
43. Mackey, S. and Wong, F.K.C., "The Effective Width of a Composite Tee-Beam Flange", The Structural Engineer, Vol. 39, Sept. 61.
44. Melosh, R.J., "Basis for Derivation of Matrices for the Direct Stiffness Method", AIAA Journal, Vol. 1, No. 7, July 63.
45. Mikkola, M.J. and Schnobrich, W.C., "Material Behaviour Characteristics for Reinforced Concrete Shells Stressed Beyond the Elastic Range", Civil Engineering Studies, SRS No. 367, Univ. of Illinois, Urbana, Illinois, Aug. 70.
46. Moffat, K.R. and Dowling, P.J., "British Shear Lag Rules for Composite Girders", Journal of the Structural Division, ASCE, Vol. 104, No. ST7, July 78.
47. Park, R. and Paulay, T., "Reinforced Concrete Structures" John Wiley and Sons, New York, 1975.

48. Phillips, D.V. and Zienkiewicz, O.C., "Finite Element Nonlinear Analysis of Concrete Structures", Proceedings, Institute of Civil Engineers, Part 2, March 76.
49. Robinson, G.S., "Behaviour of Concrete in Biaxial Compression", Journal of the Structural Division, ASCE, Vol. 93, No. ST2, Feb. 67.
50. Robinson, H. and Wallace, I.W., "Composite Beams with 1-1/2 in Metal Deck and Partial and Full Interaction", Transaction of the Canadian Society for Civil Engineering Vol. 16, No. A-8, Sept. 73.
51. Robinson, H., "Tests on Composite Beams with Cellular Deck", Journal of the Structural Division, ASCE, ST4, Aug. 67.
52. Römstad, K.M., Taylor, M.A. and Herrman, L.R., "Numerical Biaxial Characterization for Concrete", Journal of the Engineering Mechanics Division, ASCE, Vol. 100, No. EM5, Oct. 74.
53. Scanlon, A. and Murray, D.W., "An Analysis to Determine the Effects of Cracking in Reinforced Concrete Slabs", Proceedings of the Specially Conference on Finite Element Methods in Civil Engineering, McGill Univ., Engineering Institute of Canada, Montreal, June 72.
54. Schnobrich, W.C., "Finite Element Determination of Nonlinear Behaviour of Reinforced Concrete Plates and Shells", Transport and Road Research Laboratory, Dept. of Environment, Univ. of Illinois, Urbana, 1974.
55. Schnobrich, W.C., "Behaviour of Reinforced Concrete Structures Predicted by the Finite Element Method", Proceedings of the Second National Symposium on Computerized Structural Analysis and Design, George Washington, D.C., March 76.
56. Scordelis, A.C., "Finite Element Analysis of Reinforced Concrete Structures", Proceedings of the Specially Conference on Finite Element Methods in Civil Engineering, McGill Univ., Engineering Institute of Canada, Montreal, June 72.
57. Timoshenko, S., "Bending of Rectangular Plates with Clamped Edges", Proceedings, Fifth International Congress of Applied Mechanics, Cambridge, Mass., 1938.
58. Timoshenko, S. and Goodier, J.N., "Theory of Elasticity", McGraw-Hill Book Company, Inc., New York, 1951.

59. Wanchoo, M.K. and May, G.W., "Cracking Analysis of Reinforced Concrete Plates", Journal of the Structural Division, ASCE, Vol. 101, No. ST1, Jan. 75.
60. Wegmuller, A.W., "Overload Behaviour of Composite Steel-Concrete Bridges", Journal of the Structural Division, ASCE, Vol. 103, No. ST9, Sept. 77.
61. Wegmuller, A.W., "Overload Behaviour of Composite Steel-Concrete Highway Girder Bridges", Report ST 76-2, Dept. of Structural Engineering and Applied Mechanics, Univ. of Alabama, Birmingham, Oct. 76.
62. Wegmuller, A.W., "Finite Element Analysis of Elastic-Plastic Plates and Eccentrically Stiffened Plates", PH.D. Thesis, The Univ. of Lehigh, 1971.
63. Zienkewicz, O.C., "The Finite Element Method", 3rd Edition, Mcgraw-hill Book Company, Inc., New York, 1977.
64. Zienkewicz, O.C. and Cheung, Y.K., "The Finite Element Method for Analysis of Elastic Isotropic and Or the Tropic Slabs", Proceedings, Institute of Civil Engineers, Aug. 64.